Interrelation Between H-Bond and Pi-Electron Delocalization

ARTICLE *in* CHEMICAL REVIEWS · NOVEMBER 2005

Impact Factor: 46.57 · DOI: 10.1021/cr030083c · Source: PubMed

3 AUTHORS, INCLUDING:

Lucjan Sobczyk
University of Wroclaw
245 PUBLICATIONS **3,579** CITATIONS

Interrelation between H-Bond and Pi-Electron Delocalization

Lucjan Sobczyk

Faculty of Chemistry, University of Wrocław, Joliot-Curie 14, 50 383 Wrocław, Poland

Sławomir Janusz Grabowski*

Department of Crystallography and Crystal Chemistry, University of Łódź, Pomorska 149/153, 90 236 Łódź, Poland

Tadeusz Marek Krygowski

Department of Chemistry, University of Warsaw, Pasteura 1, 02 093 Warsaw, Poland

Received November 30, 2004

Contents

* To whom correspondence should be addressed. E-mail: slagra@uni.lodz.pl or slagra@ccmsi.us. Fax: +48-42-6790447.

1. Introduction: Definitions, Commonness, and Importance in Natural Sciences

Among many various kinds of molecular interactions, the H-bond has a special position. The term is ubiquitous in the world that surrounds us, but also it is often applied in different ways. The H-bond is of great importance in natural sciences. This relates particularly to biological aspects, such as molecular recognition that could be a basis for the creation of life,[1−4] formation of higher order structures of peptides and nucleic acids,[5] and biochemical processes, particularly the enzymes catalyzed.[6,7] One can say that the H-bond plays a double role in biological systems: on one hand, as a relatively strong directional interaction, it leads to relatively stable supramolecular structures, and on the other hand, because of dynamic features of the proton, it is an active site for initiation of chemical reactions.

H-bonds are the source of specific properties of associated liquids, with water being the most popular among them.[8] Water as a medium in which life was most probably created is saturated by H-bonds with highly mobile protons in between, even in the solid state.[9]

In many crystal lattices of organic compounds, the H-bonds are a decisive factor governing packing.[10] In designing new interesting crystal structures, which is the subject of fast developing crystal engineer-

10.1021/cr030083c CCC: $53.50
Published on Web 09/21/2005

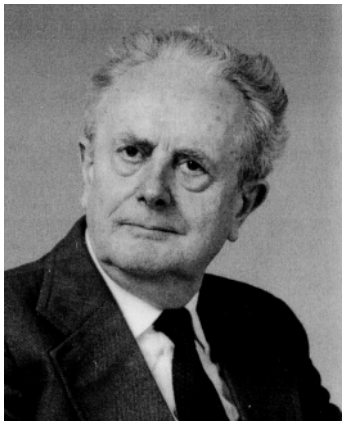

Lucjan Sobczyk was born in 1927 in Natalin (at present Belorussia). He obtained a M.Sc. from Wroclaw Technical University and a Ph.D. from the Institute of Fine Chemical Technology, Moscow, under the supervision of Ya. K. Syrkin. He trained at the Universities of Paris (M. Magat) Aberystwyth (M. Davies), and Ljubljana (D. Hadži). His current research interests are applications of physical methods (particularly dielectric and spectroscopic) in structural studies of organic compounds. The main area of interest is molecular interactions and particularly hydrogen bonds and charge-transfer complexes. He is engaged in organizations of International Conferences Horizons in Hydrogen Bond Research. He was president of the Polish Chemical Society (1979–1984), distinguished by several medals and awards. Since 1976, he has been a member of the Polish Academy of Sciences, D.h.c. of the Leningrad and Wroclaw Universities. Professor emeritus at the Faculty of Chemistry, University of Wroclaw.

Sławomir Grabowski was born in Warsaw, Poland (1956) and received his M.Sc. degree (1981) and his Ph.D. (1986) at the University of Warsaw. He received his D.Sc. (1998) at the Technical University of Łódź, Poland. Since 1986, he has been working at the University of Białystok, Poland, from 1994 as a Head of the Theoretical Chemistry Group and from 2000 as a Professor of the university. He worked under the direction of Professor Ivar Olovsson at the University of Uppsala, Sweden (1988), and at the University of Grenoble, France (1992), under the direction of Prof. Janine Lajzerowicz. In 2002, he moved to Łódź and currently is employed as the Professor of the University of Łódź and a Head of the group working on crystallography and crystal chemistry. His research interests are connected with the intermolecular interactions in crystals, especially different kinds of hydrogen bonds. The important part of research concerns dihydrogen bonds and the application of the Bader theory to analyze the nature of interactions. He has published about 90 papers and a few book chapters. He cooperates with Professors Tadeusz M. Krygowski (University of Warsaw, Poland), Jerzy Leszczynski (Jackson State Univerisity, Jackson, MS), Steve Scheiner (Utah State University, Logan, UT), and Cherif Matta (Dalhousie University, Canada).

ing,[11−13] one of the main parameters is the engagement of H-bonds. In such designing, the main thing to do is classification of synthons defined by groups that are able to form H-bonds and the graph-set analysis.[14−16]

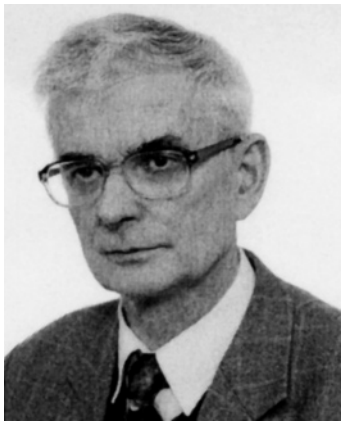

Tadeusz Marek Krygowski was born in Poznan, Poland (1937), and received his M.Sc. degree at the Adam Mickiewicz University (Poznan, 1961) and his Ph.D. (1969) and D.Sc. (1973) both from the Department of Chemistry of the Warsaw University. Since 1964, he has been working at this university, from 1983 as a Professor of Chemistry. He has lectured at many universities, in many countries, serving as an invited Professor in Canada (Guelph, Ontario), France (Nantes), Austria (Linz/D), Israel (Beer Sheva), and South Korea (Busan). He has been president of the Polish Chemical Society (1994–1997), titular member of III Division of IUPAC (2002–present), and since 2002, is a chairman of the Subcommittee of Structural and Mechanistic Organic Chemistry of IUPAC. He is an honorary member of the Polish Chemical Society. He was awarded the Prime Minister price for outstanding scientific achievements (2002), Maria-Sklodowska Medal of the Polish Academy of Science (2004), and J. Zawidzki medal of the Polish Chemical Society for scientific achievements in physical chemistry (1999). His main research interests are in studies of structural effects of intra- and intermolecular interactions, various phenomena associated with σ- and π-electron delocalization, definition of aromaticity, and long-distance consequences of H-bonding. His hobbies are national music and hiking on not too high mountains.

Also, the field of hydrogen-bonded functional materials, first of all ferroelectrics and ferroelastics as well as superprotonic conductors, is of great importance.[17,18] Finally, one should mention hydrogen-bonded photoactive materials in which the optical excitation leads to proton transfer.[19] Such phenomena play an important role in biological systems and can be used in various applications.[20,21]

The IUPAC definition[22] is "the hydrogen bond is a form of association between an electronegative atom and a hydrogen atom attached to a second, relatively electronegative atom. It is best considered as an electrostatic interaction, heightened by a small size of hydrogen, which permits proximity of the interacting dipoles or charges. Both electronegative atoms are usually (but not necessarily) from the first row of the Periodic Table, i.e., N, O, or F. With a few exceptions, usually involving fluorine, the associated energies are less than 20−25 kcal/mol. Hydrogen bonds may be intermolecular or intramolecular". This definition is limited to an already classical conception of this specific molecular interaction. It does not embrace cases such as π-electron systems as proton acceptors, charge-assisted H-bonds of the OHO^+ and OHO^- type, and finally unconventional so-called blue-shifting H-bonds. Moreover, in cases of strong H-bonds, a covalent nature of interaction is revealed. According to Pauling's definition[23] "under certain conditions an atom of hydrogen is attracted by rather strong forces to two atoms, instead of only one, so that it may be considered to be acting as a bond between them. This is called the hydrogen bond".

Table 1. H-Bond Energies (E_{HB}s) Corrected for BSSE (in kcal/mol); HF/6-311++G(d,p) and MP2/6-311++G(d,p) Results Are Given[a]

complex acceptor−donor	E_{HB}(HF)	E_{HB}(MP2)
$(F\cdots H\cdots F)^-$	−40.5	−39.9
$(F\cdots H-Cl)^-$	−19.4	−20.9
$CH_2O\cdots HF$	−6.1	−5.4
$H_2O\cdots HF$	−8.2	−7.5
$H_3N\cdots HF$	−10.2	−11.2
$HLi\cdots HF$	−10.6	−12.6
$\pi(C_2H_2)\cdots HF$[b]	−2.7	−3.2
$H_2O\cdots HOH$	−4.3	−4.5
$HCOOH\cdots HCOOH$	−6.1	−5.9
$H_2O\cdots HCCH$	−2.5	−2.5
$\pi(C_2H_2)\cdots H_2O$[b]	−1.4	−1.8
$\pi(C_2H_2)\cdots HCCH$[b]	−0.7	−1.1
$LiH\cdots HCCH$[c]	−3.1	−3.7
$H_3N\cdots H_2O$	−5.0	−5.8

[a] The results of H-bond energies taken from ref 25. [b] T-shaped configuration. [c] Dihydrogen bond.

Pauling also states that the hydrogen bond "is formed only between the most electronegative atoms."[23] The terms "typical hydrogen bond" or "conventional hydrogen bond" are related in this review to the Pauling definition of hydrogen bonding.

The H-bond is most often formed between atoms, which have already saturated valencies. Moreover, unlike typical chemical bonds, the H-bond ranges over a large scale of energy, from very weak ones, with the energy around a fraction of kcal/mol, up to very strong ones, with the energy around a few dozen kcal/mol.[24−26] This is illustrated in Table 1, which presents the binding energies for different kinds of complexes connected through conventional H-bonds as well as some unconventional ones. Also see Table 1 in ref 27, where the weakest interaction cited was for $CH_4\cdots FCH_3$, with the energy equal to 0.2 kcal/mol. It should be mentioned here that for the intermolecular H-bond the stabilization energy because of its formation is usually calculated as the difference between the energy of the complex and the energies of the isolated monomers ($E_{HB} = E_{AB} - E_A - E_B$).[28] Hence, for the energetically stable systems, such a difference is negative. For the convenience of discussion, the absolute positive values of H-bond energies ($-E_{HB}$) are presented in the text, while E_{HB} values are given in tables and are presented in figures.

There is a variety of typical H-bonds, for example, O−H···O existing for water dimer and formic acid dimer, or charge-assisted $(F\cdots H\cdots F)^-$, as well as nonconventional H-bonds, such as the one for acetylene−water dimer (C−H···O), C−H···π for T-shaped conformation of hydrogen fluoride and acetylene, dihydrogen bonds, etc.

Figure 1 shows three cases of hydrogen-bonded complexes: linear-trans configuration of the water dimer often treated as a reference species in comparative studies on H-bonds,[25,29] the centrosymmetric dimer of formic acid, where two equivalent O−H···O bonding forms exist, and the unconventional F−H···π H-bond for T-shaped configuration of the complex C_2H_2−HF.[30,31] It is worth mentioning that the formic acid dimer represents the pattern often existing within crystal structures of carboxylic acids, especially the derivatives of benzoic acid,[14,32,33] and also that, because of resonance effects, the O−H···O interactions belong to moderate or even strong H-bonds. According to Gilli,[34] the centrosymmetric dimers of carboxylic acids are attributed to intermolecular resonance-assisted hydrogen bonds. This topic will be described in detail in the next sections of our review.

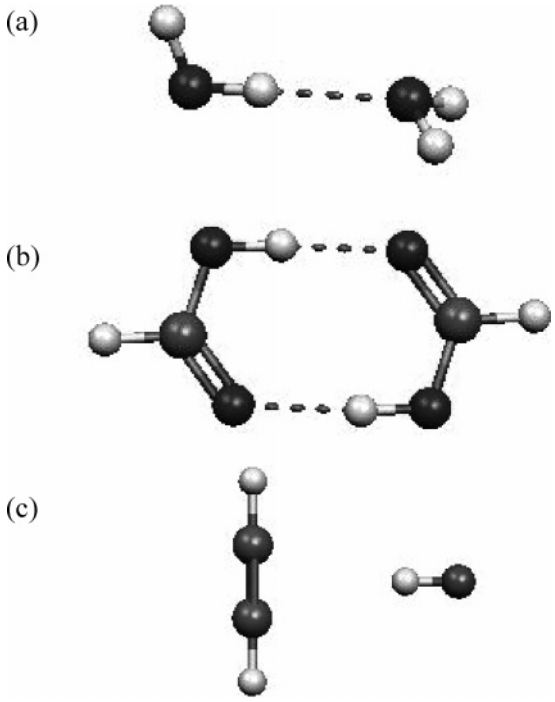

Figure 1. H-bond patterns; (a) linear-trans water dimer, (b) centrosymmetric dimer of formic acid, and (c) T-shaped complex of acetylene and hydrogen fluoride.

The HF and MP2 results of Table 1 show the importance of the electron-correlation energy contribution, which, for example, for $H_2O\cdots HF$ complex, amounts to ca. 10% of the total binding energy, while for the water dimer it may be estimated as approximately 5%.

One can see that there is a tendency to extend the definition of hydrogen bonding,[35,36] but our considerations in this review are in principle limited to conventional H-bonds, close to Pauling's or at most to the IUPAC definition, which can be written in the form

$$R_1 - \overset{\delta-}{A} - \overset{\delta+}{H}\cdots B - R_2 \qquad (1)$$

where A and B are more electronegative atoms than the hydrogen atom. Most often A and B contain $2p_z$-type electrons, and hence, they may be conjugated with R_1 and R_2, if they are π-electron systems. It is worth mentioning that structural consequences of the H-bond interaction are extended beyond the A and B bridge atoms embracing all (or at least part of) the R_1 and R_2 groups.

Two different cases have to be considered (i) with intermolecular H-bond in which R_1 and R_2 may function almost independently and (ii) with intramolecular H-bond, which, owing to charge redistribution caused by the bonding, may exert substantial

Table 2. ΔG and ΔH Values of the Reaction AH = A^- + H^+ in the Gas Phase (in kcal/mol)

AH	ΔG	ΔH
CH_3CH_3	411.7	420.1
CH_2CH_2	401.0	409.4
CHCH	370.0	379.0

structural effects on R_1 and R_2. They may be correlated via the spacer, because R_1 and R_2 are in this case linked by a chemical bond and may be involved in a variety of interactions. Some aspects of these interactions are associated with Gilli's resonance-assisted hydrogen bond (RAHB) model.[37]

In both cases, the geometry patterns in R_1 and R_2 change, and this reflects the changes in π-electron delocalization. Those changes are often discussed in terms of aromaticity indices.[38−41] In the present review, the above-mentioned aspects will be discussed as one of the important subjects of investigation.

It was pointed out[42] that the H-bond could be treated as an acid−base interaction in the Brønsted−Lowry formulation.[43] If the acidity of the proton-donor bond A−H and the basicity of the proton-acceptor B are strong, then a case where a proton transfer from A to B occurs and the creation of another kind of H-bond takes place A−H···B ⇔ A^-···HB^+ with reverse proton-donor−acceptor function of the bridge A and B atoms. In many cases, as will be shown later, there is equilibrium between two protonic states described by a double minimum potential for the proton motion. A can be any atom that can form a polar $A^{\delta-}-H^{\delta+}$ bond, thus, the atom of any element more electronegative than hydrogen. This is nicely illustrated by an increase in bond polarity and Brønsted acidity of the C−H bond in alkane, alkene, and alkine. In this sequence, electronegativity (in the Pauling scale)[23] of the carbon atom increases: 2.48, 2.75, and 3.29 for sp^3, sp^2, and sp hybridized atomic orbitals, respectively.[44] This may be compared with the value for hydrogen electronegativity equal to 2.2.[23] The acidity increases in the same direction as may be described by a decrease of the changes in free energy ΔG and enthalpy ΔH of deprotonation of ethane, ethylene, and acetylene in the gas phase given[45] in Table 2.

This is also illustrated for the complexes of methane, ethylene, and acetylene (Figure 2) connected with water through the C−H···O H-bonds. Their binding energies calculated at the MP2/6-31+G(d,p) level of theory amount to 0.29, 0.86, and 2.51 kcal/mol, respectively.[29,46] Figure 2 presents the latter complex, where the binding energy is the greatest.

B as an acceptor can be any atom with a lone electron pair. The negatively charged hydrogen atom can also play a role in the proton acceptor. In such a case, the so-called dihydrogen bond is formed.[47−50] On

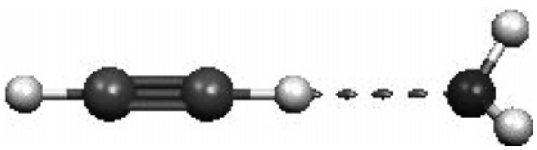

Figure 2. Complex of acetylene with water. The C−H···O H-bond is indicated.

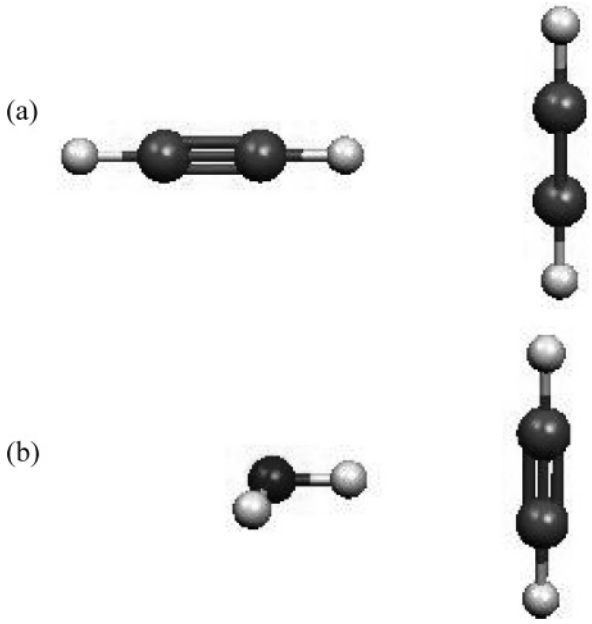

Figure 3. (a) T-shaped configuration of acetylene dimer. (b) π electrons as an acceptor of proton for the complex of water with acetylene.

the other hand, the π-electron systems, such as acetylene, may act as the proton-acceptor centers, forming A−H···π bridges,[51] and even the T-shaped configuration of acetylene dimer is energetically stable because its binding energy calculated at MP2/aug-cc-pVDZ level of theory (BSSE included) amounts to 1.4 kcal/mol.[52] Figure 3 presents the above-mentioned systems.

It shows two examples of complexes where π electrons act as an acceptor of the proton within weak, unconventional C−H···π and O−H···π H-bonds. For the latter complex, the water molecule acts as a donor of the proton. Another configuration is known (see Figure 2) where the acetylene molecule is a proton donor and the water molecule is an acceptor. These two configurations were investigated,[25] and it was pointed out that the C−H···O H-bond, where water acts as an acceptor, is stronger than the O−H···π H-bond, where the water molecule is a proton donor. Other π-electron systems are also known to act as the proton acceptors, such as for example aromatic moieties.[53,54]

Extensive literature is already available relating to the H-bond.[35,36,55−63] Note that since 1977 every 2 years an international conference, Horizons in Hydrogen Bond Research, has been organized, the last of which was held in 2003 in Berlin. The proceedings of those conferences have been published in special issues of *J. Mol. Struct.* (last issue, see ref 64). Recently, several review papers have also been published.[26,27,65−73] Of particular interest seems to be the review devoted to intramolecular H-bonds,[74] strongly related to the subject of the present review.

2. Nature, Variety of Appearance, and Properties Associated with the H-Bond

As it was pointed out in many theoretical studies,[60,65,75,76] in H-bonds, the same forces are manifested as in other molecular interactions. Those forces

are electrostatic in nature. However, one can distinguish a few specific features that make it possible to discriminate H-bond complexes from the universal van der Waals associates and electron-donor−acceptor (EDA), named usually charge-transfer (CT) complexes.

The easiest, most important, and widely applicable is a geometric criterion. When the H-bond is compared with the van der Waals interaction, the equilibrium distance between H and B atoms is dramatically different. In the case of van der Waals interactions, the distance between H and B is close to the sum of van der Waals radii,[77] whereas in the case of H-bond, the H···B distance is much smaller. Thus, for instance, the H···O distance in the most frequently observed O−H···O bridges ranges between 1.6 and 2.2 Å, while from summing the H (∼1.2 Å) and O (1.52 Å) van der Waals radii, one obtains for $R_{H\cdots O}$ ca. 2.7 Å. Thus, a dramatic shortening is observed. This effect is even more remarkable for strong OHO bridges for which the distance between oxygen atoms, $R_{O\cdots O}$, ≈2.4 Å. Note that the sum of van der Waals radii of two oxygen atoms is of 0.6 Å greater than this value and amounts to ∼3 Å! Hence, the H atom (or more precisely, an almost bare proton) is hidden in the electron clouds of both oxygen atoms approached so near!

It is worth mentioning that the van der Waals cutoff works very well for conventional H-bonds, both weak and strong, but it is criticized in many studies because of weak unconventional hydrogen bonds. The hydrogen bond is mostly an electrostatic interaction and acts far beyond the cutoff mentioned above. This is very important for the proton-acceptor distances, which are approximately equal or even greater than the corresponding sum of van der Waals radii. Hence, the use of the geometrical criterion described above may lead to the nonclassification of weak and unconventional C−H···Y interactions as H-bonds.[36]

This simple picture is well-supplemented by a more subtle criteria of the H-bond, which results from the application of the AIM theory[78] or experimental charge-density studies (for recent review, see ref 79). Even if these criteria, because of a high level of theoretical or experimental procedures, may be applied only to a limited number of systems, they give a much deeper insight into the nature of charge distribution in the region of the H-bond. Koch and Popelier[80] used the AIM theory,[78] providing a few necessary criteria to allow the conclusion that hydrogen bonding is present. A more detailed analysis of the application of the Bader theory to study H-bond interactions is performed in the next sections of the present review.

Coming back to purely geometric features, it was already pointed out by Morokuma[81] that such unusual relations for geometrical parameters of the H-bond result from the particular repulsion potential when the A−H bond is polarized and the molecular contact undergoes via the H atom. A simplified demonstrative illustration of the situation is shown in Figure 4, in which a less steep repulsion potential is visualized as compared with the usual van der Waals interaction. For simplification, it was assumed

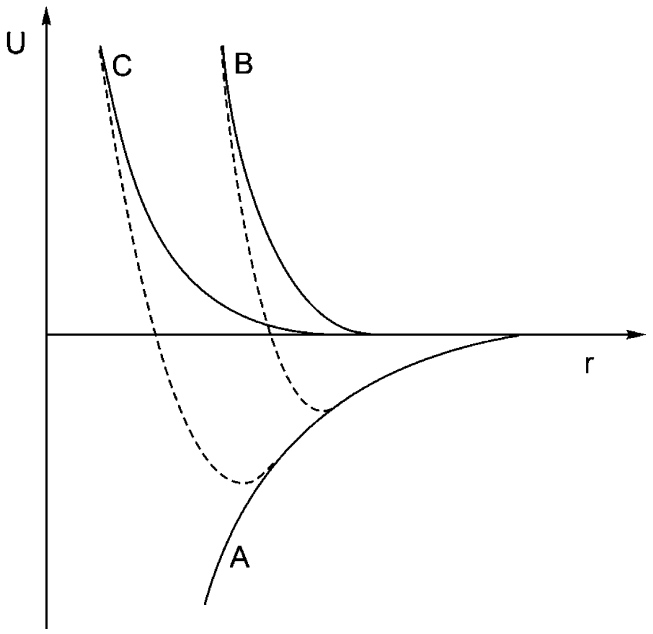

Figure 4. Attraction (A) and repulsion potentials for the van der Waals interaction (B) and H-bond (C).

that the attraction potential is the same in both cases. The unusual repulsion potential seems to be understandable if one takes into account the fact that the hydrogen atom is the only one which, when deprived of the electron, becomes itself a naked nucleus. If the AH bond is polarized, the interaction in the bridge leads to further polarization.

In Figure 4, one can see that the minimum on the total energy curve is shifted to shorter distances and the potential well becomes much deeper. The interaction energy of the typical H-bond is a few times higher than that of the van der Waals interaction.[24] A particular interaction potential of hydrogen bonding can easily be expressed in an analytical form by using the Lennard−Jones potential.[82,83]

$$E(R) = -\frac{A}{r^6} + \frac{B}{r^n} \qquad (2)$$

Although the Lennard−Jones equation has to be treated as semiquantitative, its simple form demonstratively illustrates the "softness" of the repulsion potential in the H-bond interaction.[84]

In the cases of the van der Waals interaction, the exponent $n = 12$. However, in the case of the H-bond, this exponent is much smaller, approximately on the order of 8−10.[85] The mutual approach of interacting atoms to a much smaller distance than the sum of van der Waals radii causes on one hand some increase of the A parameter in eq 2 and, on the other hand, what is more important, a decrease of the n exponent because of further polarization of the A−H bond.

A peculiar interaction potential in H-bonds finds some reflection in high-pressure studies. From the analysis performed by Katrusiak,[86−88] it follows that at medium high pressures the compressibility through the van der Waals contacts is decisive, but it is highly nonlinear. At higher pressures around 2 GPa, this van der Waals compressibility becomes comparable

with that of H-bonds. The fact that the compression at lower pressures undergoes mainly on van der Waals contacts results from various effects such as the molecule deformation, reduction of rotation of some groups, and dynamical disorder of molecules. When the compression reaches a saturation connected with those effects, the repulsion potential becomes steeper than that of the H-bond.

The softness of H-bonds is also manifested in intramolecular steric phenomena and lattice effects. One can consider such effects in terms of the internal pressure. It has been proved that chemically the same or very similar H-bond systems can differ markedly in geometry depending upon the environment.[89] Particularly convincing are data collected for the charge-assisted (NHN) bridges. It seems that we should always take into account some discrepancies when comparing the H-bond lengths in various crystals.

The quantum mechanical calculations enable estimation of the contributions of various effects to the total interaction energy. For example, it was shown early by Jeziorski and van Hemert[90] that, in the case of the water dimer, in which the H-bond is moderately strong, the exchange (repulsive) energy $E_{exch} \approx +5$ kcal/mol and the attractive contributions $E_{electr} \approx -7$ kcal/mol, $E_{pol} = -1.6$ kcal/mol, and $E_{disp} = -1.5$ kcal/mol. The relatively high value of the repulsive term E_{exch} is balanced by large attractive effects at small distances. The authors applied a basis set (11,7,2/6,1) contracted to (4,3,2/2,1) within the exchange perturbation formalism.[91] Similar results were obtained after applying other interaction energy-partitioning schemes; for example, for the most frequently applied Morokuma partitioning scheme,[92] the interaction energy terms calculated for the water dimer at the MP2/6-31+G(d,p) level of theory amount to $E_{exch} = +4.24$ kcal/mol, $E_{electr} = -7.58$ kcal/mol, $E_{pol} = -0.71$ kcal/mol, $E_{CT} = -0.93$ kcal/mol, and $E_{corr} = -0.30$ kcal/mol.[29] The correlation energy E_{corr} was calculated as a difference between the MP2 energy and the one estimated at the Hartree−Fock level of theory. One can see that the electrostatic energy is the most important attractive term, which outweighs the repulsive exchange energy; it is often true for conventional hydrogen bonds that the first-order energy contribution is attractive ($E_{exch} + E_{electr}$) and that the electrostatic term is the most important. This is also in line with the Pauling definition of the H-bond interaction.[23] A slightly different picture is usually obtained for weak H-bonds with π-electrons as proton acceptors. For the T-shaped dimer of acetylene,[52] the following contributions to the interaction energies are calculated within the Morokuma scheme at the MP2/6-311++G(d,p) level: $E_{exch} = +2.1$ kcal/mol, $E_{electr} = -2.2$ kcal/mol, $E_{pol} = -0.3$ kcal/mol, $E_{CT} = -0.5$ kcal/mol, and $E_{corr} = -0.4$ kcal/mol. One can see comparable values of exchange and electrostatic energy terms; similar decomposition was obtained for the benzene−water dimer where π electrons of benzene are the proton acceptor and the water molecule is a proton donor and where the exchange repulsive term is approximately equal to the attractive electrostatic term.[93] Hence, for these cases of unconventional hydrogen bonds, the T-shaped complex of acetylene and benzene···water complex, the electrostatic attractive interaction is compensated by the exchange interaction energy term and the other attractive terms are very important to stabilize the systems. Among these terms, there is the correlation energy. The Hartree−Fock method does not include the electron correlation; MP2 is one of methods where these effects are included. One should mention here the DFT (density functional theory) methods,[94,95] which are often used in studies on H-bonds.[69,96] DFT methods are often applied because they are much less computationally demanding than beyond Hartree−Fock methods. DFT methods work well for H-bond systems in terms of geometries' reproduction, dipole moments, and vibrational properties. DFT energy includes an exchange term and a contribution to the electron correlation energy. It is worth mentioning that none of the most often applied functionals of DFT describes the London dispersion energy, and hence, the corresponding DFT calculations are not suitable for weaker molecular complexes and also for large systems of biological importance.[69]

The very characteristic feature of hydrogen bonds is associated with a possibility of appearance of two potential wells.[97] The shape of the double minimum potential can vary depending upon the chemical nature of interacting components expressed by means of the acid−base parameter ΔpK_a, which is defined in a thermodynamic approach as $pK_a(B^+-H) - pK_a(AH)$ for water solutions. This parameter was introduced for the first time by Huyskens and Zeegers−Huyskens[42] to analyze the proton-transfer phenomena in hydrogen-bonded systems. Interpretation of this parameter is clear: the greater the Brønsted acidity of A−H (lower pK value), the stronger the binding effect with a base B becomes and the greater the Brønsted basicity of the base B is. In other words, the greater the pK value and the smaller the acidity of the Brønsted conjugated acid B−H, the stronger the tendency to create the H-bond is. For $\Delta pK_a = 0$, the proton is statistically located on both centers in equal weight. In media other than water, the ΔpK_a values determined in water should be corrected and the normalized parameter ΔpK_N was proposed $\Delta pK_N = \Delta pK_a - \Delta pK_a$ (crit), where ΔpK_a (crit) refers to the condition where K_{PT} (proton-transfer equilibrium constant) is equal to 1.[98]

The evolution of the potential energy surfaces for the proton motion in AH···B hydrogen bonds is presented in a simplified manner in Figure 5. This presentation does not take into account the two-dimensional shape of the potential and a continuous change of the A···B distance. In the critical region with the centralized proton localization, the bridges are the shortest ones and the mutual coupling between both moieties of the H-bond complex becomes the strongest one. The complete proton transfer leads to state F, which is a mirror image of state A; the H-bond with reverse functions of B and A atoms is formed. The overall energy of the system after proton transfer is accompanied by the Coulomb interaction between the counterions.

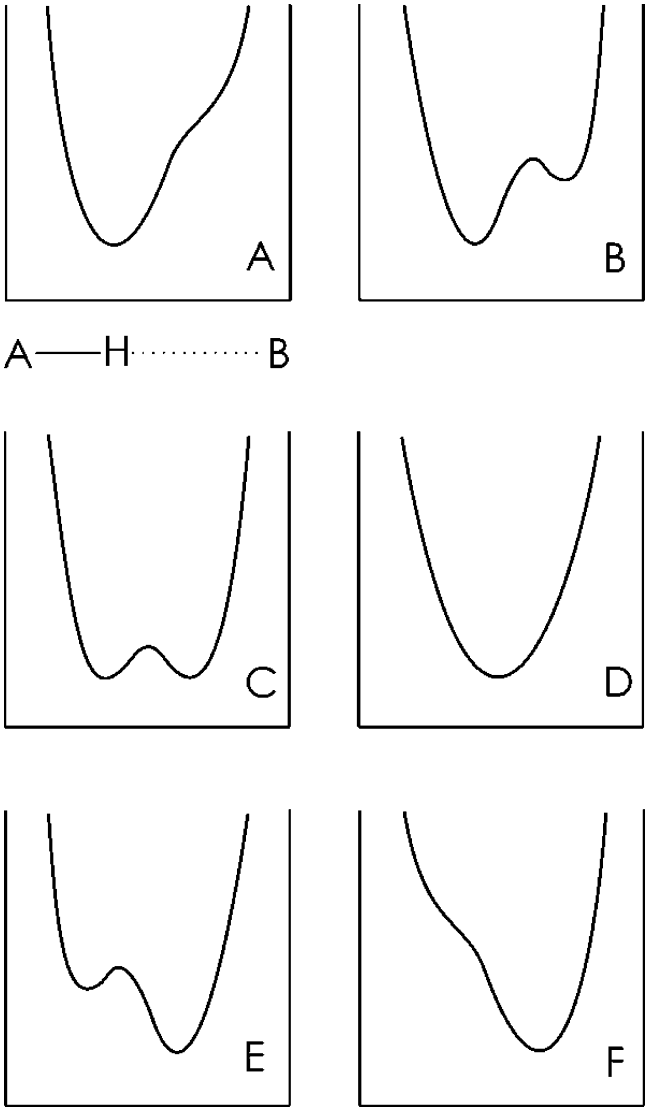

Figure 5. Evolution of the one-dimensional potential for the proton motion with the increasing ΔpK_N, from the usual H-bond (A) through the double minimum (C) or from the single minimum (D) to the H-bond ion pair (F).

A special treatment is needed in cases of symmetrical or nearly symmetrical potential energy curves C and D. In cases of different A and B atoms, we are dealing in fact with a quasisymmetrical situation. True symmetrical bridges are formed in charge-assisted hydrogen bonds or within the molecules of the ketoenol type.

The proton potential in HF_2^- and $H_5O_2^+$ ions was theoretically analyzed by Kollman and Allen,[99] while that in the $H_3NHNH_3^+$ cation was theoretically analyzed by Scheiner.[100] The results of Scheiner's calculations are illustrated in Figure 6. They nicely show how much the barrier can be changed for the proton motion and overall energy depending upon the distance between the A and B bridged atoms. As it was shown, the minimum of the overall energy corresponds to rather long distances and medium high barriers. Simultaneously, these results show how easily the H-bond length can be changed, so that they show how soft the repulsion potential is. Scheiner has shown later[101] that low-barrier hydrogen bonds (LBHB) are not particulary stabilized in

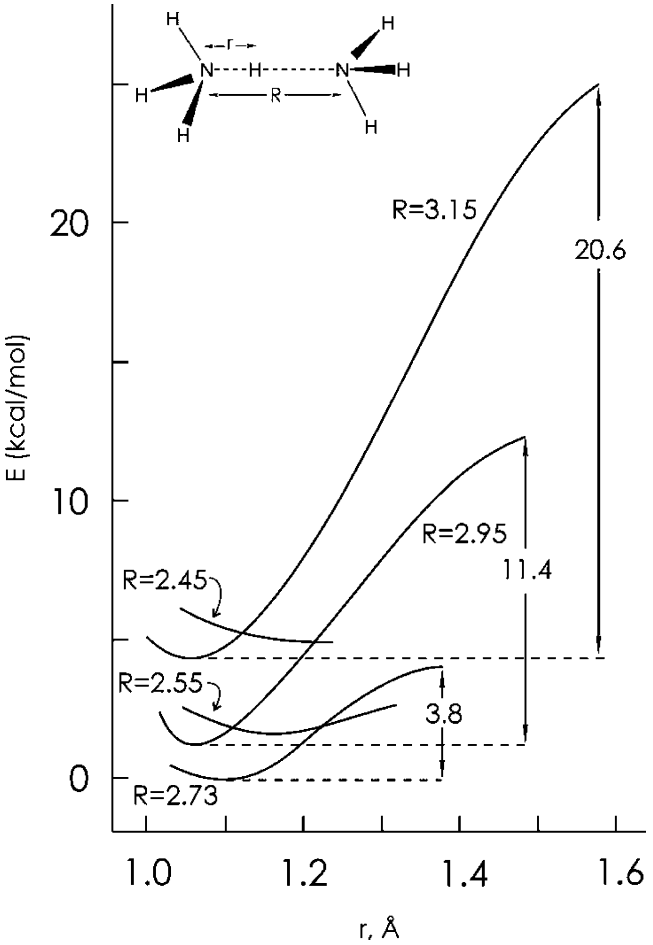

Figure 6. Symmetrical potential for the proton motion in charge-assisted $[H_3NHNH_3]^+$ H-bond for four different N···N distances. Energies are all shown relative to that of the fully optimized structure (R = 2.73 Å, and r = 1.087 Å). Reprinted with permission from (Scheiner, S. *J. Phys. Chem.* **1982**, *86*, 376), copyright 1982, American Chemical Society, Washington, DC.

enzymatic processes as postulated earlier.[6] It seems that the importance of such LBHBs consists of high polarizability and strong coupling of two moieties of homo- or heteroconjugated ions.

Here, we would like to mention the interesting problem of the potential energy shape for the proton movement when the barrier is sufficiently low and the vibration zero-point energy is located close to the barrier top. Such a situation is certainly taking place in protonated naphthalene proton sponges and particularly in 2,7-disubstituted 1,8-bis(*N*,*N*-dimethylamino)naphthalene.[102,103] The short distance between the nitrogen atoms is constrained by the steric conditions. The shortest $R_{N\cdots N}$ values are on the order of 2.54−2.55 Å. The double minimum potential in such cases was evidenced by using various methods including *ab initio* and DFT theoretical methods. Most convincing conclusions come from isotope effects in NMR spectra.[104] Using the IR spectra, it was shown that the isotopic ratio ν_H/ν_D (ISR) exceeds markedly $\sqrt{2}$ and the highest value reported to date equals to 2.08.[103] This means an inverted anharmonicity of the potential resembling a rectangular potential well. The calculations confirmed the distribution of the excited protonic levels expected in

such a case. There are increasing energy differences between those levels for higher quantum numbers.

One should mention here also other interesting aspects of the situation when the depths of two minima are similar and the barrier for proton transfer is low as it was pointed out in the extensive literature[105] and the other studies of this series.[106,107] Because of proton tunneling, such systems are characterized by unusual polarizability that was evidenced by both theoretical and experimental studies.[108−111] One can look for some analogy to the hard/soft acid−base interaction in the Lewis formulation,[112] a concept based on the polarizability of interacting atoms. In cases of H-bond systems, we are dealing with atomic, i.e., vibrational polarizability, which, according to Whiffen,[113] is related to vibrational frequencies and integrated intensities of IR absorption bands. The systems with LBHB are characterized by very high intensities of continuous absorption extended to an extremely low-frequency region.

One should mention here another parameter describing precisely the proton-donor−acceptor properties of interacting components. It is based on experimentally determined proton affinities (PA) in the gas phase. The thermodynamics of H-bond formation in the gas phase and in the solution was analyzed by Zeegers−Huyskens[114,115] based on the ΔPA parameter. In the studies on XH (X = F, Cl, Br, and I) complexes with bases (B) in the low-temperature argon matrices, Pimentel[116] introduced a normalized proton-affinity parameter defined as

$$\Delta PA_n = \frac{PA(B) - PA(X^-)}{PA(B) + PA(X^-)} \quad (3)$$

where PA(B) and PA(X^-) are proton affinities of the base and X^-.

Our considerations in this review are based mainly on the ΔpK_N parameter, which can be applied to various systems in condensed phases. Using such a parameter, it was possible to describe numerous physical properties of hydrogen-bonded complexes in various conditions. As an example, we present in Figure 7 the dependence of the interaction dipole moment $\Delta\vec{\mu}$ (increase of the dipole moment along the bridge) on ΔpK_N for various phenol−amine complexes. Note that the $\Delta\vec{\mu}$ value is a quantity describing the change of charge distribution as a result of H-bond formation and may be assumed as an electron delocalization parameter for the region building up the H-bond.

To obtain a strictly quantitative description, an additional parameter $\xi < 1$ was introduced, so that the general expression of log K_{PT} was formulated in a useful form

$$\log K_{PT} = \xi \Delta pK_N \quad (4)$$

The ξ parameter can be related to softness of the H-bond interaction, i.e., to the barrier height for proton transfer.[98]

Similar correlations were accomplished for other physical properties such as ^{35}Cl nuclear quadruple resonance in the solid state for various chlorine-containing proton donors,[117] ^{15}N nuclear magnetic resonance in complexes of carboxylic acids with pyridines[118,119] expressed in chemical shifts, and coupling constants $J(^1H, ^{15}N)$; the geometry of hydrogen-bonded complexes formed between phenols and amines reflected in the dependence of the C−O bond length on ΔpK_N.[120] In the cases of the ^{1}H NMR chemical shift of the bridge proton[121,122] position of broad protonic bands in IR spectra[123] and the intensity of broad continua,[124] extrema are observed exactly when $\Delta pK_N = 0$.

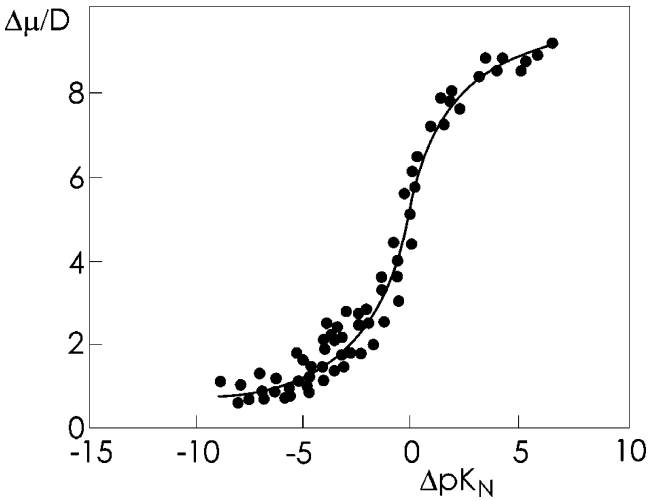

Figure 7. Dependence of the polarity of OH···N H-bond ($\Delta\vec{\mu}$) expressed as a vector of the increase of the dipole moment, on ΔpK_N; lowest values of $\Delta\vec{\mu}$ correspond to nonproton-transfer species governed by the electrostatic inductive effect, while the highest polarity relates to the proton-transfer state. Reprinted with permission from (Huyskens, P.; Sobczyk, L.; Majerz, I. *J. Mol. Struct.* **2002**, *615*, 61), copyright 2004, Elsevier, Amsterdam, The Netherlands.

As an example, we show in Figure 8 the dependence of the intensity of broad (continuous) absorption on ΔpK_N for octylamine-substituted phenol systems. The maximum of intensity corresponds to the critical region where the proton-transfer degree is close to unity.[124]

Another example, which we would like to present and which, as will be seen, is related to the main subject of our review, is the interrelation between ΔpK_N and the geometry of hydrogen-bonded complexes. In Figure 9, the correlation between the C−O bond length in 2,6-dichloro-substituted phenols complexed with N bases and ΔpK_N is presented. One can see a typical sigmoidal plot that can be fitted to the curve analogous to that for $\Delta\vec{\mu}$, i.e., formally to the degree of proton-transfer according to eq 4. The state without proton transfer (HB) corresponds to d(CO) = 1.330 Å, whereas that after proton transfer (PT) = 1.268 Å, with ξ being equal in this case to 0.78.

The conditions when $\Delta pK_N = 0$ can be treated as critical are when the proton occupies either one broad minimum or is equally distributed between the donor and acceptor atoms. One should also note that the critical point is also well-reflected in the plot of ΔH (enthalpy of H-bond formation) versus ΔpK_N.[125]

Some discontinuity in the evolution of charge distribution (expressed in the dipole moment) in

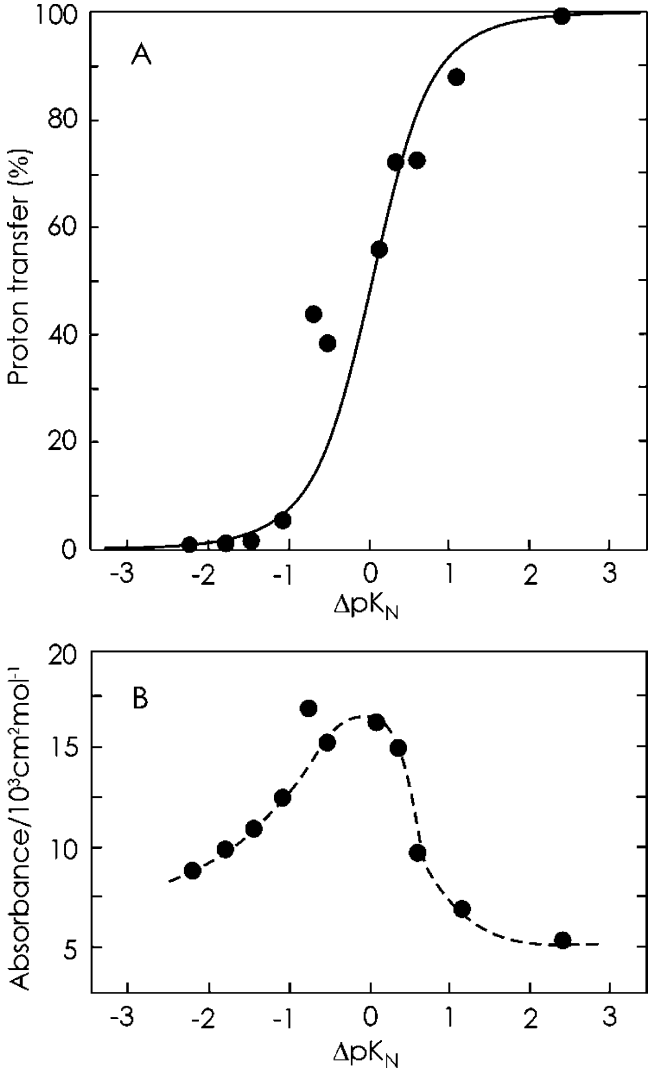

Figure 8. Proton-transfer degree (A) and absorbance of continuous IR absorption (B) plotted against ΔpK_N for trioctylamine-substituted phenols systems. Reprinted with permission from (Albrecht, G.; Zundel, G. *J. Chem. Soc., Faraday Trans. I* **1984**, *80*, 553), copyright 2004, Royal Society of Chemistry, London, U.K.

H-bond complexes, which will be discussed later, as compared with the CT complexes is a consequence of the appearance of the second potential minimum. Huyskens[126] suggested that it is the reason of the exceptional properties of H-bonds. The existence of a double minimum potential for the proton motion prompted the investigators to search for the best expression of such a potential in an analytical form. One should mention here two useful empirical functions. The best seems to be the Lippincott−Schroeder potential[127,128] that was fitted successfully for various types of H-bonds. Of some importance seems to be also the simple potential of Somorjai and Hornig.[129] A very approximate expression estimating the energy of interactions A−H···B (B= O, N, and Cl^-) was given by a simple exponential formula well fitted to the Lippincott−Schroeder potential.[130−132]

At the present time, when it is possible to calculate both adiabatic and nonadiabatic paths of proton transfer with a high level of accuracy, the potential can be approximated by using an *n*-order polynomial, e.g., via fitting of the *ab initio* energy for a varying

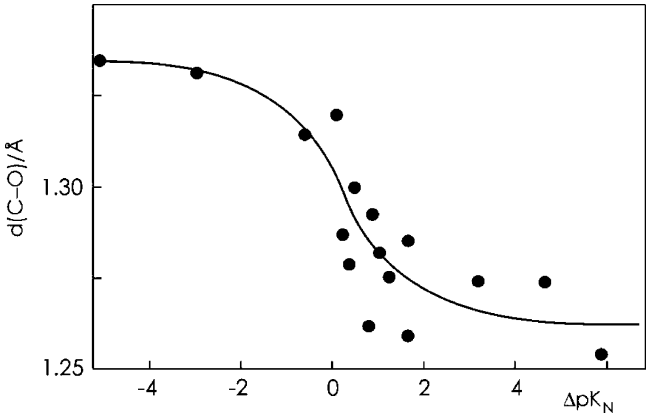

Figure 9. Correlation between the C−O bond length and ΔpK_N for complexes of pentachlorophenol and 2,6-dichloro-4-nitrophenol. Reprinted with permission from (Majerz, I.; Malarski, Z.; Sobczyk, L. *Chem. Phys. Lett.* **1997**, *274*, 361), copyright 2004, Elsevier, Amsterdam, The Netherlands.

position of the proton by using the six-order polynomial.[133]

The specific interaction via H-bond is manifested in several physical properties of systems. The phenomena observed in IR absorption spectra related to stretching ν(AH), δ(AH), and γ(AH) bending vibrations are most characteristic. Undoubtedly, these phenomena are due to the changes in charge distribution, which may be related to electron delocalization. Because both heavy-atom components usually contain electrons described by np orbitals (or similar ones, able to conjugate with π-electron systems), the IR spectroscopy gives some indirect information about π-electron delocalization. The spectacular red shift of the ν(AH) band and an increase of its intensity and width (in many cases accompanied by a substructure) are considered by the majority of specialists as a basis of the operational definition of conventional (proper) H-bonds. The behavior of H-bond systems in the IR spectra is explained by taking into account a decrease of the force constant of ν(AH) vibrations, an increase of anharmonicity of those vibrations, which leads to stronger coupling with low-frequency [mainly bridge σ(A···B) vibrations] modes and the coupling of Fermi resonance type, an increase of the polarizability of the H-bond, particularly when approaching the critical region with a double minimum potential, a remarkable increase of the intensity of IR ν(AH) bands, the possibility of a deviation from the Born−Oppenheimer approximation, and some coupling of the proton and electron motions. The last factor is particularly important when considering the phenomena that are in focus of our interest in this review.

A decrease (sometimes drastic) of the force constant of ν(AH) vibrations and an increase of the force constants of δ(AH) and γ(AH) vibrations seem to be natural if one remembers the polarization of the AH bond and a shift of the proton toward the proton acceptor. Extensive literature is available related to the coupling effects; here, we only refer to the main discussion and review.[134−137] We would also like to mention here that there are attempts to understand the broad IR protonic bands by assuming overdamping of low-frequency modes and a stochastic approach

both for weak and strong hydrogen bonds in condensed media[138−140] or taking into account the unusual polarizability of hydrogen bonds that can govern the relaxation mechanism of librational energy.[109,141] One should remember that we are dealing in this case with vibrational, atomic polarizability.

From the point of view of the problem of the hydrogen-bond effect upon π-electron distribution, which is the main topic of the present review, of special importance seems to be the concept of the coupling of proton and electron motions expressed in Witkowski papers.[142,143] In the approach to the separation of electronic and nuclear motion, Witkowski went beyond approximation of infinitely quick electrons by including into the Hamiltonian the change of the nuclear coordinate as a function of the ratio of the nuclear to electronic velocity. In such a way, the Hamiltonian of a quantum harmonic oscillator may be considered as corrected by a quadratic time-dependent term, the strength of which depends on the velocity ratio. This effect should appear first of all in vibrations of the lightest nucleus, performing large amplitudes and in contact with electrons, which can easily be displaced. It seems that such conditions are present in hydrogen-bonded systems. Naturally, the effect is mass-dependent and should be diminished by substitution of hydrogen by deuterium. This may cause an anomalous intensity isotope effect in the IR spectra. The unusual electrical anharmonicity of proton vibrations in hydrogen-bonded systems could find a physical explanation.[144,145]

The polarization of the AH bond and the shift of the proton toward the B atom finds a spectacular manifestation in ^{1}H magnetic resonance. The value of the chemical shift, exceeding in very strong H-bonds 20 ppm, correlates very well with the strength of interaction and IR spectral characteristics, which are reflected in extensive literature on the subject.[121,122,146,147] Substantial information on charge distribution (as well as proton distribution) is provided by the NMR spectra of the bridge B atoms, e.g. ^{15}N isotope.[118,119] Of particular importance is the value of the $J(^1H^{15}N)$ coupling constant, which informs us about the dynamical proton distribution and thus about the shape of the potential for the proton motion.[148,149] However, most attractive from the point of view of charge distribution in π-electron systems seems to be the information provided by the studies of the isotope H/D effect on ^{13}C chemical shifts in π-electron systems.[150,151] Exchanging H for D causes either a weakening or a strengthening of H-bonds[152] (see anomalous isotope effects in hydrogen bonds, which are reflected in subtle but well-measurable effects in ^{13}C chemical shift). Let us mention here that other isotope effects such as in IR spectra,[153] the geometry of hydrogen bonds,[154] H/D exchange equilibria fractionation factor,[155] or phase transitions[156] are also spectacularly reflected in hydrogen bonds.

Dipole moments are directly connected with the charge distribution in H-bond systems. The detailed studies of dipole moments were carried out for both intra- and intermolecular hydrogen bonds, leading to important conclusions that are summarized in ref 157.

Thus, in agreement with theoretical analysis, the change of the dipole moment expressed as a vector directed along the A···B bridge arises in cases of weak hydrogen bonds almost entirely from the electrostatic (inductive) effects. The results of dipole moment studies appeared to be very convincing for numerous complexes, which showed that the $\Delta\mu$ value for weaker complexes did not depend on proton-donor−acceptor properties of the interacting components.[158]

$$A-H\overset{\Delta\vec{\mu}}{\cdots}B \qquad (5)$$

Only for stronger complexes, one observes a nearly linear dependence of $\Delta\mu$ on ΔpK_a of the interacting components.[159] In a particular region (called critical), a stepwise increase of $\Delta\mu$ is observed, which is ascribed to the appearance of proton-transfer equilibrium with the formation of $A^-\cdots H-B^+$ ion pairs.[98,117] The proton jumping is connected with complete reorganization of charge distribution both in donor and acceptor molecules. This is strongly manifested in aromatic systems, particularly with intramolecular hydrogen bonds, such as those in Schiff bases and related systems. It seems important to note here that in electron-excited states one observes in H-bonds the photoinduced proton transfer. Extensive literature is available on the subject.[19,160]

Also electron absorption spectra, both related to the donor (AH) and acceptor B, are sensitive to hydrogen-bond formation.[161] Thus, the H-bond causes a bathochromic shift of the $\pi \rightarrow \pi^*$ band of a proton donor, frequently with a remarkable increase in intensity because of enhancement of the transition dipole moment. The bathochromic shift of the $\pi \rightarrow \pi^*$ bands can be very large, giving evidence that H-bond causes a substantial change in charge distribution, particularly in the excited state. In the case of the proton-acceptor molecules involved in the H-bond, a hypsochromic shift of the $n \rightarrow \pi^*$ transition (transition of the electron from the lone electron pair to the excited π^* level) is very characteristic. This results in a natural way from the engagement of the lone electron pair in the formation of the H-bond.

The intramolecular H-bonds playing the role of the π-electron-conjugating element deserve special treatment. Such a role was already discussed during the first international meeting on the H-bond in Ljubljana in 1957. Nowadays, it is commonly accepted to call such hydrogen bonds as resonance assisted (RAHBs).[37,162−164] The π-electron conjugation via H-bonds occurs in all systems when both AH and B groups are coupled with a joint π-electron-conjugated system. Chart 1 presents the system with an intramolecular resonance-assisted hydrogen bond and representing enolones. One can see (Chart 1) the O=C−C=C−O(H) π-electron-conjugated bonds; such

Chart 1

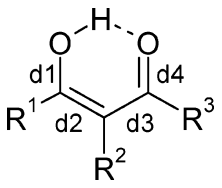

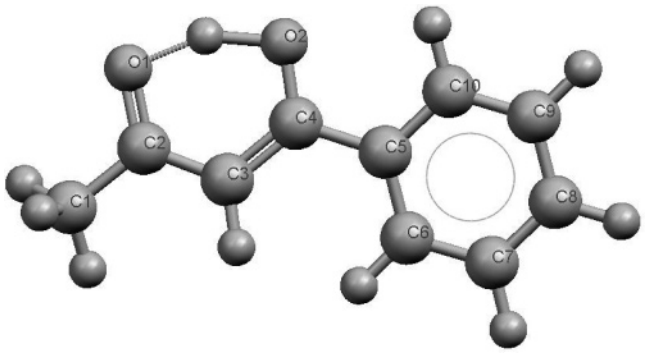

Figure 10. Molecular structure of benzylacetone. The crystal structure was determined by Madsen et al. (ref 165), and the crystal data needed to draw that structure were taken from Cambridge Structural Database. Non-hydrogen atoms are labeled, while hydrogen ones are not.

conjugation is enlarged, owing to the intramolecular O−H···O H-bond formation.

If R_1, R_2, and R_3 are H atoms, then Chart 1 represents malonaldehyde. RAHBs are often described in studies on crystal structures of organic compounds. Gilli et al. classify enaminones, enaminoimines, and enol-imines as intramolecular RAHBs and amide dimers, amide−amidine complexes, as well as DNA H-bond base pairs as intermolecular H-bonds.[162] Figure 10 presents the benzoylacetone molecule taken from the crystal structure.[165] There is the equalization of CC and CO bonds because of the π-electron conjugation within the chelate H-bond ring; the hydrogen atom of the proton-donating OH bond is shifted toward the middle of the O···O distance.

One can observe that the benzylacetone−RAHB system nicely corresponds to Chart 1 because R_1, R_2, and R_3 are methyl, hydrogen, and phenyl substituents, respectively. The characteristic of RAHB is one of the main topics of the present review. Although it is impossible to estimate directly whether the H-bond itself in such cases is stronger or weaker, there are various attempts to evaluate its strength approximately[73,166] and there is no doubt that the whole system with a resonance-assisted hydrogen bond is markedly more stable as compared with the complexes with intermolecular H-bonds. Moreover, it is worth mentioning that intramolecular hydrogen bonds differ substantially from intermolecular ones, irrespective of whether or not they are coupled with the π-electron system.

π-Electron delocalization in the hydrogen-bonded systems, as presented in eq 1, may be considered in three ways: (i) when the delocalization is considered within the H-bond itself, i.e., in the $A^{\delta}-H^{\delta+}\cdots B$ system, (ii) when the more distant structural consequences are taken into account; the changes in π-electron delocalization in R_1 and R_2 of eq 1 are considered, and (iii) when a mutual interaction between these two kinds of delocalizations is considered.

All of these three kinds of relations between the H-bond and π-electron delocalization will be considered in the present review.

3. Methods Applied to Study Electron Delocalization in H-Bond Systems

3.1. IR and NMR Spectroscopies Based on Analysis of Charge Delocalization in H-Bond Systems

It is commonly accepted that the most characteristic appearances of H-bond interactions are visible in the IR spectra. This relates to the stretching ν(AH) vibration frequency and the intensity of IR ν(AH) bands. The deformation in-plane δ(AH) vibrations are less characteristic because they are, as a rule, coupled with vibrations of other atoms. The red shift of ν(AH) vibrations and their IR band intensity are frequently treated as a criterion of formation of conventional H-bonds.

The formation of such bondings weakens the A−H bond and decreases the force constant of vibrations, the coordinate of which is the A−H bond axis. Note that these vibrations are characterized by a large amplitude. The increase of intensity of the IR ν(AH) band is a consequence of the increase of $d\mu/dQ$ (Q, the coordinate of vibrations, which in the case of ν(AH) vibrations is the A−H distance). A "neat" protonic vibration is also γ(AH). Its frequency increases with an increase of interaction strength, but this quantity is rarely used in estimation of the H-bond energy. A sensitive measure of H-bond energy is the NMR ^{1}H chemical shift δ^1H of the bridge proton. The conventional H-bonds lead as a rule to an increase of δ^1H (deshielding), reaching in several cases of critical range the values above 20 ppm.

Approximately linear correlations between the H-bond energy and various physical parameters describing the interaction are fulfilled for concrete types of H-bonds and limited energy ranges. However, even then, some exceptions should be expected. As a good example, the comparison of H-bonds in RNA and DNA manifested in NMR data can be mentioned.[167] These data show that the NMR shielding does not reflect univocally the H-bond stability.

In most cases, linear correlations between the energy of H-bond and $\Delta\nu$(AH), $\Delta\gamma$(AH), δ^1H, as well as integrated intensity (A) of ν(AH) bands were analyzed.[58,68,168−170] It seems interesting to note that a linear correlation between the $\Delta\nu$(AH) and basicity of the proton acceptor expressed in pK_a was reported very early.[171]

One should remember that all such simplified approaches are limited to weak and medium strength H-bonds. Limitations arise from the fact that for stronger H-bonds very broad bands are observed. Moreover, when we approach the critical range of interaction (see the previous section of this review), there are no IR or NMR correlations with the energy at all.

In early studies, in the mid-fifties, peculiar features of H-bonds were observed if the A−H bond and B acceptor were linked to the π-electron systems. Then, this had become a subject of interest for a long time. During the first international conference devoted to H-bonds at Ljubljana in 1957, a few papers dealing with that problem were presented.[172] Already since that time, special names for this type of H-bonds were

proposed, such names as "pseudoaromatic hydrogen-bonded rings" or "conjugate−chelate systems". However, according to researchers dealing with the problem of aromaticity, these kinds of interactions are named more properly as quasiaromatic,[173] because pseudoaromatic are considered nonbenzenoid compounds exhibiting aromatic properties, such as asulene, etc.[174] Therefore, to avoid the double meaning, the terms "quasiaromatic" or better "conjugate−chelate" are preferred in this review. One should remember, however, that all such terms do not define satisfactorly the nature of the phenomenon as pointed out in the new literature.[37,162−164,175] Peculiar behavior of such systems, as it will be shown, is revealed for instance in vibrational spectra, mainly in the region of ν(AH) vibrations, in the charge distribution expressed by dipole moments, and in unusual stability, independent of the fact that all intramolecular H-bonds are thermodynamically more stable than intermolecular ones because of the entropy contribution to the free energy.

2-Nitrophenol and its derivatives occupy an important place among the systems considered. According to the behavior of nitrobenzene as a base, the nitro group belongs to weak proton acceptors, so that the intermolecular hydrogen bonding with participation of this group is very weak. The π-electron coupling presented schematically in Chart 2 leads to

Chart 2

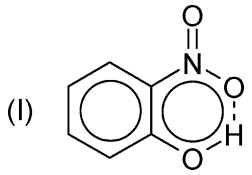

a particular kind of stability. The estimated enthalpy for transition from the closed (cis) to the broken trans conformation of *o*-nitrophenol equals 6.2 kcal/mol.[176] In the IR spectra, as shown by Schreiber,[177] the following features of H-bond in **I** are visible.

If one compares the ν(OH) band of **I** with that of phenol itself or *p*-nitrophenol measured in CCl_4, the frequency is shifted by 350−370 cm^{-1} to lower frequencies, which corresponds to rather strong H-bonds. This shift is markedly smaller for the phenol in nitrobenzene solution, although it is known that intramolecular H-bonds as bent species are characterized by a small frequency shift. As already mentioned, the ν(OH) band shift is taken as a measure of H-bond strength (this is commonly accepted); hence, the peculiar stability of H-bond in **I** is well-reflected. Another even more important feature of H-bonds is a remarkable increase of the intensity of ν(AH) bands. However, in our case of molecule **I**, the integrated intensity of the ν(OH) band is only negligibly higher as compared with that of phenol itself and many times lower as compared with H-bonds in the systems with similar shifts of ν(OH) bands. If we link the integrated band intensity with the dipole moment induced in the lone electron pair and the OH bond polarization, the conclusion should be drawn that this dipole moment is compensated by the dipole moment induced in the conjugate−chelate system. In more quantitative considerations, as it will be shown later, one should take it into account that intramolecular H-bonds are not linear; i.e., the OH group is oriented by ∼130° with respect to the lone electron pair axis.

A direct analysis of molecular dipole moments is burdened with considerable uncertainty arising from the assumption about the additivity of bond and group moments that may not be fulfilled in all cases. However, the comparison performed for the charge distribution in 2-nitro- and 2-chlorophenol (Chart 3)

Chart 3

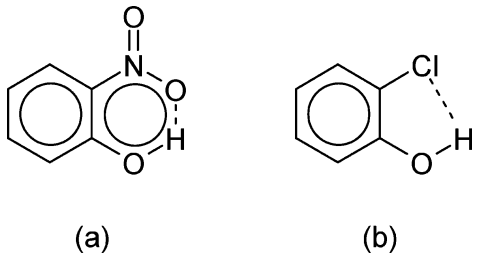

seems to be very interesting.[178] The analysis has shown that the sense of the vector of the induced dipole moment is entirely different in both cases.

In case b, the vector of the interaction dipole moment is directed "normally" along the bridge and results from the usual electrostatic inductive effect, whereas in case a, this moment is directed from the benzene ring toward the quasiaromatic hydrogen-bonded ring, which shows electron-accepting properties as a whole. Such a charge distribution based on the electronic spectra was suggested by Burawoy and Chamberlain.[179]

With respect to the stability of the H-bond in 2-nitrophenol, the analysis of a situation when the additional di-*N*-alkylaminomethyl group is introduced in the ortho position (**II**) seems to be interesting (Chart 4), where a competition between two

Chart 4

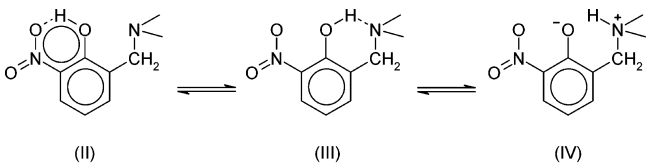

different proton acceptor centers could be expected. In the case of intermolecular hydrogen bonds, the amino group is among the strongest proton acceptors. However, in our case, it appeared that in nonpolar solvents the molecules are exclusively in conformation **II**. Only in strongly polar solvents or in the solid state, the proton transfer takes place and the formation of the tautomeric ion pair (**IV**) is observed. The IR protonic bands of **II** and **IV** forms are located in different regions, and their integrated intensities differ by 1 order of magnitude.[180] Similar results were obtained by Lutskii et al.[181] for di- and trinitro derivatives of phenol studied in solutions with aliphatic and aromatic amines. The general conclusion can be drawn from these results that the intramolecular H-bond to nitro groups is weaker but the whole π-electron system is markedly stabilized. With

Table 3. Physical Properties of Nitrophenols

	mp (°C)[a]	μ (D)[a] (benzene)	solubility (water)	M (dm^3)[a] (benzene)	pK_a[a]
ortho	43−45	3.08 ± 0.05	0.02	4.6	7.21
meta	94−95	3.92 ± 0.02	0.077	0.216	8.39
para	110−114	5.0 ± 0.1	0.084	0.097	7.15

[a] The mp, μ, M, and pK_a values were taken from Merck KGaA, Darmstadt, Germany, 2002 (www.chemdat.de), A. L. McClellan, Tables of Experimental Dipole Moments, Rahara Enterprises, El Cerrito, CA, 1989,T. Dziembowska, Intramolecular Hydrogen Bonds (in Polish), D.Sc. Thesis, Agriculture Academy, Szczecin, Poland, 1990, G. Kortum, W. Vogel, and K. Andrussow, Dissociation constants of organic acids in aqueous solution, Butterworths, London, U.K. 1961, respectively.

respect to these results, the data related to macroscopic properties of nitrophenols collected in Table 3 seem to be interesting.

The data in Table 3 clearly show unusual behavior of *ortho*-nitrophenol as compared with *meta* and *para* derivatives, which can be ascribed to the increase of lipophilicity. Particularly expressive are data related to the solubility in water and benzene. Less expressive are data related to the acidity, but also in this case, a strikingly high value of pK_a as compared with *para*-nitrophenol is visible. One could expect much higher acidity because of the proximity of the strongly affecting highly polar nitro group. The example of *o*-nitrophenol seems to be very important because one observes in this case a dramatic decrease of hydrophilicity and a simultaneous increase of lipophilicity.

Qualitatively similar results were obtained for other chelate H-bonds such as in salicylaldehyde, enolized β-diketones,[182] and peri-hydroxyquinones.[183,184] In peri-hydroxyquinones, the intensity of ν(OH) bands is so low that it can be observed only with very thick layers of solution. Hadži et al. discussed the behavior of other systems with an intramolecular H-bond of this type.[136,182]

Very suggestive results were published by Takasuka and Matsui[168] who compared the behavior of several ortho-substituted phenols and in particular **V** and **VI** (Chart 5).

Chart 5

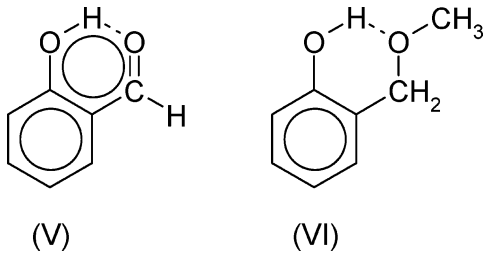

Although the H-bond in **V** is markedly stronger, the intensity of the ν(AH) band is much lower than that of **VI**. Takasuka and Matsui have shown for the first time the difference between conjugate−chelate and nonconjugate intramolecular H-bonds expressed in the relationship between the integrated intensity and the red shift of the ν(OH) bands. Such relationships are shown in Figure 11.

In several papers by Shigorin et al.[185−188] related to numerous examples of intramolecular H-bonds

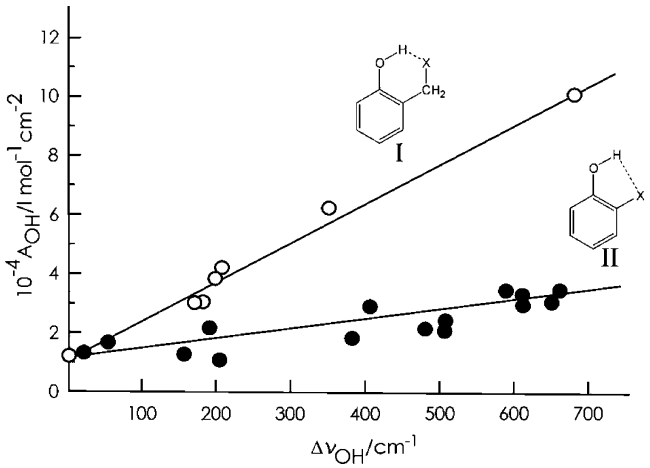

Figure 11. Integrated intensity of the ν_{OH} band plotted versus frequency shift $\Delta\nu_{OH}$ for two types of intramolecular H-bonds: conjugate chelate (II) and isolated (I). Reprinted with permission from (Takasuka, M.; Matsui, Y. *J. Chem. Soc., Perkin Trans. 2* **1979**, 1743), copyright 2004, Royal Society of Chemistry, London, U.K.

with participation of π-electron conjugation, it was shown that the interaction energy can be approximated in agreement with the already cited literature by a simple equation (eq 6)

$$E_{HB} = \frac{1}{K}\frac{\Delta\nu}{\nu} \tag{6}$$

where ν is the frequency of ν(AH) vibrations and K is a constant. For intermolecular H-bonds, another equation (eq 7) was proven, namely

$$-E_{HB} = K'A^{1/2} \tag{7}$$

where A is the integrated intensity of the ν(AH) band and K' is another constant. It was shown that in the case of intramolecular π-electron conjugate H-bonds this relation is not fulfilled.

Brzezinski and Zundel[189] have shown that in the case of certain compounds such as 2-quinuclidinecarboxylic acid *N*-oxide (**VII**) (Chart 6) a continuous

Chart 6

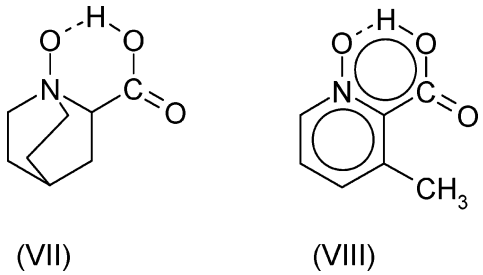

intense IR absorption is observed that can be interpreted in terms of high polarizability of a low-barrier H-bond. In the case of compound **VIII** with a conjugate−chelate H-bond, this continuous absorption either drops in intensity or disappears. Again, we are dealing with a phenomenon of the coupling between proton vibrations and π-electron density distribution.

Of great importance in recognition of unusual behavior of π-electron-conjugated H-bonds can be the

Chart 7

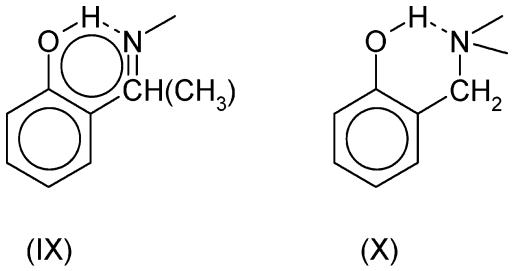

(IX) (X)

comparison of Schiff (**IX**) and Mannich (**X**) bases (Chart 7) that was done in several papers by Koll et al.[190−195]

The π-electron coupling of the imino group in **IX** causes the planarity of the chelate ring in contrast to the Mannich base **X**, where the nitrogen atom is located out of the benzene ring plane, independent of the strength of the H-bond (after proton transfer, too). Even more, the exchange of the hydrogen atom at the bridge carbon atom for the bulky alkyl or aryl group does not disturb the planarity of the chelate ring, while the distance between the H-bridge O and N atoms undergoes a decrease. This is excellent evidence of the softness of the repulsion potential. The shortening of H-bond can reach 0.1 Å. This is reflected in spectroscopic behavior; namely, the IR ν(AH) band is shifted to lower frequencies interpreted by the cited authors as the strengthening of the H-bond.

The most important quantitative results in papers by Koll et al. are related to integrated intensities of ν(AH) bands for four groups of H-bond systems, namely, Mannich bases, Schiff bases, and complexes with intermolecular hydrogen bonds composed of related phenols with *N*,*N*-dimethylbenzylamine and *N*-benzylidenemethylamine. The collected results are illustrated in Figure 12, where the correlations between $\Delta A^{1/2}$ and $(\Delta\nu)^{1/2}$ are presented for four discussed systems. $\Delta\nu_{cg}$ is the shift of the center of gravity of the ν(AH) band, whereas A is the integrated intensity of that band. The interpretation of the results is as follows. The intensity of intramolecular H-bonds is markedly lower as compared with intermolecular ones because of some unfavorable geometry. The polarizability tensor of the lone electron pair of the nitrogen atom is not a sphere. Therefore, in a bent H-bond typical of an intramolecular bridge, the induced dipole moment in the proton acceptor should be lower as compared with a linear intermolecular bridge. However, as can be deduced from data in Figure 12, in addition to the geometrical decrease of intensity, a remarkable decrease of intensity in Schiff bases should be ascribed to the formation of the quasiaromatic H-bond ring.

The impact of the H-bond on charge distribution over the whole interacting systems is well-reflected in NMR spectra of various nuclei and particularly based on H/D isotope effects. In NMR spectra of H-bond systems, one can distinguish a few H/D isotope effects that are suitable in the charge distribution analysis. In the case of the primary H/D isotope effect, a basic is the change in chemical shift, i.e., the $\Delta\delta(^1H,^2H)$ value that informs about changes

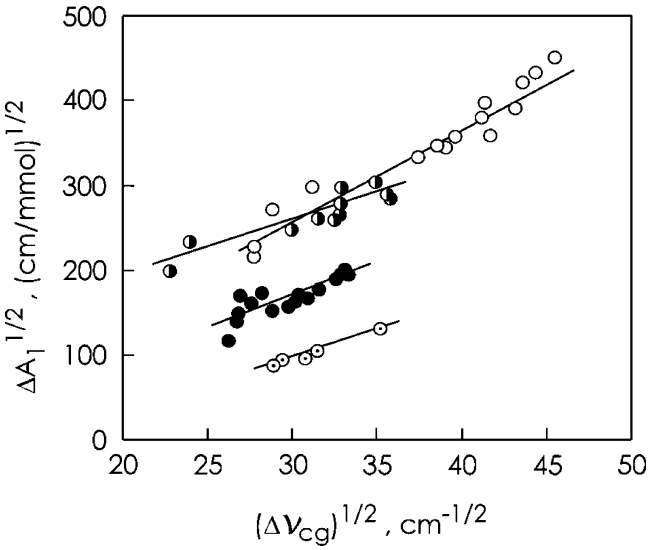

Figure 12. $\Delta A_1^{1/2}$ versus $(\Delta\nu_{cg})^{1/2}$ for (○) complexes of phenols with *N*,*N*-dimethylbenzylamine ($\Delta A_1^{1/2} = 11.04(\Delta\nu_{cg})^{1/2} - 75.36$, $R^2 = 0.9503$, $n = 16$); (◑) complexes of phenols with *N*-benzylidenemethylamine ($\Delta A_1^{1/2} = 6.33(\Delta\nu_{cg})^{1/2} + 60.29$, $R^2 = 0.8487$, $n = 11$); (●) Mannich bases ($\Delta A_1^{1/2} = 8.16(\Delta\nu_{cg})^{1/2} - 77.02$, $R^2 = 0.8903$, $n = 16$; and (⊙) Schiff bases ($\Delta A_1^{1/2} = 6.29(\Delta\nu_{cg})^{1/2} - 92.13$, $R^2 = 0.9622$, $n = 8$). Reprinted with permission from (Filarowski, A.; Koll, A. *Vibr. Spectr.* **1998**, *17*, 123), copyright 2004, Elsevier, Amsterdam, The Netherlands.

in H-bond itself after deuteration. The source of such changes can be either an increase (weak H-bond) or a decrease of the interaction strength (strong H-bond, particularly of LBHB type). In the case of a double minimum potential, a strong isotope effect can appear, named equilibrium isotope effect: deuteration leads to a change in the population of two minima. The analysis of secondary isotope effects consisting of a change of the chemical shift of nuclei participating in the H-bond or located far from the bridge separated by two or more bonds can be very useful. Deuteration can lead to substantial changes in chemical shifts of such nuclei (most frequently analyzed ^{13}C isotopes). If one takes into account the high precision of NMR measurements, they are of primary importance in analysis of the H-bond influence on the charge distribution.

There is extensive literature related to this problem both for inter- and intramolecular H-bonds.[150,196−199] Most of the papers are devoted to intramolecular H-bonds, which is due to the thermodynamic stability of such species and a marked reduction of additional effects connected with the association and conformation equilibria. Numerous papers deal with primary and secondary H/D isotope effects for various nuclei.[200−212] Because the H/D exchange leads to a marked change in the H-bond strength, the isotope effect yields direct information on the H-bond influence on charge distribution.

In the case of strong H-bonds, the proton-transfer equilibrium can appear and one should expect overlapping of the two effects, the intrinsic and equilibrium isotope effects. The latter effect is particularly strong when the contribution of zwitterionic and nonproton-transfer states are comparable. In many cases, one can easily estimate the contribution of the

proton-transfer state based on the correlations between chemical shifts of the interacting atoms or coupling constants. For instance, in the case of O−H···N hydrogen bonds (Chart 8), the $J(^1H, ^{15}N)$

Chart 8

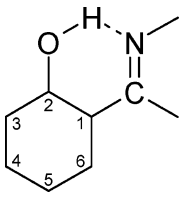

value appeared to be very useful. The overall effect in the Schiff base for the secondary C2 deuterium isotope effect can be approximated in the form[210]

$$^{n}\Delta\text{C-2(XD)}_{obs} = (1 - \chi)^{n}\Delta\text{C-2(XD)}_{intr} + \chi^{n}\Delta\text{C-}\alpha\text{(XD)}_{intr} + \Delta\chi\,(\delta\text{C-2}_{OH} - \delta\text{C-2}_{NH}) \quad (8)$$

where χ is the mole fraction of the proton-transfer state, while $\Delta\chi$ is the change in the mole fraction upon deuteration. The dependence of the observed secondary isotope effect on χ has an S-shaped dependence as shown in Figure 13 for the carbon atom in position 2 in Schiff bases.[210]

This type of correlation has a general character, but for various atoms, the local maxima and minima can interchange. Exactly the same picture is observed for intermolecular H-bonds in complexes of carboxylic acids with pyridine when correlating $^1\Delta^{15}N$ (D) with the proton-transfer degree.[118] To show the intercorrelation between the H-bond and charge delocalization reflected in the secondary ^{13}C H/D isotope effect, it seemed justified to look again into the situation in the Schiff and Mannich bases. The Schiff bases were studied by several authors, whereas data for Mannich bases (incomplete) resulted from only one paper. The main difference between the simplest Schiff and Mannich bases arises from the mesomeric forms presented in Chart 9. In these forms, those present in the phenol molecule itself are omitted.

Thus, in Schiff bases, the keto form occupies a marked place after proton transfer. In the cases of Mannich bases, the mesomeric effect is localized only within the phenol ring and, after proton transfer, the positive charge is localized on the nitrogen atom.

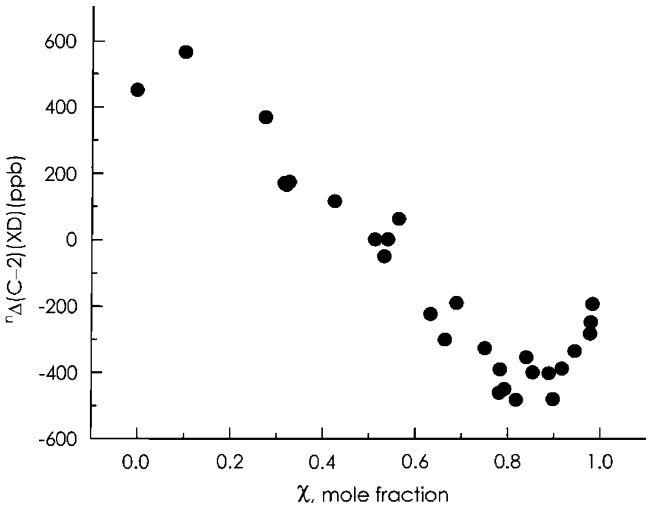

Figure 13. Dependence of the secondary H/D isotope effect for the carbon atom in position 2 in Schiff bases on the mole fraction of the proton transfer state. Reprinted with permission from (Rozwadowski, Z.; Majewski, E.; Dziembowska, T.; Hansen, P. E. *J. Chem. Soc., Perkin Trans. 2* **1999**, 2809), copyright 2004, Royal Society of Chemistry, London, U.K.

Because a strictly quantitative comparison of Mannich and Schiff bases is not possible as a result of different steric conditions and the resulting difference in H-bond energies as well as because of limited data for Mannich bases and some complications arising from association phenomena, only some general conclusions can be drawn.

It seems that analogously to other isotope phenomena, the primary and secondary NMR isotope effects are of vibrational nature. Generally, the H/D isotope effects in H-bond systems, as it was shown,[152] consist of three parts. The first part is connected with the deformation vibrations of the proton-donor group: because the deuteronic vibrations are characterized by smaller amplitude deuteration, this leads to a strengthening of the H-bond. The opposite effect comes from the stretching vibrations because of their marked anharmonicity. The third contribution can appear in the cases of LBHBs connected with tun-

Chart 9

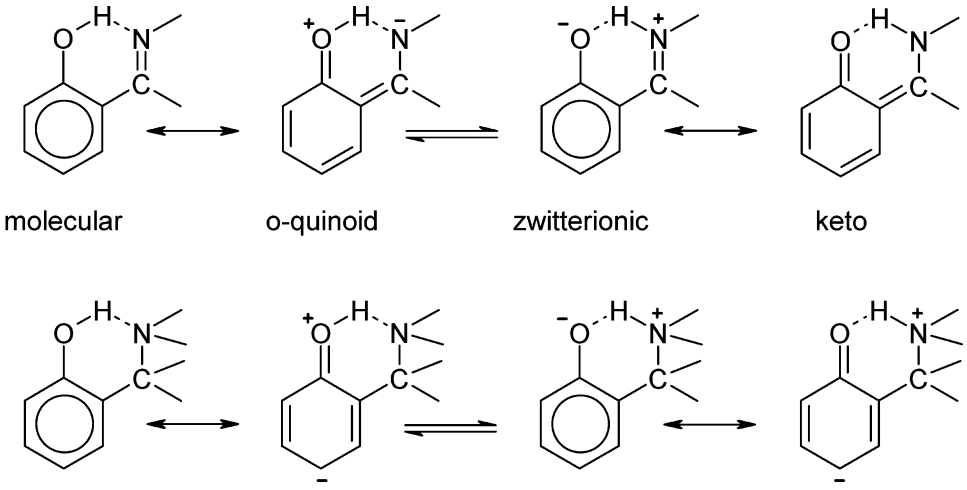

neling: in this case, deuteration leads to a weakening of H-bonds. The vibrational source of isotope effects was analyzed in several papers.[196,213,214] As argued earlier,[215] the isotope substitution should cause the change of charge distribution. In the case of some Mannich bases, a linear correlation was shown[216] between the ^{13}C (H,D) isotope effect and the calculated charge distribution, which is in agreement with the prediction of Karplus and Pople.[217]

When comparing the behavior of Mannich and Schiff bases, the most characteristic is the difference in the value of $^{n}\Delta C\text{-}2(D)$ for the proton-transfer state and more exactly in the depth of the minimum shown in Figure 13. For Mannich bases, the minimum is about 2 times deeper as compared with Schiff bases, and this is best evidence of the role of the keto form in Schiff bases after proton transfer.

3.2. Diffraction Methods in the Study of H-Bond Systems

Crystallography provides very powerful experimental techniques, which may be applied to study hydrogen bonds in crystals. X-ray and neutron diffraction crystal structures' analyses allow us to get an insight not only into the symmetry of crystal lattices but also into geometries of species constituting crystals. Because the symmetry relations are provided by X-ray and neutron diffraction measurements, it is also possible to analyze the intermolecular contacts, among them hydrogen bridges. It is very important that these two diffraction techniques allow us to obtain the full information on geometries of molecules and hence also on H-bonds; it is usually not common for the other experimental tools. However, one should mention important differences between X-ray diffraction and neutron diffraction results. Such differences are analyzed and described in detail in numerous monographs[35,36,218] and review articles.[27,73,219] Hence, they are only briefly mentioned in this review. Strickly speaking, one may mention that for the X-ray measurement there is the diffraction of X-rays on electrons, and hence, one obtains as a result the positions of the maxima of electron densities attributed to positions of atoms. For the neutron diffraction technique, there is the diffraction of neutrons on nuclei, and hence, one obtains directly their positions. Of course that is the simplification of the description of these two important crystallographic techniques, but it allows us to indicate the main results' differences. For X-ray diffraction measurements, for heavy, non-hydrogen atoms, the electron-density maxima are practically at the same positions as corresponding nuclei. However, for the hydrogen atom "possessing one electron", the electron-density maximum is significantly shifted, usually toward the heavy atom connected by a covalent or polar bond with hydrogen. Hence, the effect of the shorter distances between the electron-density maxima than the corresponding distances between nuclei for A−H covalent and polar bonds is very well-known for X-ray measurements. Additionally, one should mention the other effect of the X-ray diffraction technique, that is, the lower accuracy of the determination of the positions of the electron-density maxima for H atoms in comparison with such positions for non-hydrogen atoms. It is connected with the limits of the X-ray technique,[220] that is, different for neutron diffraction measurements, where exactly the distances between nuclei are determined and where the accuracy of the positions of H atoms is of the same order as for the other atoms. The differences between X-ray and neutron diffraction results are sumarized by Jeffrey.[35]

The information on the crystal structures of organic and metallorganic compounds is accessible from the Cambridge Structural Database (CSD).[221] This base contains information on the symmetry of crystals as well as on positions of atoms in crystal structures. Hence, it is a very useful tool to analyze hydrogen bonds in crystals. X-ray and neutron diffraction results are collected there. At present, the base contains over 300 000 crystal structures, mainly X-ray measurements as the number of neutron diffraction structures amounts to about 1200. Hence, if one describes hydrogen bonds for the selected related crystal structures, then the sample of neutron diffraction results may be not sufficient for statistical analyses. Also, there is the necessity to analyze X-ray diffraction data to enlarge the data sample. There are different approaches to correct inaccurate X-ray A−H bonds. In the normalization procedure, the distances obtained in an X-ray analysis are corrected by extending the A−H bond to the average neutron-derived A−H bond length or to the values known from gas-phase spectroscopy experiments.[36] For example, the standard, normalized bonds listed by Desiraju and Steiner[36] amount to 1.083, 1.009, and 0.983 Å for C−H, N−H, and O−H bonds, respectively. Such an approach is justified for weak C−H···O and even N−H···O hydrogen bonds, where the effect of the lengthening of the proton-donating A−H bond is negligible[163,219] but not for stronger O−H···O H-bonds. The lengthening of the proton-donating O−H bonds for species taken from CSD was analyzed in detail.[222] The refined normalization of A−H bonds within A−H···B bridges for strong hydrogen bonds was proposed by Steiner.[223]

It was mentioned above that CSD is a useful tool to analyze hydrogen bonds in crystals. One can mention numerous examples of statistical analyses of such interactions with the use of crystal data taken from CSD. First of all, there is the very important study of Taylor and Kennard,[224] where the CSD was used and further the statistical approaches were applied to prove the existence of C−H···B (B = O, N, and S) hydrogen bonds in crystals. Since that time, the number of studies on so-called weak and unconventional (i.e., with the C−H bond as the proton donor) hydrogen bonds increased rapidly. Before the appearance of the study of Taylor and Kennard, the existence of such hydrogen bonds was the subject of controversy. There are the other studies on H-bonds with the use of CSD or where at least the X-ray or neutron diffraction data are used. One can mention the topics considered by Desiraju and Steiner[36] such as effects of donor acidity and acceptor basicity, statistical studies and distance cutoffs, angular properties of H-bonds, etc. Among them, there are the

studies on correlations between geometrical parameters of hydrogen bonds[35] as for example between O−H bonds and H···O distances within O−H···O H-bonds,[73] the lengthening of the C=O bond because of the complexation if it is the proton acceptor in C−O−H···O=C H-bond systems,[225] the attempt of substantiation that for the weak C−H···O bonds there is the lengthening of the C−H bond as an effect of the complexation, similarly as for the conventional H-bonds,[36] etc.

The charge-density studies, where X-ray and neutron diffraction measurements are applied, were performed for a number of crystal structures, also those containing hydrogen bonds. In such studies, very often, a deformation electron density is calculated that allows us to gain insight into the nature of the H-bond interaction. Recently, the number of studies where the topological Bader theory is applied for experimental electron densities increases rapidly. Such experimental approaches are not analyzed in this review in detail because they were described in the other monographs[35] and studies.[79] However, the results of calculations based on the Bader theory are described in the next and further sections.

3.3. Use of the Bader Theory for Studies on Hydrogen Bonds

There are different tools to detect the H-bond interaction and to estimate its strength;[5,36,73] they have been mentioned in the first section of this review. However, in the past few years, the Bader theory ("Atoms in Molecules" theory, AIM) has become a powerful method to study different kinds of interactions, especially hydrogen bonding.[78] It seems that the characteristics of critical points derived from AIM are particularly useful as such descriptors of interactions. For the critical points (CPs), the gradient of electron density $\rho(r)$ vanishes,[226−228] which may be expressed by eq 9

$$\nabla\rho(r_c) = 0 \tag{9}$$

CPs are classified according to the number of negative eigenvalues of the Hessian of ρ (matrix of partial second derivatives with respect to $\{x, y, z\}$)

$$h_{pq} = \frac{\partial^2}{\partial p \partial q}\rho(r_c) \qquad p, q = x, y, z \tag{10}$$

Stable critical points fall into one of four categories: the maxima in $\rho(r)$ correspond to attractors, which are almost always attributed to nuclei, whereas the minima correspond to cage critical points (CCPs), bond critical points (BCPs), or ring critical points (RCPs).

Another important feature of the electron-density function ρ is that its Laplacian $\nabla^2\rho$ determines where the electronic charge is concentrated and where the electronic charge is locally depleted. For the former, $\nabla^2\rho$ is negative, and for the latter, it is positive. The sign of Laplacian of the electron density at the critical point of the pair of atoms considered is often treated as decisive of the kind of interaction. In principle, the negative value of Laplacian corresponds to the covalent bond-shared interaction, while the positive Laplacian value showing the depletion of the electron density corresponds to the interaction of closed-shell systems: ionic interaction, hydrogen bond, and the van der Waals interaction.[229] Figure 14 shows the electron-density relief map of the Li−H···H−F complex considered previously in detail using *ab initio* methods as well as the AIM theory.[48] One can see that there are considerable differences between the shared H−F interaction on one hand ($\nabla^2\rho_{BCP} < 0$) and the ionic Li−H and H···H interactions ($\nabla^2\rho_{BCP} > 0$) on the other.

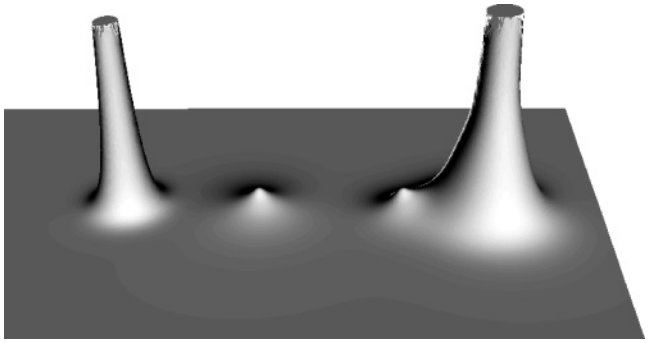

Figure 14. Relief map of the electron density of the Li−H···H−F complex (atoms order is the same as that in the picture).

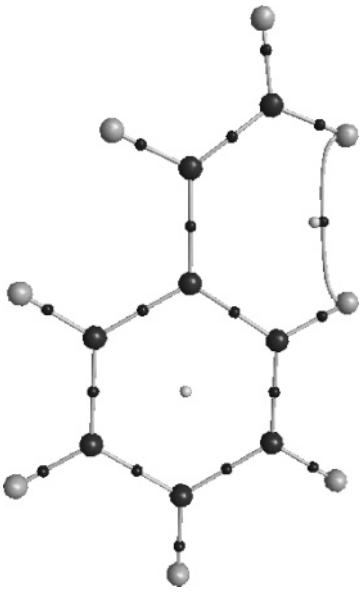

Figure 15. Molecular graph of styrene. Big circles correspond to attractors attributed to nuclei, and small ones correspond to critical points. Reprinted with permission from (Grabowski, S. J.; Pfitzner, A.; Zabel, M.; Dubis, A. T.; Palusiak, M. *J. Phys. Chem. B* **2004**, *108*, 1831), copyright 2004, American Chemical Society, Washington, DC.

Figure 15 presents the molecular graph of styrene,[230] where the attractors attributed to nuclei are designated as big circles and small circles represent the bond and ring critical points. One of the ring critical points is connected with the benzene ring and the second one with the C(aromatic)−C(aromatic)−C=C−H···H−C pseudoring of the typical covalent bonds and the H···H interaction.

Owing to the wide application of the AIM theory to H-bond systems, there has been a substantial

development as far as the formation of various criteria of this kind of interaction is concerned. Koch and Popelier proposed eight criteria based on the AIM theory to detect hydrogen bonds:[80,229] (1) there is a BCP for the H···B (proton···acceptor) contact, which topologically proves the existence of a hydrogen-bonding interaction; (2) the value of electron density at the BCP of H···B ($\rho_{H\cdots B}$) lies within the range of 0.002−0.040 au; (3) the corresponding Laplacian ($\nabla^2\rho_{H\cdots B}$) is in the range from 0.024 to 0.139 au; (4) there is a "mutual penetration" of the hydrogen and acceptor atoms; (5) there is a loss of charge of the hydrogen atom; (6) there is energetic destabilization of the hydrogen atom. This means that the atomic energy of hydrogen decreases in the hydrogen bond because of the complexation (page 152 of ref 229); (7) a decrease of dipolar polarization of the hydrogen atom; and (8) a decrease of the hydrogen atom's volume.

One should mention here that the criteria proposed by Koch and Popelier were intended to discriminate weak and very weak hydrogen bonds from van der Waals interactions. However, they are not applicable for stronger hydrogen bonds where the characteristics of proton···acceptor (H···B) bond critical points are often outside of the limits proposed; i.e., electron density at BCP is greater than 0.139 au and the Laplacian of the electron density at BCP has a negative value as was stated for covalent and polar bonds. This is in line with the electrostatic covalent H-bond model (ECHBM).[163,231] According to this model, one can state the covalent nature for some strong and very strong H-bonds. That statement was supported by accurate X−N electron-density measurements, which showed such covalency along the H···O interaction in negative charge-assisted hydrogen bonds (−)CAHB[232,233] and RAHBs.[165]

Among the criteria given by Koch and Popelier, the first three are most frequently applied in the studies on the hydrogen-bonding interaction. Besides, they are very useful because the geometrical criteria are sometimes not sufficient to decide if the hydrogen bonding exists. For example, the topological criteria were applied to detect C−H···O hydrogen bonds[80] or to characterize dihydrogen bonds.[234] The characteristics of the H···B bond critical point seem to be the most frequently used. For example, it was pointed out for clusters of water with methanol that there is a good linear correlation between the charge density at H···B BCP and the strength of hydrogen bonding.[235,236] It has been detected many times that the electron density at H···B BCP and its Laplacian correlate well with the hydrogen-bond energy;[237−242] the relationships between the H-bond energy and the characteristics of the proton-donating bond are also known for various groups of compounds.[25] Hence, the Bader theory provides additional topological parameters that may be applied to determine the hydrogen-bond strength: electron densities at the BCP of the proton-donating bond and at the BCP of the proton−acceptor contact, as well as the Laplacians of these densities. Roughly speaking, the increase of the H-bond strength is connected with the elongation of the proton-donating bond A−H, the shortening of the proton···acceptor distance, and the change of the corresponding topological parameters.[73] Certainly, the correlations between the geometrical, energetic, and topological parameters are in force only for groups of related compounds. However, one can observe that the topological parameters, such as for example electron densities at BCPs, are less sensitive to the diversity of the species analyzed than the geometrical parameters. For example, the complexes of hydrogen fluoride and hydrogen chloride molecules as the proton-donating moieties with the species containing the N≡C group as the proton acceptor were investigated.[243] For the relationship between the H···N (N atom as the proton acceptor) distance and the H-bond energy, two separated regression lines were obtained, one connected with FH···N≡C−R complexes and the other with ClH···N≡C−R ones. However, while the relationship between the electron density at H···N BCP and the H-bond energy was analyzed, the single regression line was obtained for both subgroups of complexes with the linear correlation coefficient of 0.991.

There are also other properties of the BCP, the electronic energy density H_C of the charge distribution, which may be expressed as[227,228]

$$H_C = G_C + V_C \tag{11}$$

where G_C is a local one-electron kinetic energy density and V_C is the local potential energy density. The relation between the Laplacian and the components of local energy density H_C is given by the equation

$$(\hbar^2/4m)\nabla^2\rho(r_{BCP}) = 2G_C + V_C \tag{12}$$

or in atomic units

$$(1/4)\nabla^2\rho(r_{BCP}) = 2G_C + V_C \tag{13}$$

The sign of Laplacian at a specific point determines whether the negative potential energy or the positive kinetic energy is in excess of the virial ratio amounting to 2. In negative regions of Laplacian, the potential energy dominates, whereas in positive regions, the kinetic energy dominates. It was pointed out that, in bonds with any degree of covalent character, $|V_C|$ is greater than G_C and H_C is less than 0. Bonds in which this condition holds and where $|V_C|$ is less than $2G_C$ have been attributed to being partially covalent, while $H_C > 0$ corresponds to purely closed-shell interactions.[244,245] Rozas et al. have introduced a new classification of hydrogen bonds according to their strength.[238] Weak hydrogen bonds show both $\nabla^2\rho(r_{BCP})$ and H_C values as being positive. For medium H-bonds, $\nabla^2\rho(r_{BCP})$ is greater than 0 and H_C is less than 0. For strong hydrogen bonds, the electron energy density as well as the Laplacian value are negative because these interactions are often classified as covalent or at least partly covalent in nature.[163,244−246]

It is worth mentioning that the features of ring critical points may also be applied to characterize intramolecular H-bonds. The ring critical point (RCP) is a point of the minimum electron density within

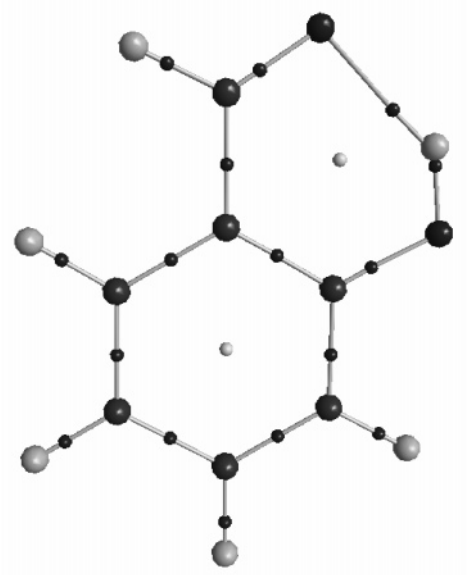

Figure 16. Molecular graph of the *o*-hydroxybenzaldehyde indicates a noncentric position of RCP for a pseudo-ring containing H-bond.

the ring surface and a maximum on the ring. For example, in the case of benzene, the RCP lies in the center of the ring, owing to symmetry constraints. In the absence of symmetry, an RCP can be found anywhere inside the ring.

Figure 16 shows the molecular graph of the *o*-hydroxybenzaldehyde, bond paths, bond critical points and two RCPs: one for the benzene ring and the other for the ring created owing to the intramolecular H-bond formation. This moiety and the other related fluoroderivatives were investigated,[247] and it was found that the characteristics of RCP created because of intramolecular H-bond formation correlate well with the strength of such an interaction. In other words, the features of such an RCP may be treated as new measures of hydrogen-bonding strength. These finding were confirmed for intramolecular H-bonds (IHBs) of enaminones.[248] Because IHBs for enaminones represent the resonance-assisted hydrogen bonds existing partly because of the effect of π-electron delocalization, therefore, their description will be the subject of the next few sections.

Since 1995, numerous applications have been published about the AIM theory to multipole-modeled experimental densities in crystals.[79] The studies on electron density in crystals of 1,8-bis(dimethylamino)-naphthalene[249] and its ionic complexes with different acids[250−252] are one of the examples. For the ionic complex of 1,8-bis(dimethylamino)-naphthalene with 1,2-dichloromaleic acid,[250] the proton in the cation is covalently bonded to one of the nitrogen atoms because the electron density at N−H BCP is high, as for typical covalent bonds, and its Laplacian is negative. In the case of the second H···N interaction, the electron density at the corresponding BCP is lower and its Laplacian is positive, indicating the closed-shell interaction. In the case of the O···H···O hydrogen bond in the 1,2-dichloromaleic acid anion, both Laplacians of the electron density at O···H BCPs are negative, suggesting covalent in nature interactions.

Another early example of the AIM application to the experimental electron density concerns the crystal structure of methylammonium hydrogen succinate monohydrate,[232] where the symmetric O···H···O hydrogen bond exists because the H atom is at the inversion center and the H···O distance amounts to 1.221 Å. The high value of electron density at H···O BCP and the negative Laplacian show the covalent character of this interaction.

It is also possible to evaluate the local energetic electron-density properties at BCP from the electron-density distribution. Abramow has proposed the relation between electron density and the local electronic kinetic energy density at BCP.[253]

$$G_C = 3/10(3\pi^2)^{2/3}\rho^{5/3} + 1/6\nabla^2\rho \qquad (14)$$

In such a way, many of the characteristics of the H-bond may be obtained from experimental electron density. Espinosa et al. have found the exponential relationships between the H···O distance and V_C and G_C topological energetic parameters as well as between the H···O distance and dissociation energy for 83 A−H···O (A = C, N, and O) hydrogen bonds that were observed experimentally by accurate X-ray diffraction measurements.[237] The authors also proposed a relationship between the H-bond energy and the potential electron energy density at H···O BCP because it fits well into the experimental systems considered.

$$E_{HB} = 1/2V_C \qquad (15)$$

For the experimental charge density distributions in ionic complexes of 1,8-bis(dimethylamino)-naphthalene, the characteristics of the variety of interactions such as $[O\cdots H\cdots O]^-$, C−H···O, $[N-H\cdots N]^+$, O−H···O, C−H···N, Cπ···Nπ, Cπ···Cπ, and C−H···Cl were investigated.[251] The authors have found exponential relationships between different properties of BCP and the length of the interaction line. For example, the Morse-type dependence between the length of the interaction line and the Laplacian of the electron density at BCP allowed them to divide the plot into three regions of the H···Y distance (Y designates here the acceptor center if the H-bond systems are taken into account). For this distance, smaller than 1.3 Å, there is the region of covalent bonds with the negative Laplacian value; within the range of the H···Y distance from 1.3 to 2.1 Å, there is the transition region from the covalent to ionic interactions; and if that distance is greater than 2.1 Å, there are closed-shell interactions. A division of this type was proposed by Espinosa et al. on the basis of the H···F distance versus the Laplacian relationship for A−H···F−Y interactions considered theoretically.[254] This is also in line with the experimental X-ray electron-density investigations on the O−H···O systems. Thus, one can see that the Bader theory is also a powerful tool to analyze experimental electron density. The applications of the AIM theory to study π-electron effects will be discussed in the next sections.

4. Electron Delocalization in the Region of the H-Bond

4.1. Intramolecular O–H···O Resonance-Assisted Hydrogen Bonds—Assumptions and Descriptions

There are two aspects of hydrogen-bond cooperativity. The first one concerns molecules with multiple π bonds, and it is usually designated as resonance-assisted hydrogen bond; the second one concerns continuous chains or cycles of the hydrogen-bonded functional groups having both donor and acceptor properties.[35] The latter occurs mainly between hydroxyl groups and was first found in the crystal structures of carbohydrates,[255] although there are experimental and theoretical studies on the other functional groups participating in H-bonds for this kind of cooperativity. For example, hydrogen-bond cooperativity and electron delocalization in hydrogen fluoride clusters were studied,[256] and it was pointed out that the binding energy per hydrogen bond increases with the increase of cluster size; other measures of the H-bond strength also confirm such a tendency because electron density at the monomer-bond critical point decreases with cluster size and the density at the hydrogen-bond critical point increases. The authors of this study[256] also pointed out that the short H-bond interactions in chains of hydrogen bonds in crystals could be explained by an increase of the electric field felt by each molecule because of the polarization of its neighbors. It was also pointed out that cooperativity enhancement occurs in C−H···B weak hydrogen bonds.[36] Among numerous cases of such cooperativity, one can mention the hydrogen-bond chain C≡C−H···O−H···C≡C−H···O−H in the crystal of danazole.[257] One of the recent studies nicely shows the importance of the cooperative effect because both the experimental approach (rotational spectroscopy) as well as *ab initio* calculations were applied to investigate the complexes of H_3N−HF and H_3N−HF−HF in the gas phase.[258] The experimental results show the N···H hydrogen-bond length of 1.693(42) Å for the first complex, whereas for the second one, this distance amounts to 1.488(12) Å, a value that is shorter by 0.205(54) Å.

The aim of this section is to present the first kind of cooperativity existing for the so-called RAHBs. This kind of hydrogen bond is connected with the occurrence of two interrelated effects: π-electron delocalization and that the species analyzed may be treated as mixtures of resonance forms. The influence of these effects on the hydrogen-bonding strength was pointed out early; however, a detailed description of this kind of cooperativity was given by Gilli and co-workers.[37] The first observations related to the concept of RAHB are those of Higgins[259] who found the O−H···O=C chains in carboxylic acids and carboxylate hydrates. Coulson[260] has pointed out that because of the chains of molecules connected through the O−H···O bonds for β-oxalic acid the O···O distance is decreased from 2.8 to 2.5 Å and hence the H-bonds are stronger. It was pointed out that there are strong intramolecular H-bonds for *o*-nitrophenol because of the contribution of the following resonance form (see Chart 10).[261]

Chart 10

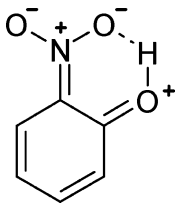

It was also pointed out that for the cyclic dimers of carboxylic acids the double hydrogen bonding is stronger, owing to the effect of resonance, resulting from the existence of two resonance forms.[32,33,262] A case of centrosymmetric dimers of carboxylic acids (Chart 11) was later classified as one of the most

Chart 11

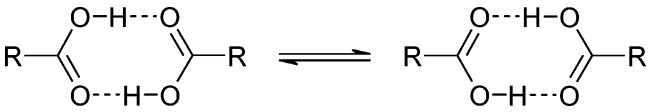

frequently occurring types of the resonance-assisted hydrogen bond.[231]

Emsley has found that for the HOCR=CR−CR=O system the π-electron delocalization is greater if the intramolecular H-bond or the chain of intermolecular H-bonds exists.[263] Gilli and co-workers have investigated in detail the case of intramolecular hydrogen bond, where two oxygen atoms are interconnected through the system of conjugated single and double bonds.[37,162,163,264] Such a situation occurs for malonaldehyde and its derivatives (Chart 1).

The increasing π-electron delocalization is connected with the increased contribution of the ionic resonance form (Chart 12).

Chart 12

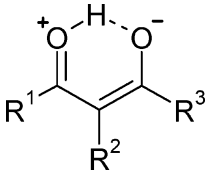

The following characteristics for the O−H···O intramolecular resonance-assisted hydrogen bond were observed and summarized;[37] the increase of π-electron delocalization and hence the changes of geometrical parameters were described. (1) The equalization of C−O and C=O bonds, i.e., the decrease of the $q_1 = d_1 - d_4$ value (see Chart 1), (2) the equalization of C−C and C=C bonds, i.e., the decrease of the $q_2 = d_3 - d_2$ value (Chart 1), (3) the decrease of O···O and H···O distances, in the case of O···O down to about 2.4 Å, and (4) the elongation of the O−H proton-donating bond, for the extreme cases of full delocalization, the shift of the H atom toward the midpoint of the O···O distance.

The correlation between symmetry coordinates q_1 and q_2 mentioned above was observed and the $Q = q_1 + q_2$ parameter, which may be treated as a measure of π-electron delocalization, was introduced.[37] The value of Q is smaller for the greater π-electron delocalization and up to 0 for the full delocalization, resulting in complete equalization of

the corresponding bonds. It was pointed out that the Q parameter interconverts the enol−keto form into the keto−enol one through the totally delocalized form, where Q is equal to 0.

The ground state of the RAHB system may be treated as a linear combination of tautomeric forms **I** (enol−keto) and **II** (keto−enol) (see Chart 13), λ **I**

Chart 13

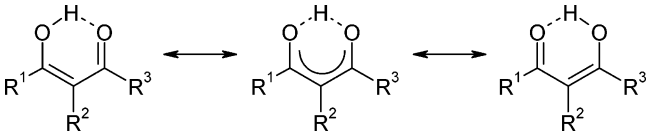

$+ (1 - \lambda)$ **II**, and λ is a coupling parameter, $\lambda = (1 - Q/Q_0)/2$. Q is the parameter described earlier in this section, while the Q_0 corresponds to the standard single and double CO and CC bonds. $d_1 = 1.37$ Å, $d_2 = 1.33$ Å, $d_3 = 1.48$ Å, and $d_4 = 1.20$ Å; thus, $Q_0 = 0.320$ Å. One can see that, for the enol−keto form, the λ parameter is equal to 1, for the keto−enol form, is it equal to 0, and for the fully delocalized structure, it is equal to 0.5. Because it is often unimportant whether one considers the enol−keto form or the keto−enol one (they are indistinguishable for malonaldehyde and when $R_1 = R_3$), it is rather the degree of π-electron delocalization that is important; thus, the λ parameter is often given as $|1 - Q/Q_0|$.[265] In such a case, the full delocalization corresponds to the value of λ of unity and the lack of this effect is connected with λ being equal to 0.

Very recently another parameter, Δ_{rp}, describing π-electron delocalization as an effect of the formation of the intramolecular H-bond, was introduced.[266] To define the Δ_{rp} parameter, the geometry of the so-called "open conformation" is needed, where the intramolecular H-bond does not exist (Chart 14).

Chart 14

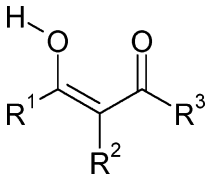

This conformation is often treated as a reference state to estimate the strength of the intramolecular H-bond and may be obtained from the "closed" conformation after the rotation of O−H 180° around the vicinal C−O bond and then the full geometry optimization using *ab initio* or DFT methods. Hence, the roughly estimated H-bond energy is the difference between the energies of the closed and open conformations.[267,268] Coming back to the Δ_{rp} parameter, if we consider the differences between the corresponding C−O, C=O and C−C, C=C bonds for the open conformation, we can write

$$\Delta d_1' = d_3' - d_2'$$
$$\Delta d_2' = d_1' - d_4' \qquad (16)$$

d values of eq 16 correspond to those presented in Chart 1 but for the open conformation.

The same equations may be written for the closed conformation

$$\Delta d_1 = d_3 - d_2$$
$$\Delta d_2 = d_1 - d_4 \qquad (17)$$

The resonance parameter describing the changes connected with the transformation of the open conformation into the closed one was defined.[266]

$$\Delta_{rp} = 1/2[\,(\Delta d_1' - \Delta d_1)/\Delta d_1' + (\Delta d_2' - \Delta d_2)/\Delta d_2'] \qquad (18)$$

One can point out the main differences between the λ parameter and Δ_{rp} one. The latter refers to the changes between two conformations: closed and open, whereas the former considers the differences between the reference system with single and double CC and CO bonds not perturbed by any kind of delocalization (hence, the Q_0 value within the definition of the λ parameter) and the analyzed system with the intramolecular H-bond. It is worth mentioning that for the open conformation there is also π-electron delocalization but not as strong as for the closed system, where the H-bond formation makes this effect stronger.[266] Δ_{rp} is equal to 0 if there is no difference between the closed and open conformation, in other words, if the formation of the intramolecular H-bond does not cause any further π-electron delocalization and it is equal to unity if there is full equalization of C=O, C−O and C−C, C=C bonds. One can see that the physical meaning of the Δ_{rp} parameter is similar to that of λ. It has been shown very recently[269] that both parameters, λ and Δ_{rp}, correlate mutually for different groups of RAHB systems. It should be mentioned here that the Δ_{rp} parameter correlates well with the other measures describing the H-bond strength.[266] For example, it was pointed out that for the simple chloro and fluoro derivatives of malonaldehyde for which full geometry optimizations were performed at the MP2/6-311++G(d,p) level Δ_{rp} correlates with electron density at the H···O bond critical point; the linear correlation coefficient for this relationship is equal to 0.997.

It seems that if there is the effective mixing of two enol−keto and keto−enol forms, then there is also greater π-electron delocalization.[231] Hence, according to the valence bond theory, the RAHB system may be described by the wave function being a linear combination of wave functions of two forms: $\Psi = c_1\Psi_1 + c_2\Psi_2$. Referring to the coupling parameter described earlier, this may also be expressed as follows: $\Psi = \lambda\Psi_1 + (1 - \lambda)\Psi_2$.[37]

It was pointed out that for intramolecular RAHBs, such as malonaldehyde and its derivatives, or for the other similar systems different effects might make H-bonds stronger. Owing to such effects, there is a more efficient mixing of two resonant forms and hence the π-electron delocalization becomes greater.

R_1 and R_3 substituents (Chart 1) influence on the π-electron delocalization within the RAHB system and hence on the O−H···O hydrogen bonding.[162] The similar influence is observed if the oxygen-accepting

center (O=) is additionally involved in the intermolecular H-bond.[162] The influence of R substituents on the H-bond strength has been investigated for malonaldehyde and its simple derivatives at the MP2/6-311++G(d,p) level of theory.[268]

4.2. Geometrical and Energetic Consequences of the Existence of RAHBs

The correlations between geometrical parameters of RAHBs were found in crystal structures of organic compounds, such as for example the relationship between the O−H bond length and H···O distance. This correlation is very well-known for different samples of O−H···O bonds, not only those concerning RAHB systems.[35,73,225]

The other relationships between H-bond energy, geometrical, and topological parameters derived from the Bader theory have been found for derivatives of malonaldehyde mentioned in the previous section as an example. The factor analysis was applied for this sample, and it was pointed out that, for such parameters as the elongation of the O−H bond, the H···O distance, H-bond energy, electron densities at the O−H and H···O bond critical points, and their Laplacians, the main factor covers over 91% of the total variance.[25] This means that, similarly as for typical O−H···O intermolecular H-bonds, for intramolecular RAHBs, the interrelations between different parameters describing the H-bond strength exist. It seems that the hydrogen-bonded systems where proton transfer is detected may be classified as RAHBs because in such a case there should be an effective mixing of resonance forms. Such a situation exists for example for C=O···H−O−C systems, where the following proton-transfer process may be observed:

$$\underset{\text{form A}}{\text{C=O···H−O−C}} \Leftrightarrow \underset{\text{form B}}{\text{C−O−H···O=C}} \qquad (19)$$

One may expect that the analyzed system is an effective mixture of forms A and B. It is worth mentioning that the proton-transfer process for malonaldehyde and its derivatives may also be described by the reaction mentioned above. The reaction path for this kind of proton transfer was investigated with the use of high-precision neutron diffraction data.[270]

It was stated that correlations between structural parameters of molecules are reminiscent of structural changes occurring during chemical reactions. This concept named the "principle of structural correlation" was introduced by Bürgi and Dunitz[218,271,272] and may be applied to many different reactions, among them to the proton-transfer process. The idea of Bürgi and Dunitz may be summarized for practical use in the following way. If someone is interested in the changes of a selected molecular fragment or more generally a geometrical fragment of the more complex system, then it is possible to find such a fragment within the greater set of crystal structures and to analyze its changes. In particular, the changes during the proton-transfer reaction of the C=O···H−O−C geometrical fragment were analyzed.[270] Therefore, the neutron diffraction (ND) data of high accuracy was taken from CSD (e.s.'s ≤ 0.005 Å, and $R \leq 8\%$)

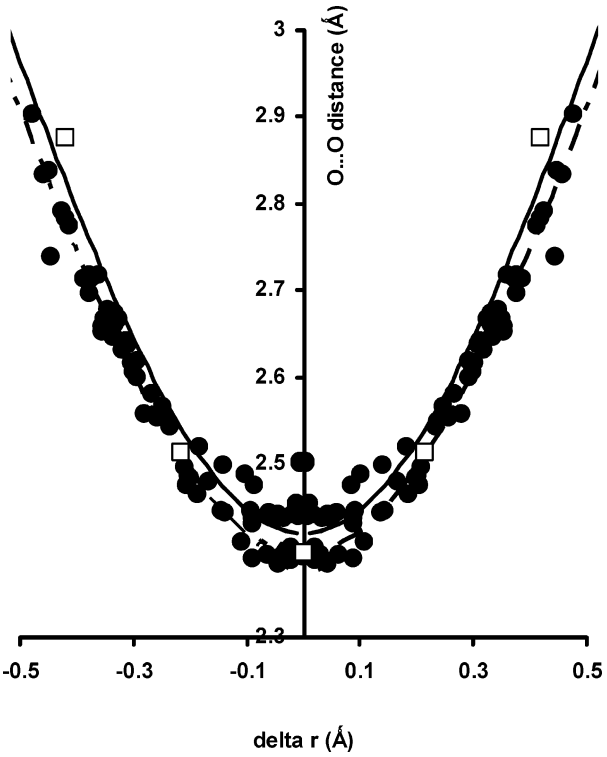

Figure 17. Reaction path for the proton-transfer reaction, with the variables corresponding to coordinate axes in Å and □ representing the *ab initio* results for formic acid dimer. The solid line corresponds to the BV model as well as the broken line; however, for the latter, the constants proposed by Gilli et al. were applied (see the text).

to view different stages of the reaction process. It was very important to use the ND results but not the X-ray measurements because it is well-known that X-rays are scattered at the electron shells and the positions of H atoms are not well-determined.[273] Neutrons are scattered at the atomic nuclei, and hence, the positions of H atoms are of similar accuracies as the other atoms. This was explained in the previous section. Figure 17 shows the dependence between the positions of protons measured from the middle part of the O···O distance and the O···O distance; they are denoted by full circles. The solid line that was obtained from the bond number conservation rule (BNC)[218,274,275] is in good agreement with the ND results, particularly for shorter O···O distances. The broken line was also obtained from the BNC rule. However, the other constants proposed by Gilli et al. were applied in this case.[163] Figure 17 was obtained in the same way as it was earlier done[270] for the accurate neutron diffraction data taken from CSD; however, in this case (Figure 17), the recent CSD release (CSD, November 2004 release) was applied.

The BNC rule is based on the concept of the bond number n originally introduced by Pauling for metal crystal structures,[276]

$$r_n - r_1 = \Delta r = -c \log n \qquad (20)$$

where r_n is the considered interatomic distance for which the bond number is equal to n, c is the constant, and r_1 is the reference distance for which the bond number is usually equal to unity. The bond

number may be understood as the number of electron pairs attributed to the considered pair of atoms, and it usually correlates with the strength of the interaction. On the other hand, n may also be understood as a numerical measure of the electron delocalization observed in the given bond. The bond number idea and particularly BNC rule were often applied in many chemical problems such as for example the analysis of chemical reactions, the construction of reaction paths, and the correlation analysis for geometrical parameters of the systems considered.[222,271,272,277−280] Figure 17 presents one of the applications of the bond number idea, particularly BNC, and concerns the proton-transfer reaction. The bond number concept and BNC rule are also useful for studies of intra- and intermolecular interactions,[281] and they are frequently used to study hydrogen-bond interactions. For example, for the O−H bond undisturbed by any kind of intermolecular interactions, the bond number is equal to unity. When the O−H bond interacts with the oxygen atom being the proton-acceptor center within the O−H···O H-bond, then it is elongated and the n value decreases according to eq 20. However, the decrease of n is compensated by the H···O contact. The sum of bond numbers of O−H and H···O should be equal to unity. It is known as the bond number conservation rule mentioned above.[218]

A similar and more general idea of bond valence was developed by Brown[282−284] within the consistent and simple model known as the bond valence (BV) model. According to the BV model, the BNC rule is only the particular case of the more general valence sum rule. The BV model was also frequently applied in physical and chemical problems as well as described in reviews and monographs.[219,223,285]

The solid line of Figure 17 was obtained in accordance with the constants of Dunitz,[218] the length of the single O−H bond $r_0 = 0.957$ Å and $r_{1/2} = 1.22$ Å, the length of the partial OH bond for which the bond number is equal to 0.5. Figure 17 also presents the broken line corresponding to the constants proposed by Gilli and co-workers: $r_0 = 0.925$ Å, and $r_{1/2} = 1.22$ Å.[163] Gilli and co-workers claimed that such an attitude is in better agreement with the character of interactions within the O−H···O systems because the electrostatic part of the interaction is greater for greater O···O distances and the use of such constants takes this into account.

Figure 17 may be generally understood in the following way. The contour of the experimental neutron diffraction results represents possible geometries of C−O−H···O=C bonds during the proton-transfer process. It was pointed out[270] that this contour is in line with high-level *ab initio* results on formic acid dimer.[286] In Figure 17, □ represent the pretunneling, post-tunneling, and energetic stable configurations of the formic acid dimer (FAD). The same or similar configurations during the proton-transfer exist for the other carboxylic acids. For example, the benzoic acid dimer in the solid state was investigated extensively.[287]

It was demonstrated[270] that the proton-transfer reaction path presented in Figure 17 also shows approximately the potential barrier height for this process. The greater the differences between configurations for which the proton-transfer reaction occurs, the greater is the way within the contour of Figure 17 and the greater is the barrier height. Hence, the distribution of theoretical points representing the formic acid dimer configurations (Figure 17) confirms the high barrier of 8.9 kcal/mol as it was calculated by Kim.[270] Figure 17 also shows the area of the so-called LBHBs for which the O···O distance is usually less than 2.5 Å and the potential energy barriers are of about ∼1 kcal/mol or even less.[288−291] The species corresponding to single well hydrogen bonds may also be indicated in Figure 15. For O···O distances shorter than about 2.5 Å, one can see the concentration of points representing neutron diffraction results (●); there are systems described above in this region. The similar approaches to analyze reaction paths for the proton-transfer reactions of N−H···O, O−H···N, and N−H···N H-bond systems were used by Limbach and co-workers; the BNC rule was also applied in these studies.[107,118]

There are also examples of low-barrier and very strong O−H···O hydrogen bonds investigated with the use of the AIM theory to multipole-modeled experimental densities in crystals (see the previous section). In the crystal structure of methylammonium hydrogen maleate,[233] the asymmetric unit contains a methylammonium ion and two hydrogen maleate ions. The latter contains O···H···O H-bonds, because both H atoms are at the mirror planes and oxygen atoms of H bridges are symmetry-related. The O···H contacts for both maleate ions have the covalent character because the electron densities at H···O BCPs are equal to 0.167 and 0.162 au, while the corresponding Laplacians are equal to −0.245 and −0.295 au, respectively. The study on the crystal structure of benzoylacetone,[165] mentioned briefly in the previous section, provides excellent justification of the RAHB model. One can observe for this structure considerable equalization of the corresponding CC and CO bonds, and what is most important, one can analyze the topological parameters of the O···H···O H-bond. The system is almost symmetric with the O···H distances of 1.25(1) and 1.33(1) Å, and the electron densities for the corresponding BCPs amount to 0.132 and 0.113 au, respectively, whereas the Laplacians are equal to −0.378 and −0.187 au, indicating the covalent character of both contacts.

The same type of the reaction path as for C−O−H···O=C bonds, obtained from ND results taken from the Cambridge Structural Data,[292] was investigated for the deuterated C−O−D···O=C systems.[293] It was found that the differences between the O−H···O geometries and the O−D···O ones are in agreement with the geometrical changes known as the Ubbelhode effect.[294,295] It was also pointed out that the geometrical parameters for the O−H···O H-bonds as well as for the O−D···O ones correspond to the relationships obtained from the bond number conservation rule.[293] Figure 18 presents the relationship investigated previously[293] and based on the results taken from CSD. However, in this review, the last release of CSD was used (November 2004 release of

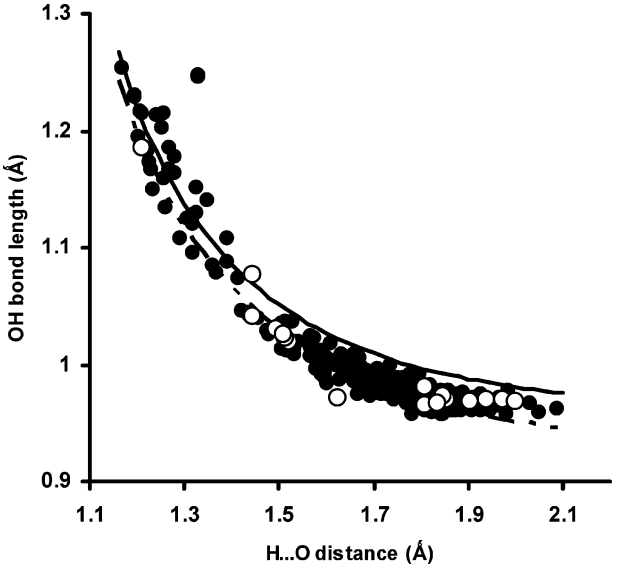

Figure 18. Relationship between H(D)···O distance and O−H (O−D) bond length (both variables in Å) for O−H···O (O−D···O) systems taken from neutron diffraction results. The solid line corresponds to the BV model as well as the broken line; however, for the latter, the constants proposed by Gilli et al. were applied (see the text).

CSD). The solid line of Figure 18 corresponds to the relationship obtained from the BNC rule; the empty points correspond to the O−D···O systems, and the full ones correspond to the O−H···O systems. It is worth mentioning that the relationship between the H···O distance and the O−H bond length is well-known and has been frequently cited in the literature since it was found.[35,59]

4.3. Very Strong O–H···O Bonds and the Electrostatic Covalent H-Bond Model

RAHBs described in previous sections may often be classified as strong or very strong hydrogen bonds. This is rather true for homonuclear O−H···O systems. The strong hydrogen bonds are also often related to LBHBs[296,297] or to single well hydrogen bonds, where the hydrogen atom is located in the middle of the O···O distance or nearly so. These systems are often important in many chemical and biochemical processes as the other weaker H-bonds. For example, the attempts to explain the catalytic activity of enzymes owing to the existence of LBHBs are known.[296,298−300] However, there are also opposite opinions about the nonexistence of specially stabilized and strong H-bonds in enzymes.[101,301] This problem was discussed in detail by Perrin and Nielson,[7] and the authors conclude that "the LBHB is probably not the key feature for enzymatic acceleration, which instead is probably the sum of many different contributions, including hydrogen bonds, electrostatic and hydrophobic interactions, and the proper positioning of substrates on the enzyme".

The situation of the existence of one potential minimum occurs for the $[H-O\cdots H\cdots O-H]^-$ ion in the crystal structure of the mixed salt $Na_2[Et_3MeN][Cr(PhC(S)=N(O)_3] \times {}^1/_2NaH_3O_2 \times 18H_2O$, where the O···O distance amounts to 2.29(2) Å.[302,303] This salt contains sodium and triethylmethylammonium cations and tris(thiohydroximato)chromate(III) and hydroxide anions. These are the X-ray crystal structure results. However, there is no doubt as to the central position of the proton exactly in the middle of the O···O distance because it lies in the special position (the center of inversion). There are also other examples of symmetrical $[O\cdots H\cdots O]^-$ hydrogen bonds in crystals from neutron diffraction studies, such as imidazolium hydrogen maleate,[304] potassium hydrogen maleate,[305] potassium hydrogen chloromaleate,[306] and lithium hydrogen phthalate methanolate[307] In all of these cases, the proton is not lying in the special position; however, the difference between the O−H and H···O bond lengths is less than 3σ; all H···O and O−H distances are in the range of 1.195−1.206 Å. There are also neutron diffraction examples of symmetrical or nearly so $[O\cdots H\cdots O]^+$ hydrogen bonds. For the crystal structure of phenylsulfonic acid tetrahydrate,[308] the H···O distances amount to 1.128 and 1.301 Å, and in the crystal structure of the diaquohydronium ion in yttrium oxalate trihydrate,[309] the proton lies in the special position and both H···O distances are equal to 1.221 Å.

The explanation of the nature of strong and especially LBHBs seems to be important here because RAHBs for which there is the effective mixing of resonance forms as a result of π-electron delocalization often become also very strong H-bonds with low-energy-barrier height for the proton-transfer reaction. The covalent nature of very strong H-bonds and hence LBHBs was suggested many times in some of the investigations.[99,310−314]

A more general explanation of the resonance-assisted hydrogen bonds was given by Gilli and coworkers within their so-called electrostatic covalent H-bond model (ECHBM),[163,231] where the following statements were pointed out: weak hydrogen bonds are electrostatic in nature, and their covalent nature increases with the increase of their strength; very strong H-bonds are three-center-four-electron covalent bonds; and the strongest H-bonds are homonuclear and symmetrical because only for such a case the corresponding VB resonance forms are isoenergetic and their effective mixing is possible. The last statement may be expressed in terms of the condition of the minimum difference between proton affinities (ΔPA) of the proton-donor and proton-acceptor atoms or of the minimum difference between pK values. There are three ways to have the O−H···O hydrogen bond very strong by making the proton-acceptor and proton-donor atoms of identical or similar proton affinity. It is the addition of an electron, its removal, or the connection of oxygen atoms by the system of π-conjugated atoms. In such a way, we have the following types of very strong hydrogen bonds: (i) negative-charge-assisted H-bonds, (−)CAHB; (ii) positive-charge-assisted ones, (+)CAHB; and (iii) the resonance-assisted hydrogen bonds, RAHBs.

The last mentioned H-bonds, which are the subject of our special attention, in the case of O−H···O bonds, may be designated as $O{=}R_n{-}OH$. R_n designates the above-mentioned resonance spacer of n atoms. For malonaldehyde and its derivatives (Chart 1), n is equal to 3, whereas for the centrosymmetric dimers

of carboxylic acids, one has a ···O=R_1−OH··· motif (Chart 11). Different types of O−H···O RAHBs with different values of n were classified, among them the ···O=R_7−O−H··· motif existing for the structure of 2,3-diacetyl-5-nitrocyclopentadiene and the O···O distance of 2.446 Å.[315]

4.4. π-Electron Delocalization for Intramolecular Resonance-Assisted Hydrogen Bonds (IRAHBs)

For the intramolecular resonance-assisted hydrogen bonds, the following scheme (Chart 15) is often presented to show that the π-electron delocalization and, consequently, the electron movement within the ring created makes the equalization of appropriate bonds.[37]

Chart 15

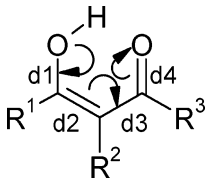

Hence, the redistribution of the electronic charge for the RAHB systems seems to be of great importance for the properties of these species. It is well-known that for the intermolecular H-bonds there is the transfer of electron charge from the proton-accepting molecule to the proton-donating one.[60] For example, for the linear (trans) water dimer, there is the transfer of 19 mē (1ē = 1000 mē) from the proton-donating water molecule to the accepting one because of complexation; it was obtained from the calculations performed at the MP2/6-311++G(d,p) level of theory.[316]

MP2/6-311++G(d,p) calculations have been performed, and the Bader theory has been applied recently to deepen the nature of π-electron delocalization.[266] The fluoro and chloro derivatives of malonaldehyde were considered, i.e., the systems where R_1, R_2, and R_3 substituents are H, F, and Cl atoms (see Charts 1 and 15). The net atomic charges for these systems were compared with the same charges for the corresponding "open" conformations (Chart 14). Table 4 shows the differences between the charges of the corresponding atoms of "open" and "closed" conformations. The following observations can be made. There is an increase of electron density for both oxygen atoms while comparing the closed configuration with the open one. There is a corresponding decrease of electron density for the H atom as a component of the O−H···O bridge; however, if one considers the OH proton-donating bond as a whole, there is also an increase of electron density. In other words, one can say that there is "the outflow" of electrons from carbon atoms into the O−H···O H bridge. Table 4 also shows the decrease of electron density for the CR_1=CR_2−CR_3 fragment.

Table 4. Changes of Atomic Charges (in me) for the Change of the Open Conformation into the Closed One[a]

R_1, R_2, R_3	Δq [O(H)]	Δq [H]	Δq [O(=)]	Δq [OH]	Δq [C(R_1)C(R_2)C(R_3)]
H, H, H	53	−37	68	16	−84
H, F, H	42	−20	82	22	−104
H, Cl, H	45	−37	78	8	−86
H, H, F	25	−9	56	16	−72
H, H, Cl	23	−18	65	5	−70
F, H, H	55	−70	80	−15	−65
Cl, H, H	81	−89	74	−8	−66
H, H, OH	40	−22	59	18	−77

[a] Data taken from ref 266.

It was pointed out[266] that a similar interpretation could be made if one considered the integrated atomic charges[317] derived from the Bader theory.[78] For example, for the results of unsubstituted malonaldehyde, there are the following changes of these charges after the change of the open conformation into the closed one; Δq(O−) = 57 mē, Δq(H) = −55 mē, and Δq(O=) = 36 mē. This means that there is an increase of electron charge for both oxygen atoms of the O−H···O bond and a decrease of this charge for the hydrogen atom; there is also a decrease of electron charge for the remaining part of the molecule (the R_1C−CR_2=CR_3 fragment), 38 mē. It is worth mentioning that similar conclusions on the redistribution of electronic charge because of the creation of the ring system may be drawn for the other intramolecular hydrogen bonds. Even for intramolecular dihydrogen bonds, an increase of electronic charge within the A−H···H region was observed.[318]

The following approach was also applied in the studies cited here.[266] The changing of the open conformation into the closed one may be considered as consisting of two stages. The first stage is the rotation of the O−H bond 180° around the C−O single bond (Chart 14), as a result of which the closed conformation is obtained (Chart 15). The second stage is connected with changes of the geometry of the system because of the process of π-electron delocalization; thus, the previous molecular structure obtained after the rotation of the OH bond is optimized. Hence, one can see the following energies of the systems considered: for the open conformation (E_O), the closed one without any change of geometry (E') and the most stable conformation existing after the system is closed, as well as the optimization of geometry (E_C). Therefore, the modulus of the energy difference between the closed configuration and the open one, $|E_{C-O}|$, consists of two terms; $|E' - E_O|$ and $|E_C - E'|$, with the first one being the result of the closing of the system and the second one being the result of the change of geometry after the closing of the system. It is very interesting to note that for every system the first term connected only with the closing of the system is approximately 3−4 times greater than the second term.[266] For example, for malonaldehyde, the first term amounts to 9.4 kcal/mol and the second one to 2.7 kcal/mol, whereas for the fluoro derivative of malonaldehyde (R_1 = F, Chart 15) these terms amount to 9.3 and 4.2 kcal/mol, respectively. Additionally, $|E' - E_O|$ does not correlate with the electron density at the H···O bond critical point, $\rho_{H\cdots O}$, because the linear correlation coefficient amounts to 0.641, similarly as for the correlation between E_{C-O} and $\rho_{H\cdots O}$. The E_{C-O} energy is often treated as a measure of the strength of intramolecu-

lar H-bonds. It only roughly corresponds to the H-bond energy because a lot of additional effects disturb the real H-bond interaction, as for example the additional repulsion between oxygen atoms for the "open" conformation.[268,319,320]

However, $|E_C - E'|$ correlates with $\rho_{H\cdots O}$ (R = 0.981). Because the electron density at H···B BCP within the A−H···B hydrogen bonds is often treated as a good measure of the H-bond strength,[25] thus, the results presented show that for the RAHBs the H-bond energy depends mainly on π-electron delocalization. These results also show that the E_{C-O} energy should not be treated as one that describes the H-bond strength. The main part of E_{C-O}, $|E' - E_O|$, is connected with the lowering of the energy of the system because of its closing; such lowering may be connected with the lowering of oxygen···oxygen repulsion.

4.5. Heteronuclear Resonance-Assisted Hydrogen Bonds

The previous considerations on RAHBs were mainly connected with the homonuclear O−H···O systems. It was pointed out that the heteronuclear A−H···B RAHB is intrinsically weaker than the A−H···A homonuclear one. The difference between proton affinities (PA) of H-bond donor and acceptor atoms results in a less effective mixing of the A−H···B ⇔ A···H−B resonance forms than for the A−H···A ⇔ A···H−A ones.[321] Different kinds of heteronuclear RAHBs were investigated, of which the N−H···O one seems to be the most important because it plays a crucial role in protein folding and DNA pairing and its role in crystal engineering also seems to be very important.[12] Hence, the studies of N−H···O RAHBs were performed for the crystal structures of β-enaminones,[322] β-ketoarylhydrazones,[321] ketohydrazone-azoenol[264] system and a lot of other crystal structures.

Recent studies on two crystal structures of phosphorohydrazide derivatives of chromone, (*E*)-3-{[(diphenoxyphosphoryl)-2-methylhydrazone]-methyleno}-4-hydroxy-2*H*-1-benzopyran-2-ne (**1**) and 3-{[(diphenoxythio-phosphoryl)-hydrazine]-methylidene}-3,4-dihydro-2*H*-1-benzopyran-2,4-dione (**2**),[248] are very interesting because they present the evidence of the existence of O−H···N and N−H···O intramolecular RAHBs. These H-bonds correspond to two tautomeric forms that are the stages of the proton-transfer reaction: N−H···O ⇔ O···H−N. It is in line with the statement of Bürgi and Dunitz[272] described in the previous section that the molecular fragments found in crystal structures may correspond to the frozen stages of the appropriate chemical reactions. Figure 19 shows molecular structures for both crystals considered.

It is worth mentioning that the OH···N interaction in **1** was the first case of such an intramolecular hydrogen bond in pyrane derivatives observed in the crystal structures; for the other cases, such as the search through the Cambridge Structural Database,[292] there were intramolecular N−H···O hydrogen bonds.[248] This is connected with the observation that the species with the N−H···O hydrogen bonds are usually of lower energy than the corresponding tautomeric forms with the N···H−O hydrogen bonds

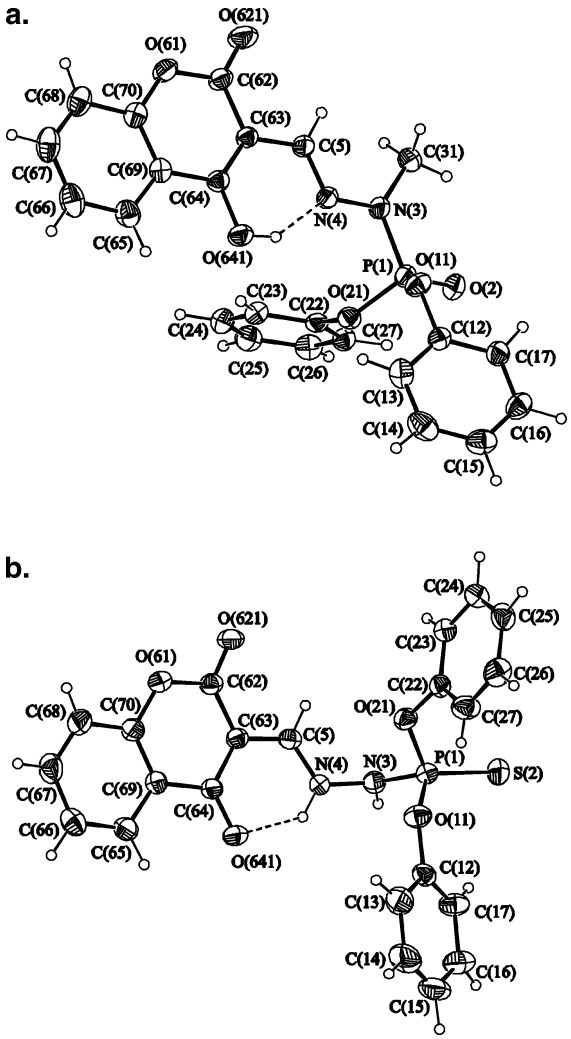

Figure 19. (a) Molecular structure of **1**; the displacement ellipsoids are drawn at a 30% probability level. (b) Molecular structure of **2**; the displacement ellipsoids are drawn at a 30% probability level. Reprinted with permission from (Rybarczyk-Pirek, A. J.; Grabowski, S. J.; Małecka, M.; Nawrot-Modranka, J. *J. Phys. Chem. A* **2002**, *106*, 11956), copyright 2002, American Chemical Society, Washington, DC.

despite the finding that contrary O−H···N bonds are stronger than the corresponding N−H···O ones. This topic is described in detail in the next section. The analysis of molecular structures **1** and **2** show that both intramolecular H-bonds are of resonance-assisted type. For **1**, there is the H−O−C=C−C=N··· system of π-conjugated bonds with the C−O bond equal to 1.335(3) Å; C=C, 1.365(3) Å; C−C, 1.454(3) Å; and C=N, 1.284 (3) Å. For the molecular structure **2**, there is the ···O=C−C=C−N−H system of bonds with C=O amounting to 1.247(3) Å; C−C, 1.433(3) Å; C=C, 1.389(3) Å; and C−N, 1.306(3) Å. One can see the shortening or lengthening of the appropriate bonds when one compares them with pure single- and pure double-bond distances: C(sp^2)=O, 1.20 Å; C(sp^2)−C(sp^2), 1.48 Å; and C(sp^2)=C(sp^2), 1.33 Å.[323] The O···N distances for **1** and **2** are equal to 2.586(3) and 2.609(3) Å, respectively. This means that the OH···N H-bond for **1** should be stronger than the NH···O bond for **2** because for the latter the N···O distance is longer. However, this probably does not correspond

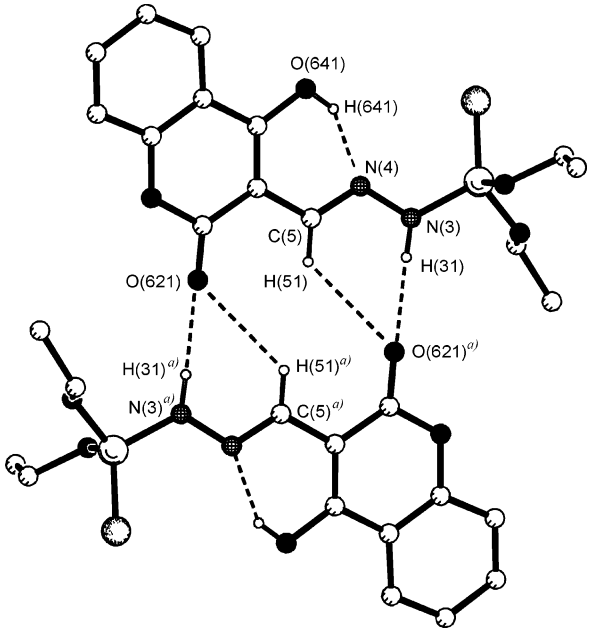

Figure 20. Dimer within the crystal structure of (*E*)-3-{[(diethoxythiophosphoryl)-hydrazon]-methyl}-4-hydroxy-2*H*-1-benzopyran-2-one. Reprinted with permission from (Rybarczyk-Pirek, A. J.; Grabowski, S. J.; Nawrot-Modranka, J. *J. Phys. Chem. A* **2003**, *107*, 9232), copyright 2003, American Chemical Society, Washington, DC.

to π-electron delocalization. One can only compare the equalization of C−C and C=C bonds; the difference between them amounts to 0.089 and 0.044 Å for **1** and **2**, respectively. One can see that there is no relationship between the equalization of CC bonds as a measure of π-electron delocalization and the H-bond strength. This is probably connected with the fact that different types of H-bonds are considered: N−H···O and O−H···N.

The other crystal structures of chromone derivatives containing intramolecular RAHBs were investigated, but only N−H···O bonds were detected.[324] The other cases of O−H···N hydrogen bonds for chromone derivatives were not found. However, a group of benzopyrane derivatives substituted with phosphorohydrazide in position 3 has been investigated recently[325] for which bifurcated hydrogen bonds exist with one acceptor center, oxygen atom, and with two proton-donating bonds, N−H and C−H. Three crystal structures were investigated, and for one of the cases considered, the crystal structure of (*E*)-3-{[(diethoxythiophosphoryl)-hydrazon]-methyl}-4-hydroxy-2*H*-1-benzopyran-2-one, there is an additional resonance-assisted O−H···N hydrogen bond. Figure 20 shows the dimer of this species where the bifurcated hydrogen bonds are visible as well as the abovementioned intramolecular H-bond. This IRAHB, O−H···N, affects strongly the strength of the bifurcated H-bond; the N···O donor−acceptor distance for this structure amounts to 2.895(4) Å, whereas for the other two related structures without RAHBs, these values within the corresponding bifurcated H-bonds amount to 2.956(3) and 2.911(3) Å. This means that IRAHB causes an increase of the acidic character of the N−H bond for the first species. Additionally, the N−H···O contact within the bifurcated H-bond for the structure with additional RAHB is close to linearity, 174(4)°, whereas for the other cases, such angles are equal to 165(3)° and 167(3)°.

Another example is the structural evidence for resonance-assisted O−H···S hydrogen bonding investigated by Steiner.[326] The author has claimed that the shortest hydrogen bonds of the O−H···S type occur in monothio-β-diketones and related substances, for which the H···O distances are of about 1.9−2.0 Å. As evidence that they are RAHBs, two relationships for the species taken from Cambridge Structural Database are given,[292] the first one between q_1 and q_2 and the second one between the Q value and the O···S distance, where q_1, q_2, and Q were described before. However, the relationships presented are based only on six points. Additionally, q_1 is the difference between different types of bonds C−O and C=S, and the parameter Q was defined for homonuclear O−H···O RAHBs.[37] Despite these reservations, it seems that the systems studied are really RAHBs because one can see considerable equalization of CC bond lengths, the elongation of the proton-accepting C=S bond, and the shortening of C−O bond. For example, for the molecular structure of mercapto-1,2-diphenylprop-2-en-1-one determined by neutron diffraction, there are the following bond lengths C−O, 1.321 Å; C=C, 1.396 Å; C−C, 1.410 Å; and C=S, 1.675 Å, showing π-electron delocalization and equalization of CC bonds (the difference amounts to 0.014 Å). Detailed studies on this type of intramolecular H-bonds, O−H···S, and additionally on the related interactions, S−H···O, were performed by González et al.[327] The authors performed B3LYP/6-31G(d) calculations on thiomalonaldehyde and its simple derivatives. The substituent effects on the strength of intramolecular hydrogen bonding were also studied. The species were not investigated in terms of RAHBs, but the results show that they may be classified as such systems and that they do follow the features described in the previous sections. If one considers the *Z*-enethiol form with the S−H···O H-bond (see Chart 16), then there are the following bond lengths of the

Chart 16

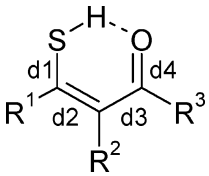

ring system: d_1, 1.741 Å; d_2, 1.358 Å; d_3, 1.455 Å; d_4, 1.232 Å, and the H···O distance is equal to 1.898 Å. The electron density at H···O BCP is equal to 0.034 au.

According to the statement of Bertolasi et al.,[162] the electron-withdrawing R_1 or the electron-donating R_3 substituents for O−H···O IRAHB (Chart 1) influence the strength of the H-bond. This is in force here because for the monofluorine derivative of *Z*-enethiol the H···O distance amounts to 1.785 Å and the electron density at the corresponding BCP is equal to 0.043 au, if R_1 = F. The H···O distance and the electron density at BCP amount to 2.015 Å and 0.026 au, respectively, if R3 = F. Hence the F substituent

makes the H-bond stronger for the former case and weaker for the latter, because the H···O distance may be treated as an approximate measure of the H-bond strength. On the other hand, if one considers the *Z*-enol form (see Chart 17), then similar findings may be pointed out.

Chart 17

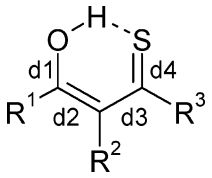

For the unsubstituent species, the H···S distance is equal to 2.062 Å and the electron density at H···S BCP is equal to 0.041 au, whereas for R_1 = F, the corresponding values are equal to 1.961 Å and 0.050 au, respectively. For R3 = F, one can have H···O equal to 2.118 Å and the corresponding electron density at BCP equal to 0.036 au. The equalization of bond lengths is the greatest for R_1 = F because the difference between C−C and C=C bonds amounts to 0.028 Å; the same difference for R_3 = F is equal to 0.050 Å.

Recently simple systems with intramolecular hydrogen bonds have been analyzed with the use of DFT and *ab initio* methods.[328] B3LYP/6-311++G(d,p) and MP2/6-311++G(d,p) calculations were performed. The OH, SH, NH_2, and CH_3 groups were selected as proton donors, and N, O, and S atoms were selected as the accepting centers. Systems similar to malonaldehyde (see Chart 1; $R_1 = R_2 = R_3$ = H) were investigated in this study. Malonaldehyde was investigated as the species with the O−H proton-donating bond; the oxygen atom was investigated as an acceptor center (Chart 1); and the other species were investigated with the mentioned donors and acceptors. The systems with two types of C−H proton-donating bonds were analyzed, with one of them originating from the CH_3 group and the other from O=C−H. For some of the systems calculated at the MP2/6-311++G(d,p) level of theory, the optimized molecular structures were not obtained, and hence, the description presented here is based only on DFT results. However, the MP2 results are in line with the DFT ones.

On the basis of the results reported earlier,[328] Table 5 presents some geometrical and topological results concerning the systems mentioned above. The H···B (where B designates the acceptor center) distances, C−C and C=C bond lengths, as well as electron densities at H···B BCPs are given. If one assumes that, for H···B, the electron density at the corresponding BCP, and its Laplacian are the rough estimators of the H-bond strength, the conclusions are as follows. The proton-donor strength may be ordered in the following sequence (Table 5): OH > SH > NH_2 > CH.

The sulfur atom may be the stronger or weaker proton acceptor than the oxygen acceptor; it depends on the kind of donor. The S−H···S hydrogen bond is stronger than S−H···O, but O−H···O is stronger than O−H···S. These results are supported by other topological parameters; the greater $\rho_{H\cdots B}$ values correspond to stronger H-bonds; also, Laplacian $\nabla^2\rho_{H\cdots B}$ correlates with the H-bond strength. However, it should be mentioned here that homonuclear H-bonds are usually stronger than the heteronuclear ones.[163] The results within Table 5 also show that the OH bond is the strongest proton donor and the nitrogen center is the strongest acceptor. There are also differences between the C−C and C=C bond lengths included within Table 5, which show that the systems analyzed are resonance-assisted intramolecular hydrogen bonds. The equalization of CC bonds within the system briefly correlates with the corresponding H-bond strength. However, such rough relationships are fulfilled within the sample of the same type of acceptor. Additionally, the species with the NH_2-donating group are out of these correlations. Figure 21 shows those dependences. Hence, the difference between the CC bond lengths (C−C and C=C, i.e., ΔCC) is the approximate measure of the degree of π-electron delocalization and reflects the H-bond strength. Thus, one can expect that for the stronger H-bonds there is the more efficient mixing of resonance forms.

Table 5. Geometrical (in Å) and Topological Parameters (in au) of the Intramolecular Hydrogen Bonds; H···B Distances, C−C and C=C Bond Lengths, and the Electron Densities at H···B BCPs and Their Laplacians Are Given[a]

system	H···B	C=C	C−C	*R*(C−C)−*r*(C=C)	$\rho_{H\cdots B}$	$\nabla^2\rho_{H\cdots B}$
CH_3···N	2.380	1.344	1.468	0.124	0.0139	0.0465
NH_2···N	1.969	1.368	1.437	0.070	0.0296	0.0973
OH···N	1.680	1.362	1.439	0.077	0.0566	0.1110
SH···N	1.879	1.355	1.450	0.094	0.0384	0.0984
O=CH···N	2.425	1.346	1.473	0.127	0.0130	0.0429
CH_3···O	2.316	1.345	1.475	0.130	0.0143	0.0485
NH_2···O	1.973	1.371	1.436	0.065	0.0267	0.0980
OH···O	1.701	1.364	1.438	0.074	0.0487	0.1347
SH···O	1.931	1.357	1.453	0.097	0.0307	0.0976
O=CH···O	2.343	1.346	1.487	0.141	0.0139	0.0466
NH_2···S	2.261	1.382	1.412	0.030	0.0275	0.0597
OH···S	2.053	1.373	1.416	0.043	0.0428	0.0547
O=CH···S	2.762	1.351	1.456	0.105	0.0112	0.0333
SH···S	2.136	1.369	1.424	0.054	0.0381	0.0564

[a] The results in this table are summarized from the values given in ref 328.

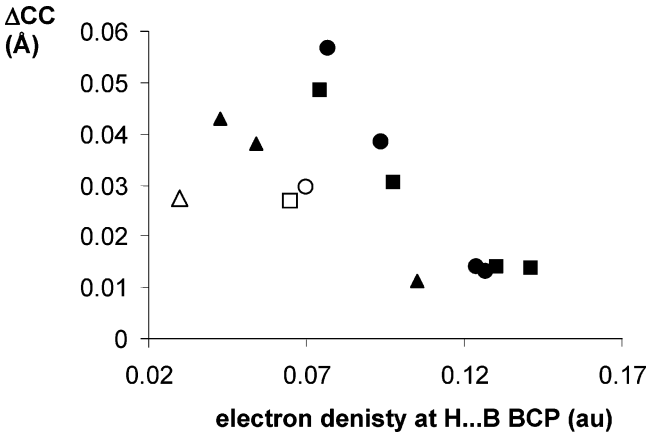

Figure 21. Relationship between the CC bond lengths' difference (in Å) and the electron density at the H···B BCP (in au). ●, ■, and ▲ correspond to N, O, and S acceptors, respectively, and ○, □, and △ correspond to those where the NH_2 group is the proton-donating one.

In recent years, some other intramolecular H-bond systems, for which the effect of π-electron delocalization may be detected, have also been investigated. For example, for the A−H···B systems where A = O and S and B=Se and Te, high-level G2(MP2) *ab initio* and DFT B3LYP/6-311+G(3df,2p) calculations have been performed.[329] The effect of π-electron delocalization was even detected for intramolecular dihydrogen bonds.[318]

4.6. Strength of Resonance-Assisted Hydrogen Bonds and the Principle of the Minimum ΔPA

It is well-known that homonuclear O−H···O H-bonds are stronger than the relative heteronuclear N−H···O ones. This is particularly evident for the intramolecular resonance-assisted hydrogen bonds. Gilli and co-workers claimed[163] that O−H···O RAHBs are stronger than the related N−H···O systems because for the latter the symmetry is broken and there is no effective mixing of two resonance forms; such mixing leads to π-electron delocalization and the enhancement of hydrogen bonding. This statement was developed later within the so-called ECHBM.[231] According to this model, the strong O−H···O RAHBs are partly if not mainly covalent interactions, whereas the N−H···O bonds are more electrostatic in nature, not covalent, and hence are weaker.

The nature of the RAHBs may also be explained within the principle of the minimum difference between A and B proton affinities ΔPA within the A−H···B H-bond or of the minimum ΔpK_a, where ΔpK_a is the difference between the two interacting groups as measured in a proper polar solvent.[330−333] According to this principle, the heteronuclear resonance-assisted N−H···O hydrogen bonds may be enhanced if, for the −N(R)H, proton-donating group, the R substituent is electron-attracting, which means it is able to decrease the ΔPA value and hence increase the acidity of the NH bond. This statement was confirmed many times by various experimental and theoretical results. For example, the proton-transfer process within simple enaminones was investigated using the MP2/6-311++G(d,p) and MP4/6-311++G(d,p) levels of theory, and the Bader theory was also applied in that bonds' analysis.[248] Generally, the results indicate that the systems with the N−H···O intramolecular hydrogen bonds are more stable than those containing O−H···N bonds, although the O−H···N H-bonds of analogous tautomeric forms are stronger. However, the inclusion of the proper R substituent within the −N(R)H, proton-donating group, may change this relation.

The enol and keto forms of simple enaminones were considered in the mentioned study,[248] the transition states for those tautomers were also taken into account (Chart 18). In the case of two tautomeric

Chart 18

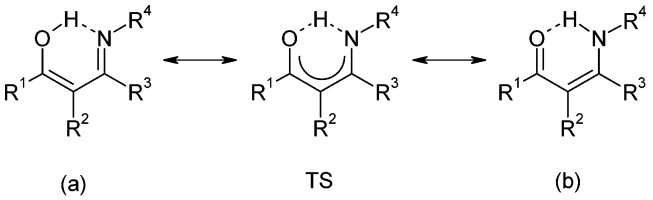

forms, iminoenol and enaminone (with $R_1 = R_2 = R_3 = R_4 = H$), and their transition state, the calculations were performed at MP2/6-311++G(d,p) and MP4/6-311++G(d,p) levels of theory. Additionally, the MP2/6-311++G(d,p) calculations were performed for such derivatives where $R_1 = F$, $R_3 = F$, and $R_4 = F$ or Li. Table 6 presents the selected geometrical, energetic, and topological parameters of the systems analyzed. If one considers the energies of the whole species with intramolecular H-bonds, one can see that for $R_1 = R_2 = R_3 = R_4 = H$ the system with the N−H···O H-bond (enaminone) is energetically more stable; for all of the systems considered, the enaminone tautomeric form exists, whereas the iminoenol form does not always exist. This is in line with most of the crystallographic studies on the related systems because in organic crystals the enaminone form is more common than the iminoenol one.[248] The situation changes if one considers the derivative with $R_4 = F$ because in such a case the form a (see Chart 18) is more stable because of the substituent effect. The fluorine atom is the electron-withdrawing substituent, which lowers the proton affinity of the nitrogen

Table 6. Selected Geometrical (in Å), Energetic (in kcal/mol), and Topological (in au, e/a_0^5) Parameters of the Simple Iminoenol and Enaminone Derivatives; for the a Form, There Is the O−H···N H-Bond, and for the b Form, the N−H···O One[a]

R_1,R_2,R_3,R_4	tautomeric form	d(O,N)	$R_{C-C} - R_{C=C}$	energy[b]	$\nabla^2\rho_{O,H}$	$\nabla^2\rho_{H,N}$
H,H,H,H	a	2.580	0.077	5.87	−2.175	0.117
	TS	2.390	0.024	8.43	−0.379	−0.863
	b	2.705	0.070	0	0.102	−1.825
H,H,H,H	a[c]	2.650	0.099	5.97	−2.392	0.115
	TS[c]	2.387	0.029	11.12	−0.331	−0.261
	b[c]	2.744	0.084	0	0.092	−1.811
F,H,H,H	b	2.765	0.070	0	0.084	−1.812
H,H,F,H	a	2.635	0.078	0.05	−2.288	0.113
	TS	2.397	0.006	5.17	−0.140	−0.390
	b	2.682	0.072	0	0.108	−1.819
H,H,H,F	a	2.668	0.088	0	−2.413	0.108
	TS	2.367	0	11.82	0.083	−0.086
	b	2.591	0.062	8.80	0.112	−1.975
H,H,H,Li	b	2.813	0.036	0	0.0292	0.3234

[a] The results in this table are summarized from the values given in ref 248. [b] The difference in energy between the system considered (tautomer or TS) and the related tautomer of the lowest energy. [c] MP4 results.

atom. This finding strongly confirms the above-mentioned principle of the minimal value of ΔPA. For R_4 = Li, only the form b exists because Li, the electron-donating substituent, causes a substantial increase of proton affinity of the nitrogen atom, which is reflected in the increase of the ΔPA value, and hence the tautomeric form a does not exist at all. The calculations were performed for the tautomer a with R_4 = Li, but the optimized structure always collapsed into the b one. Table 6 also presents the O···N distances that may be treated as an approximate measure of the H-bond strength; for the shorter O···N distances, i.e., the stronger H-bonds, the whole systems are characterized by greater energy. In the case of transition states of the highest energies, there are the strongest H-bonds studied.[248] Such a situation was also analyzed for the molecules of the keto-hydrazone-azoenol series,[334] and it was pointed out that it expresses the Hammond postulate[335] and leads to the rule stating that the less stable form, being closer on the reaction path to the transition state, always contains the stronger (shorter) H-bond. Hence, the H-bond of the transition state is the strongest one in comparison with the other H-bonds of the same system.

The results of Table 6 approximately confirm the previous findings[37,163] that the greater π-electron delocalization and further equalization of C−C and C=C bonds, the stronger is the hydrogen bond. One can see the greatest equalizations for transition states. This is also reflected in the values of Laplacians for BCPs of H···O(N) contacts that are negative, as for covalent bonds. This is in line with the electrostatic covalent model of the hydrogen bond because it shows that for very strong H-bonds the H···B interaction is partly covalent in nature.

For the same group of species, the correlation between descriptors of H-bond strength was found, i.e., the dependence between electron density at H···B BCP and electron density at RCP existing in the pseudoring with the intramolecular H-bond. Figure 22 shows this dependence. One can observe that the greatest values of both electronic densities correspond to the strongest H-bonds for the transition states.

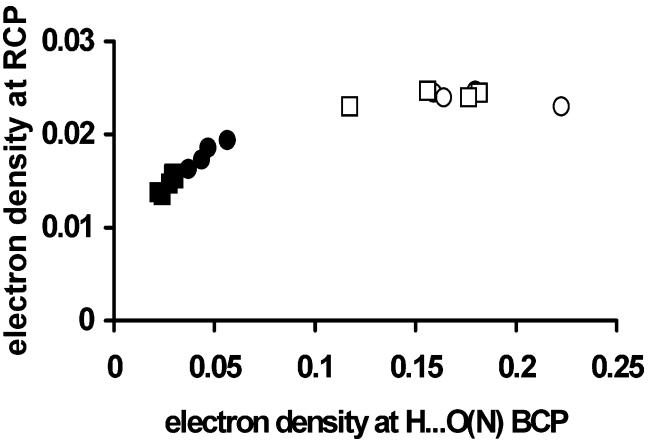

Figure 22. Correlation between the electron density at the ring critical point (RCP) of the ring created because of the formation of intramolecular H-bond (in au) and the electron density at H···B BCP (in au). (●) H···N contacts, (■) H···O contacts, and (○ and □) same values of the transition states. Reprinted with permission from (Rybarczyk-Pirek, A. J.; Grabowski, S. J.; Małecka, M.; Nawrot-Modranka, J. *J. Phys. Chem. A* **2002**, *106*, 11956), copyright 2002, American Chemical Society, Washington, DC.

4.7. Diversity of Resonance-Assisted Hydrogen Bonds

There are different kinds of hydrogen bonds assisted by resonance, both intermolecular as well as intramolecular ones. In one of their previous studies on RAHBs, Gilli and co-workers collected the molecular fragments that may be implemented in the phenomenon of RAHB.[37] The following species were indicated as intramolecular H-bond systems: enolones, enaminones, enamino-imines, and enol-imines, and the following ones as intermolecular hydrogen bonds: amide−amidine coupling, amide dimers, and thymine−adenine and cytosine−guanine couplings. In those studies, the next cases supported by X-ray crystal structure investigations and the search through the Cambridge Structural Database were indicated.[336] Among the systems indicated and investigated to a greater or smaller extent, the dimers of the Watson−Crick AT and GC base pairs seem to be the most important because of their great importance in biological processes. It was shown that AT and GC base pairs are in essence electrostatic interactions with substantial resonance assistance from the π electrons.[337] The authors performed BP86/TZ2P calculations (TZ2P designates a triple ζ plus double polarization type basis[338]), and finally, they concluded that hydrogen bonding in DNA base pairs is not only an electrostatic phenomenon. This interaction also contains the charge-transfer contribution, owing to donor−acceptor orbital interactions between the oxygen or nitrogen atom lone pairs, and N−H σ^*-acceptor orbital interactions, being of the same order as the electrostatic interaction. The effect of polarization within the π-electron system provides an additional stabilizing interaction. This effect is responsible for a decrease of the H-bond length by about 0.1 Å. The authors have concluded that in the hydrogen bonds charge-transfer and electrostatic interaction are of the same order of magnitude. There is also assistance by the π system through a delocalization; however, an order of magnitude smaller than the two attractive interactions mentioned above. Furthermore, the authors have shown with the change in the Voronoi deformation density (VDD) charges[339] that there occurs charge transfer in the σ system and delocalization in the π system, counteracting the charge flow of the σ system. Therefore, these hydrogen bonds can be named RAHBs. However, the authors also found that there is no synergetic interplay between the σ system and the π system in the meaning of enlarging the interaction of the other by acting simultaneously.

Another type of intermolecular RAHBs is that of carboxylic acid dimers. It is well-known from earlier studies on the crystal structures of carboxylic acids that these species in the solid state often form centrosymmetric dimers (Chart 11).[32,33] Usually, for such dimers, there occurs a considerable change of geometrical parameters in comparison with the single

carboxylic acid molecules existing for example in the gas phase.[32] Among various geometrical changes, there is also the equalization of C−O and C=O bonds of the carboxylic group. There are different effects causing such equalization: mesomeric effect of the carboxylic group, dynamic and static disorder enhanced in crystals by the lattice forces, etc.[270] However, such equalization, in accordance with the electrostatic covalent model of hydrogen bonding,[231] may be explained in terms of the existence of resonance forms, π-electron delocalization, and further the resonance-assisted H-bonds for dimers of carboxylic acids.

The features of intermolecular resonance assisted hydrogen bonds existing within carboxylic acid dimers were investigated extensively for the pyrrole-2-carboxylic acid molecules.[340,341] Monomeric and dimeric forms of this species were investigated using infrared and Raman spectroscopic experimental techniques as well as DFT and *ab initio* calculations performed at different levels of theory: B3LYP/6-311+G(d), B3LYP/6-311++G(d,p), MP2/6-311+G(d), and MP2/6-311++G(d,p). The crystal and molecular structure of pyrrole-2-carboxylic acid was also determined by single-crystal X-ray diffraction.[341]

Chart 19 shows which types of dimers of pyrrole-2-carboxylic acid were investigated theoretically.[341] The strongest H-bonds were detected in this study for the A and B dimers; H-bonds for the C dimer are weaker. This was confirmed by energetic, geometric, and topological (AIM) results. It was also checked that the H-bonds for A and B are stronger than those of the formic acid dimer, because the corresponding H-bond energies calculated at the MP2/6-311++G(d,p) level of theory and corrected for BSSE amount to 7.9, 7.4, and 6.6 kcal/mol, respectively (energies of the single O−H···O bonds; all dimers are centrosymmetric and hence contain two equivalent H-bonds). Hence, one may conclude that pyrrole rings would affect the geometry of pyrrole-2-carboxylic acid molecules; i.e., there would be additional π-electron delocalization, which makes H-bonds of A and B stronger.

Chart 19

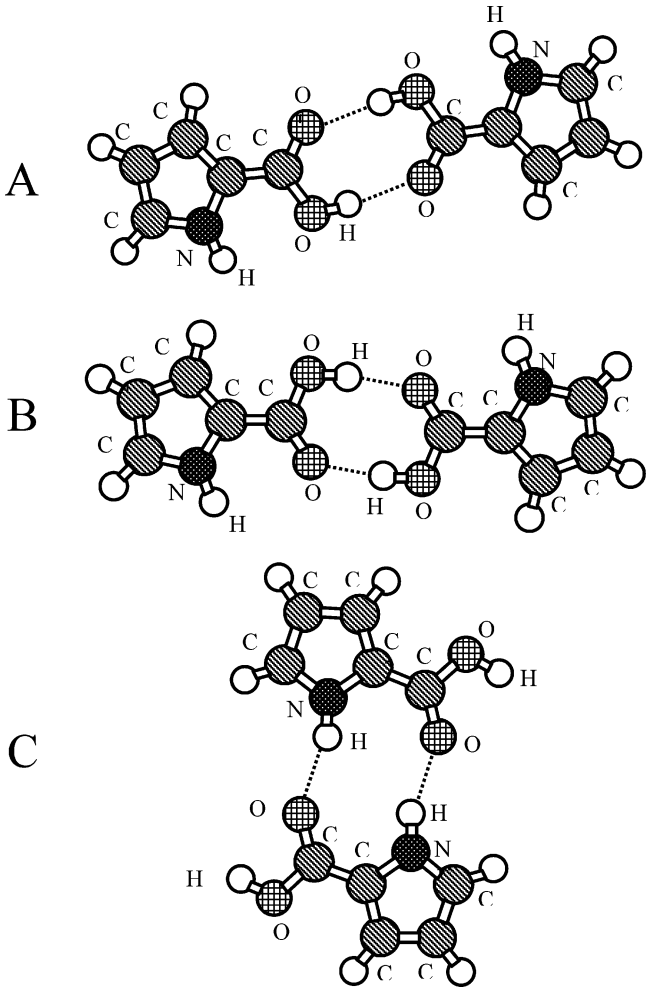

5. Distant Consequences of the H-Bond on the π-Electron Delocalization

Resonance-assisted hydrogen-bond cooperativity[37] takes into account distant interactions that associate the H-bond region with the remainder of the system. The Gilli Q or λ parameter[37] or Grabowski Δ_{rp} parameter[266] describe π-electron delocalization in the π-electron spacer, linking the proton-donating and proton-accepting parts of the H-bond. Gilli et al. in a collection of papers[37,162,163,175,264,322,334] have shown numerous dependences of the λ parameter on various parameters of the H-bond, indicating in this way association of the π-electron delocalization in the spacer with the nature of the H-bond. Moreover, geometry-based analyses applying a simple description by use of canonical forms allowed to show some distant consequences of the H-bond.[175,264,322,334]

The aim of this chapter is to show how the H-bond of various kinds and strengths affect π-electron delocalization in the remainder of the system, which may be not only the π-electron spacer but also aromatic moieties. In particular, an attention is paid for the relations between π-electron delocalization of the aromatic part of the system and the nature of the H-bond. For this purpose, indices of aromaticity will be used,[40] which well describe π-electron delocalization and allow one to relate their magnitudes to the values for well-known aromatic systems.

5.1. Aromaticity Indices as a Measure of π-Electron Delocalization

π-Electron delocalization is revealed in various ways, and many chemical and physicochemical properties of chemical compounds are associated with this phenomenon. One of the most important terms in organic chemistry, the aromaticity,[342] refers directly to π-electron delocalization observed in cyclic systems. The definition reads:[342−345] a cyclic π-electron compound is aromatic if there appears a measurable π-electron delocalization in the ground state of the molecule. This is associated with (i) an increase of stability related to the system without cyclic π-electron delocalization. In this way, the concept of resonance energy (abbreviated as RE) was defined[346,347] and had served very early as a quantitative measure of aromatic stabilization.[23,348] Actually, this quantity is defined in a more refined way and named as the aromatic stabilization energy (abbrevi-

ated hereafter ASE);[39] for an extensive review, see the paper by M. K. Cyranski, this issue; (ii) intermediate bond lengths, close to the mean value of the length for the typical single and double bonds. The first quantitative approach was done by Julg and Francoise,[349] and then it was refined in various ways.[350−353] For the most extensive review see, ref 354; and (iii) π-electron ring current formation when the molecule is exposed to the external magnetic field,[355−359] that is associated with an anisotropy of magnetic susceptibility, an increase of exaltation of magnetic susceptibility, and typical ^{1}H NMR chemical shifts.[360] A nucleus-independent chemical shift, hereafter abbreviated NICS,[361,362] is also frequently used to describe this property.

On the basis of the above presented features of aromatic molecules, many numerical descriptors of aromaticity, named aromaticity indices, have been introduced and applied in numerous discussions of π-electron delocalization (e.g., ref 40).

Even if the aromaticity indices are not equivalent,[363−369] in the case of a family containing very similar structural patterns, they may inform equally well about the changes in π-electron delocalization.[369−371]

There are many quantitative measures of aromaticity, which in principle are strongly associated with π-electron delocalization.[39,40] The choice made in the present review is based on a frequency of their use for the title problems and availability of the data in the literature.

The geometry-based aromaticity index HOMA (abbreviation from harmonic oscillator model of aromaticity) works on the assumption that geometry is strongly related to electron distribution. This is supported by the Hellmann−Feynman theorem,[372] which may be formulated as follows: distribution of electronic density in the molecule determines the forces acting on the nuclei, which in turn define the geometry of the molecule in question. Thus, geometry may provide reliable information about the electron distribution, and when employing appropriate references, it may be used to describe π-electron delocalization. The HOMA index is defined as below (eq 21),[350] extended later into π-electron systems with heteroatoms[352]

$$\mathrm{HOMA} = 1 - \frac{\alpha}{n}\sum(R_{\mathrm{opt}} - R_{\mathrm{i}})^2 \qquad (21)$$

where n is the number of bonds taken into the summation and α is a normalization constant (for CC bonds $\alpha = 257.7$) fixed to give HOMA = 0 for a model nonaromatic system (the Kekule structure of benzene) and HOMA = 1 for the system with all bonds equal to the optimal value, R_{opt}, assumed to be realized for full aromatic systems. For CC bonds, R_{opt} is equal to 1.388 Å; this bond length differs from the most precise value for the CC bond in benzene, which amounts to 1.397 Å.[373] R_{opt} is a quantity that is obtained by the use of a model allowing the users of the HOMA index to estimate the values of R_{opt} for a collection of π bonds (CC, CO, CN, NN, and NO).[352] R_{i} stands for a running bond length.

The HOMA index can be analytically dissected into two independent terms,[374] named GEO and EN, describing quantitatively whether the decrease of π-electron delocalization is due to an increase of bond alternation (GEO) or the elongation of the mean bond length (EN). The definition of this form of HOMA index is as below (eq 22)

$$\mathrm{HOMA} = 1 - \left[\alpha(R_{\mathrm{opt}} - R_{\mathrm{av}})^2 + \frac{\alpha}{n}\sum(R_{\mathrm{av}} - R_{\mathrm{i}})^2\right] = 1 - \mathrm{EN} - \mathrm{GEO} \qquad (22)$$

R_{av} stands for the average bond length.

There are many quantitative measures of aromaticity; however, in the past decade, the nucleous-independent chemical shift (abbreviated hereafter as NICS)[362,375] has deserved substantial attention. NICS[362] and NICS(1)[375] are defined as the negative values of absolute shielding in the center of the ring (NICS) and 1 Å above this [NICS(1)], respectively. Very recently, the idea of NICS was a subject of a vivid disputation at the European Science Foundation Exploratory Workshop, Exeter, U.K., July 5−9, 2003,[376] and as a consequence, an improved version of NICS was presented. It was already suggested earlier for the studies of π-electron delocalization in antiaromatic systems to use the component of the NICS tensor corresponding to the principal axis perpendicular to the ring plane, NICS(1)$_{zz}$.[377] This idea found substantial support in the discussion as a better measure for the characterization of the π system of the ring.[378] In all of the cases, the more negative were the NICS values and the more aromatic was the π-electron system.

5.2. Intermolecular H-Bond Systems and Modeling of the σ- and π-Electron Interactions between the H-Bond and Aromatic Ring

The problem of distant structural consequences of the H-bond on R_1 or R_2 (eq 1 in chapter 1) immediately raises a question: what kind of interaction causes the changes in geometry? Generally, this problem has not been solved yet, but for some cases, attempts have been made. An approximate answer was given by a systematic study of pentachlorophenol H-bond complexes with various bases. It was shown that a-bond lengths, α angle, and CO bond lengths (for labeling, see Chart 20) are nicely correlated with each other and with the correlation coefficient (or its absolute value, because it depends upon the sign of the slope) at the level of 0.94 or better.[379]

Chart 20

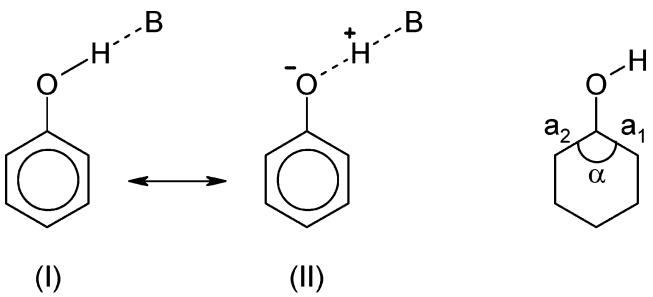

Chart 21

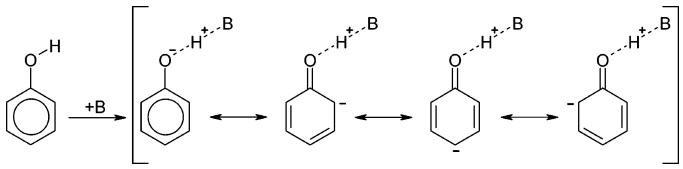

One of these dependences, viz. the C−O bond lengths d_{C-O} versus a(av), (the averaged value of a_1 and a_2) allows one to build up a qualitative model describing the σ-electronic (Chart 20) and mesomeric, i.e., π-electronic (Chart 21) effects on the geometry patterns in the ring.

Chart 20 also shows limiting resonance structures for H-bond interactions between the hydroxy group of phenol and the basicity center of the proton-acceptor B for the σ-electronic mechanism of interactions. The effects on ring geometry and basicity centers are not shown.

Chart 21 shows the resonance structures describing the consequences of π-electron delocalization because of H-bond interactions between the hydroxyl group of phenol and the basicity center of the proton-acceptor B for the mesomeric, i.e., π-electronic mechanism of interactions.

In both cases, the shortening of CO bond length leads to a lengthening of both a bonds. Thus, the differentiation may be done by analysis of the magnitude of the slope of R(CO) versus a(av) dependences. The procedure for estimating the values of the slopes for these two cases is based on a model in which the limiting cases for CO and a(av) bonds are approximated by situations in which mostly the σ- or π-electronic mechanisms operate.[379] Apart from the intermolecular case used for testing the model, it was also shown that, in the intramolecular H-bond system, *N*-salicylideneanilines, the dominant changes in geometry in the ring are due to the mesomeric effects.[380]

To differentiate the structural consequences of σ- or π-electronic mechanisms of the H-bond affecting the ring, the following approximate approach was applied.[379] Chart 20 presents two canonical structures describing the enol tautomer of the hydrogen-bonded system that allows us to describe the difference in electron distribution because of the H-bonding of the OH group. The increase in strength of the OH···B interaction increases the weight of canonical structure **II**, which then describes more adequately the system in question.

If the negative charge at the oxygen is not delocalized, its increase implies a decrease of the oxygen atom's electronegativity.[381] Application of the Walsh−Bent rule[382,383] postulates that the decrease of electronegativity causes a decrease of the 2p orbital contribution to the hybrid orbital along the CO bond ($sp^2 \rightarrow sp^{2-x}$) and an increase along both a bonds ($sp^2 \rightarrow sp^{2+x/2}$). Chart 22 presents a scheme of the changes in hybridization at the carbon atom as a result of the increase of a negative charge at the oxygen atom. In consequence, the CO bond length should be shortened and C_1C_2 and C_1C_6 bonds (i.e., bonds a_1 and a_2, Chart 20) should be lengthened (and the α angle should become sharper).

Chart 22

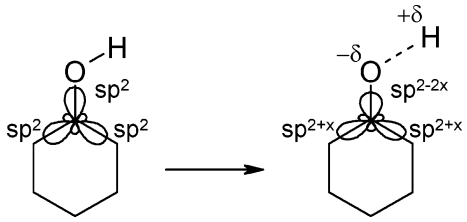

In a limiting case, when $x = 1$, the model situation reads as follows: the CO bond length for C(sp^{2-1} = sp) is as in the case of the CO_2 molecule (1.165 Å),[384] whereas the CC bond length for C($sp^{2+1/2}$) may be taken as a mean value from the CC bond length in ethane (1.534 Å)[384] and the central bond in buta-1,3-diene (1.465 Å). Thus, the CC($sp^{2+1/2}$) bond length is approximated by 1.4995 Å. Another limiting situation is for the CO bond length with C($sp^{2+1} = sp^3$) that may be modeled by the CO bond length from methanol (1.421 Å)[384] and the mean value of the central bond lengths from buta-1,3-diene (1.465 Å)[384] and buta-1,3-triene (1.284 Å), which equals 1.4245 Å. In the system of coordinates R_{CO} and R_{CC} for these two limiting cases, the straight line is defined as

$$R_{CO} = -3.4R_{CC} + 6.28 \qquad (23)$$

This equation describes the situation in which the σ-electron effect causes the changes of the CO and both a bond lengths.

Chart 21 presents the canonical structures that show the π-electron distribution because of the H-bond of the OH group and delocalized over the ring. Two limiting situations may be defined. For one situation, the $R_{C=O}$ and R_{C-C} are taken from the geometry of acroleine (1.271 and 1.484 Å),[385] respectively. For the other one, the C−OH and CC bond lengths are taken from phenol[386] with the values 1.3745 and 1.3912 Å, respectively. The equation for the straight line for these two points is

$$R_{CO} = -1.7R_{CC} + 3.74 \qquad (24)$$

In both cases, of the σ- and π-electron models of interactions, the changes are qualitatively alike and only the numerical values of the slopes may be given a chance to show which of them is dominating. The analysis of R_{CO} versus R_{CC} for 12 pentachlorophenol H-bond complexes gave the regression line $R_{CO} = -1.6R_{CC} + 3.5$ with a correlation coefficient = −0.941. Thus, it was concluded that, at least for pentachlorophenol complexes with N and O bases, the π-electron model of interactions is decisive.[379]

Recently, a much more extended study was carried out on the interrelation between the geometric parameters of the ring and the strength of the H-bond in variously substituted phenol derivatives interact-

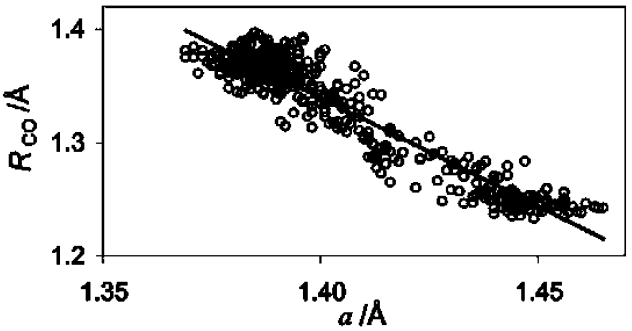

Figure 23. R_{C-O} bond lengths versus mean a-bond lengths, *correlation coefficient* = −0.952. Reprinted with permission from (Szatyłowicz H.; Krygowski, T. M. *Pol. J. Chem*. **2004**, *78*, 1719), copyright 2004, Polish Chemical Society, Warsaw, Poland.

ing with various N and O bases.[387] Figure 23 shows this scatter plot with the regression line that has the form R(CO) = −1.918a + 4.025.

As we can see, the slope is close to that for the model system presented for the π-electron model of interactions, although it is slightly greater. This means that, even for such a diversified collection of H-bond systems based on the geometry patterns retrieved from the Cambridge Structural Database (variously mono- and poly-substituted derivatives of phenol with substituents such as halogens, $-NO_2$, $-NH_2$, $-COOH$, $-CONH_2$, $-COCH_3$, $-COOCH_3$, $-CHO$, $-OH$, $-SH$, $-N{=}O$, $-Me$, $-i$Pr, $-t$Bu, $-Ph$, $-CPh_3$, $-SiMe_3$, $-SO_3H$, and $-H$) and very different bases, the main kind of H-bond effect on the geometry of the ring is mesomeric in nature, although some contribution from the electronegativity effect cannot be excluded.

It is worth mentioning that other dependences, such as R_{CO} versus ipso angle α and α versus a(av) are equally good, as it is shown in Figure 23.[387] This finding is in line with the interrelation between α versus a(av) found for 74 monosubstituted benzene derivatives (optimized at the HF/6-31G* level of theory).[388] The same kind of observation was even found for monosubstituted derivatives of *tert*-butyl,[389] supporting a σ-electron nature of the deformation.[390]

5.3. Changes in π-Electron Delocalization in the Ring of Phenol Derivatives Interacting via H-Bonds with Various Bases

Application of HOMA index (eq 21) and its extended form (eq 22) revealed how π-electron delocalization depends upon the strength of the H-bond, at least in the case of a large group of H-bond complexes of phenol derivatives. Parts a−c of Figure 24[391] show the dependences of HOMA, GEO, and EN indices on the C−O bond length, i.e., the approximate value of the H-bond strength.[392]

It results from the scatter plot in Figure 24a that the intermolecular H-bond of variously substituted phenol derivatives with a variety of bases affects dramatically with the aromatic character of the phenolic ring. The stronger the H-bond (the shorter d_{C-O}), the greater is the decrease of aromaticity.

Because of the form of the extended HOMA (eq 22), the scatter plots of HOMA (Figure 24a) and GEO

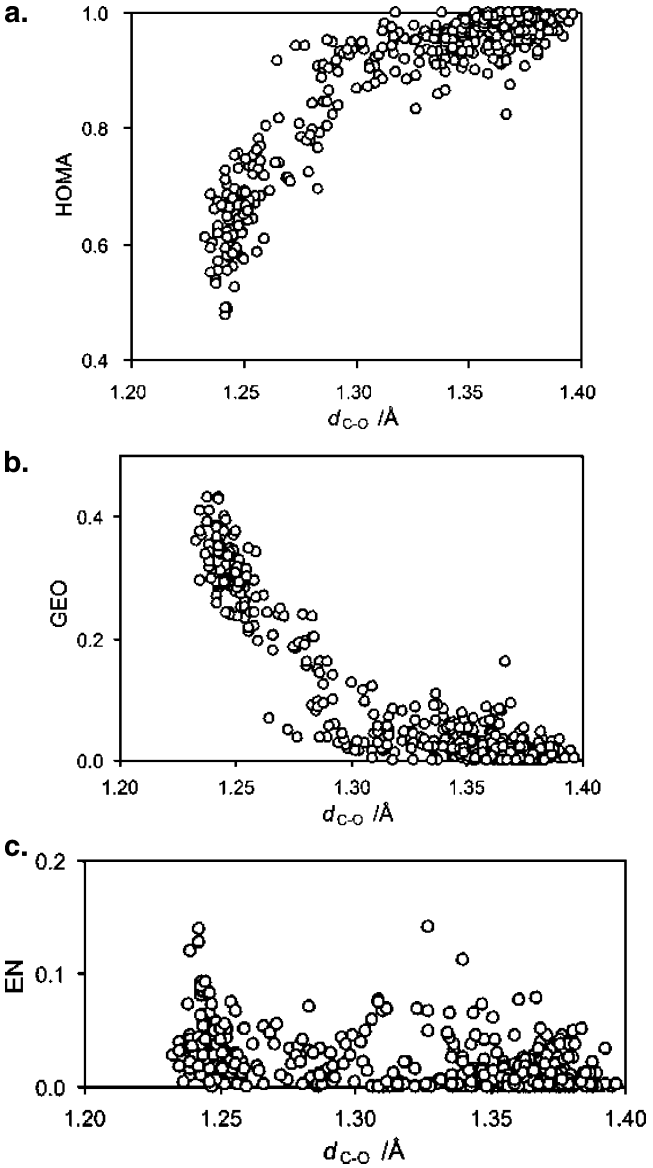

Figure 24. Relationship between (a) HOMA, (b) GEO, and (c) EN terms and C−O bond length, d_{C-O}, for H-bond complexes of variously substituted phenols. Reprinted with permission from (Krygowski, T. M.; Szatyłowicz H.; Zachara J. E., *J. Chem. Inf. Comput. Sci*. **2004**, *44*, 2077), copyright 2004, American Chemical Society, Washington, DC.

(Figure 24b) versus d_{C-O}, are almost complementary; a mediating term of EN in eq 22 is practically negligible, as shown in Figure 24c. Thus, the changes in the bond lengths alternation are the most important structural consequences of the H-bond, and the changes are remarkable. The HOMA index varies from 1.0 to about 0.5, i.e., half of the scale between the aromatic and nonaromatic systems! Substantial dispersion of points in scatter plots in parts a−c of Figure 24 results not only from a large variation of the kind of substitution of the ring but also from intermolecular interactions in the crystal, often referred to as crystal-lattice-packing forces. For a more detailed inspection, Figure 25 presents the dependence of HOMA on CO bond lengths for seven types of substituted phenols (for which the number of hits in CSD is greater than 10).[393] When the OH···base interactions were modeled by pX−Ph−

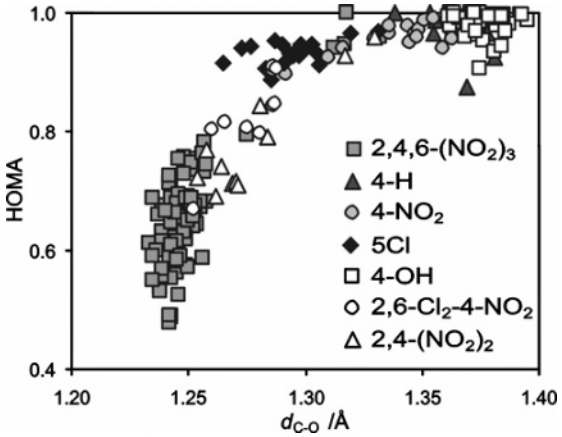

Figure 25. Dependence of HOMA on C−O bond length, d_{C-O}, for 7 types of substituted phenol. Reprinted with permission from (Krygowski, T. M.; Szatyłowicz H.; Zachara J. E. *J. Chem. Inf. Comput. Sci*. **2004**, *44*, 2077), copyright 2004, American Chemical Society, Washington, DC.

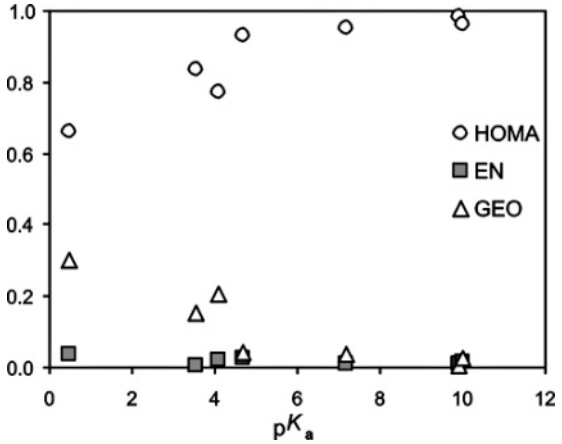

Figure 26. Plot of HOMA, GEO, and EN mean values versus pK_a for seven types of substituted phenol. Reprinted with permission from (Krygowski, T. M.; Szatyłowicz H.; Zachara J. E. *J. Chem. Inf. Comput. Sci*. **2004**, **2004**, *44*, 2077), copyright 2004, American Chemical Society, Washington, DC.

O···H···F$^-$ complexes, the HOMA versus d_{CO} plots had a much more precise shape.[394]

We should note that the scatter of the points for different complexes of a given group might result from the difference in the kind of bases interacting with the OH group of the phenol derivative.

The H-bond strength depends on the pK_a of the proton-donating system,[42] which in turn depends upon the kind of substituent and the nature of bases. The first factor is taken into account by averaging the data for a given group. The mean values of the HOMA, GEO, and EN indices plotted against pK_a values of a particular phenol derivative (i.e., uniquely substituted phenol derivative for which CSD gave more than 10 hits) give a convincing argument as to how aromaticity patterns depend upon the H-bond strength, as shown in Figure 26. The stronger acidity of the proton-donating substituted phenol, the stronger the H-bond is formed and the greater the loss of aromatic character of the ring, i.e., the lower the HOMA value. Once again, the bond lengths alternation term (GEO) is revealed as the most important in determining aromaticity of the ring in H-bond complexes of phenol derivatives, whereas the role of the EN term is chaotic and hence negligible.

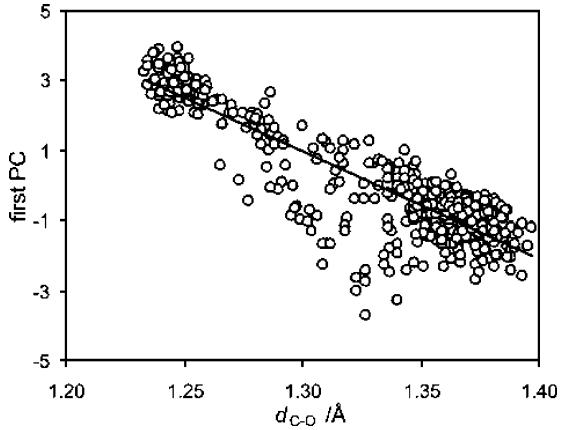

Figure 27. Dependence of first principal component of PCA (when bond lengths of the ring were taken into account) on CO bond length for variously substituted phenols, $cc = -0.902$. Reprinted with permission from (Krygowski, T. M.; Szatyłowicz H.; Zachara J. E. *J. Chem. Inf. Comput. Sci*. **2004**, **2004**, *44*, 2077), copyright 2004, American Chemical Society, Washington, DC.

It should be emphasized here that the geometry pattern of the molecules estimated by use of the X-ray crystallographic technique may be biased by crystal-packing forces. However, the bond lengths are the hardest structural parameters, and in most cases, they are less sensitive to deformation.[395] Application of the principal component analysis (PCA)[396,397] to a set of H-bond phenol derivatives of the ring bond lengths of 664 data set has revealed that the first principal component (PC) explains 47% of the total variance, and five more components are necessary to explain 98.2% of the total variance. Thus, undoubtedly the side effects affect the structural data of the ring. However, when the first PC is plotted against the C−O bond length, d_{C-O}, the dependence is encouraging, as shown in Figure 27. This means that the first PC is related to changes in the geometry parameters of the ring caused by the H-bond of which the strength is approximated by d_{CO} values.[392] Elimination of the sources resulting from the different kind of substitution and using only the data for *p*-nitrophenol H-bond complexes showed again that the first principal component explains only 51.4% of the total variance.[391] The remaining part of variance may be attributed to intermolecular interactions in the crystal lattice. However, despite side effects resulting from crystal-packing forces, it may be concluded that the main effect is due to the H-bond.

5.4. *Ab Initio* Modeling of the H-Bond Effect on the Ring in the Para-Substituted Derivatives of Phenol

Modeling of the OH···base interactions with a purpose of analysis of H-bond effects on the aromaticity of the ring in phenol and its para-substituted derivatives was carried out using the Lee−Yang−Parr correlation functional and 6-311+G** basis set [B3LYP/6-311+G(d,p)].[398−401] Two systems of H-bond

complexes are considered: $(PhO\cdots H\cdots F)^-$ and $(p\text{-}NO_2PhO\cdots H\cdots F)^-$, each in two situations. One of them deals with a stronger interaction (25a) and the other, with a weaker one (25b). Ar stands for Ph− or p-NO_2Ph−

$$ArOH\cdots F^- \quad (25a)$$

$$ArO^-\cdots HF \quad (25b)$$

The modeling was applied to the phenol− and p-nitrophenol−fluoride complexes: the fluoride is approaching the molecule of p-nitrophenol/phenol along the line, being a prolongation of the OH-bonding direction, as shown in Chart 23. Partial geometry

Chart 23

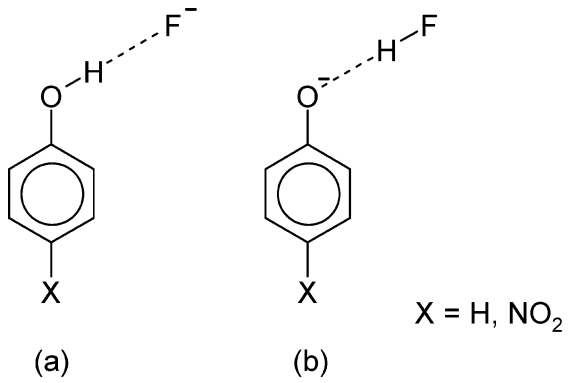

optimization (because the O···F distance was controlled and linearity of O···H···F is assumed) was performed for all of the complexes: ArOH with F^- and $ArO^-\cdots HF$.

Chart 23 shows a structural scheme of the computational model: (a) fluoride approaches the oxygen atom in hydroxyl group, and (b) hydrofluoric acid approaches the oxygen atom in phenolate anion. The shortening of the O···F distance is in case a associated with an increase of the energy of interactions because of an increase in the strength of the H-bond and in consequence with a shortening of the C−O bond length,[392] as shown in Figure 28. In case b, the opposite is true. The values of d_{C-O} have already been used as a convenient estimate of the strength of the

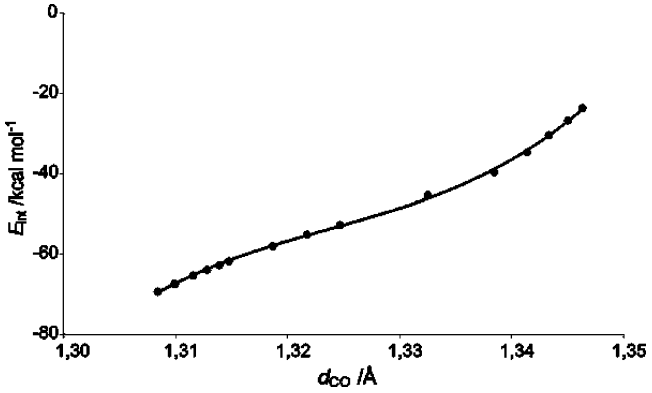

Figure 28. Calculated values of interaction energy as a function of CO bond lengths (■). Reprinted with permission from (Krygowski, T. M.; Zachara, J. E.; Szatyłowicz H. *J. Phys. Org. Chem.* **2005**, *18*, 110), copyright 2005, J. Wiley, New York.

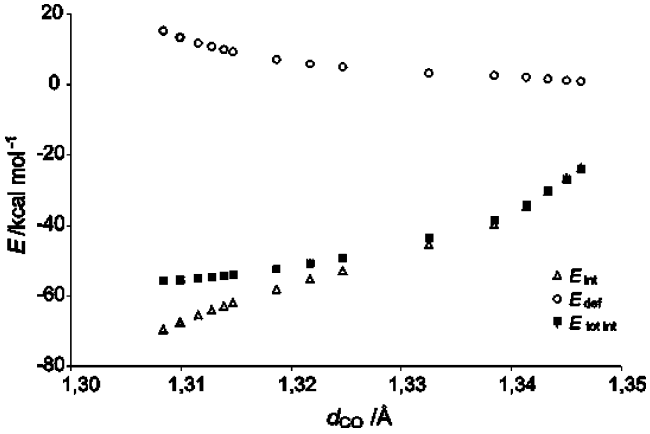

Figure 29. Calculated values of E_{int} (eq 26), E_{def} (eq 27), and the sum of these terms plotted versus CO bond lengths for the variation of O···F. Reprinted with permission from (Krygowski, T. M.; Zachara, J. E.; Szatyłowicz H. *J. Phys. Org. Chem.* **2005**, *18*, 110), copyright 2005, J. Wiley, New York.

H-bond in phenol complexes,[131] and recently, the dependence of d_{C-O} on pK_a of phenols was also found.[402]

However, it is worth mentioning that the H-bond interactions shown in Chart 23(a) are associated with the deformation of the molecule involved, and the energy of this change of geometry may be computed. Equations 26 and 27 present electronic energy of interaction and deformation, respectively.

$$E_{int} = E_{AB}(basis_{AB};opt_{AB}) - E_A(basis_{AB};opt_{AB}) - E_B(basis_{AB};opt_{AB}) \quad (26)$$

$$E_{def} = E_A(basis_A;opt_{AB}) - E_A(basis_A;opt_A) \quad (27)$$

where A is p-nitrophenol, B is F^-, and $E_A(basis_A;opt_{AB})$ means that the energy of molecule A was calculated using internal coordinates of the A molecule and for the geometry obtained during optimization of complex A−B. Note that this approach takes into account the correction for the basis set superposition error.[403] Figure 29 presents variation of energies of interaction and deformation and their sum plotted against the changes of CO bond lengths for the variation of O···F.

Closer inspection of Figure 29 shows that the deformation energy decreases with the decrease of the H-bond strength. Note that in this direction the

Chart 24

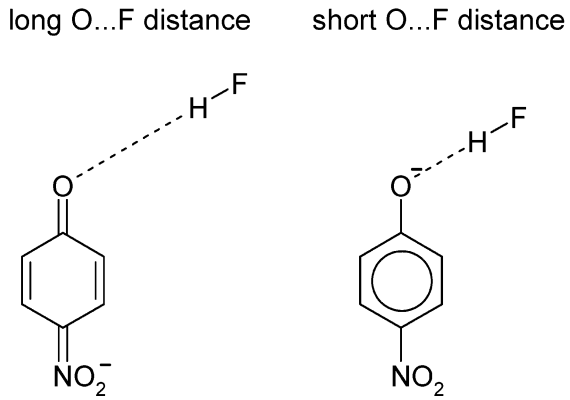

Chart 25

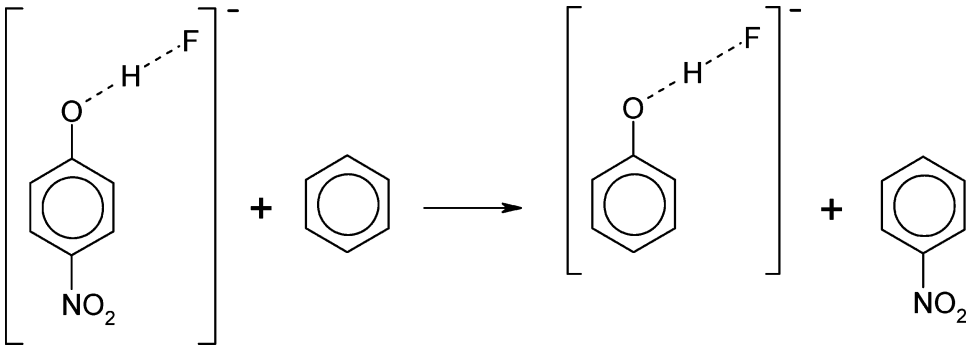

ring becomes more similar to that in benzene itself; the decrease of the quinoid structure weight is expected as illustrated in Chart 24, which shows a scheme of canonical structures associated with the geometry changes in the ring because of the formation of the H-bond (Chart 23) for extreme values of O···F distances.

Very recently an analysis of the dependences of structural changes and π-electron delocalization on the strength of the H-bond has been performed, and three kinds of approaches were investigated:[404] (i) energetic by the use of the homodesmotic reaction (scheme in Chart 25) proper for substituent effects,[405] hereafter abbreviated as SESE (from substituent effect stabilization energy) shown by the scheme in Chart 25; (ii) magnetism-based index NICS-$(1)_{zz}$,[362,375,378] and (iii) geometry-based index HOMA[370] (eqs 21 and 22).

An energetic characteristic of the substituent effect associated with the H-bond is shown by means of variation of the SESE values in dependence on the O···F distance. The changes for these two systems (eqs 25a and 25b) differ significantly, as shown in Figure 30a.

From the point of view of stabilization because of the substituent effect, the case of $O^-\cdots HF$ interactions exhibits higher energy (21−25 kcal/mol) than the other one, $OH\cdots F^-$ (7−15 kcal/mol). This is due to a much stronger through-resonance effect of O^- than OH as substituents interacting with the *p*-nitro group. The appropriate substituent constants for $-NO_2$, $-OH$, and $-O^-$ are $\sigma_p^- = 1.27$ and $\sigma_p^+ = -0.92$ and -2.3, respectively.[406] In the case of the $O^-\cdots HF$ interaction, one may visualize it by a scheme in Chart 24.

The changes in H-bond strength (resulting from and dependent on the O···F distance) cause significant changes in aromaticity indices, HOMA (Figure 30b) and $NICS(1)_{zz}$ (Figure 30c).

Clearly, the $ArO^-\cdots HF$ interactions lead to a much greater variation in the values of both NICS and HOMA indices than the $ArOH\cdots F^-$ ones, in agreement with the much expected stronger through-resonance effects of substituents in the first case. The resonance effect is also seen for phenol itself.

When the NICS and HOMA values are plotted directly against the "strength" of the H-bond, namely, against d_{C-O},[392] the dependences are still more convincing, as shown in parts a and b of Figure 31. The H-bond affects substantially π-electron delocalization in the ring in phenol and its *p*-nitro-derivative

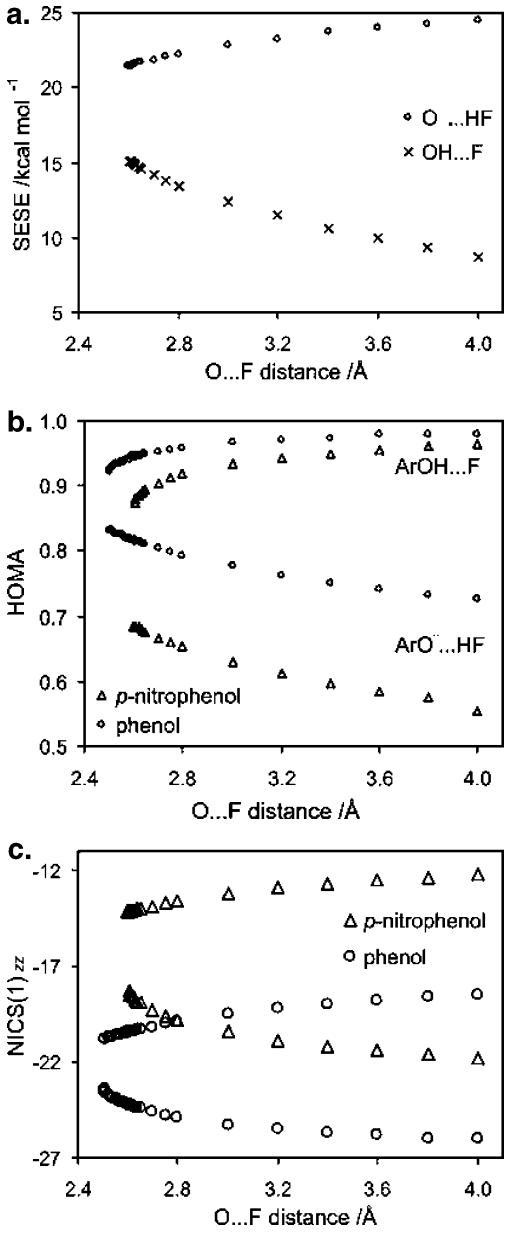

Figure 30. (a) Scatter plots of SESE values (Chart 25) for two kinds of H-bond (eqs 25a and 25b) versus the O···F distance. Variation of (b) HOMA values and (c) NICS(1)zz values for $ArOH\cdots F^-$ and $ArO^-\cdots HF$ interactions for *p*-nitrophenol (△) and phenol (○) complexes. Reprinted with permission from (Krygowski, T. M.; Zachara, J. E.; Szatyłowicz H. *J. Org. Chem.* **2004**, *69*, 7038), copyright 2004, American Chemical Society, Washington, DC.

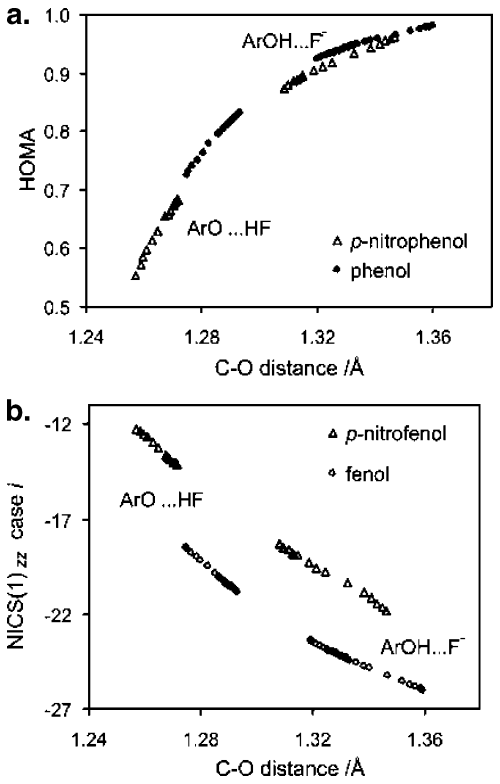

Figure 31. Plots of (a) HOMA and (b) $NICS(1)_{zz}$ values versus C−O bond length for *p*-nitrophenol and phenol complexes with fluoride. Two kinds of interactions are taken into account (eqs 25a and 25b). Reprinted with permission from (Krygowski, T. M.; Zachara, J. E.; Szatyłowicz H. *J. Org. Chem*. **2004**, *69*, 7038), copyright 2004, American Chemical Society, Washington, DC.

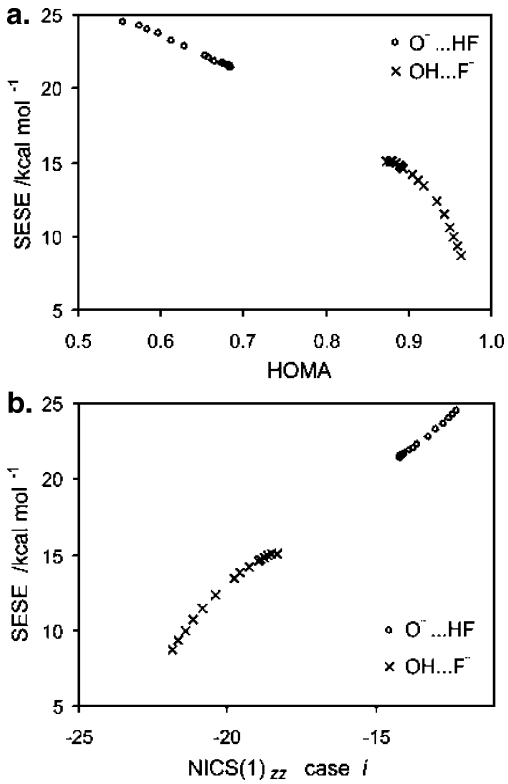

Figure 32. Relationships between SESE and (a) HOMA and (b) NICS(1)zz. Two kinds of interactions were taken into account (eqs 25a and 25b). Reprinted with permission from (Krygowski, T. M.; Zachara, J. E.; Szatyłowicz H. *J. Org. Chem*. **2004**, *69*, 7038), copyright 2004, American Chemical Society, Washington, DC.

complexes with fluoride. Again, the $ArO^{-}\cdots HF$ complexes exhibit a stronger variation of HOMA and NICS indices than $ArOH\cdots F^{-}$, following the reasoning presented for interpretation of parts b and c of Figure 30.

In the case of *p*-nitrophenol, we were able to compute the SESE values and intercorrelation between the energetic characteristic and geometry- and magnetism-based indices was made possible. Parts a and b of Figure 32 show those relationships.

In both cases of relations between the substituent stabilization effect measured by SESE and aromaticity indices HOMA and NICS, a clear monotonic dependence is observed. The strongest interaction is observed for the systems with the least aromatic character of the ring. This observation is in line with the former interpretation: for $(X)ArO^{-}\cdots HF$, a strong through resonance between X = nitro group and O^{-} groups takes place and hence increased stabilization occurs.

Recently, more detailed computational [B3LYP/6-311+G(d,p) level of approximation] analysis of the H-bond strength affecting π-electron delocalization in the ring was carried out for [*p*-X−Ph−O···H···F^{-}] complexes supported fully by the experimental data and findings discussed formerly and leading to additional observations. When the O···F distance is shortened (see Chart 23), at some value of the distance, the proton transfer from $ArOH\cdots F^{-}$ to $ArO^{-}\cdots HF$ occurs. This distance depends linearly upon σ_p-substituent constants with a correlation coefficient of 0.996, indicating an increase of stability to transfer (a larger O···F distance) with an increase of electron-accepting power of the substituent. Similarly good dependences were observed for d_{CO} versus σ_p scatter plots for $ArOH\cdots F^{-}$ and $ArO^{-}\cdots HF$ complexes, with correlation coefficients of −0.993 and −0.995, respectively. Finally, very good monotonical dependences of d_{CO} versus ^{1}H NMR chemical shifts (Figure 33a) and HOMA versus ^{1}H NMR chemical shifts (Figure 33b) showed a good mutual relationship between the approximate measure of H-bond strength (d_{CO}), magnetic property, ^{1}H NMR chemical shifts, and geometry-based aromaticity index HOMA.

It results from all of the presented scatter plots (Figure 30a, parts a and b of Figure 31, and parts a and b of Figure 33) that π-electron delocalization in the ring of phenol and its derivative depends significantly upon the strength of the H-bond.

In the case of $OH\cdots F^{-}$ interactions, the stronger the H-bond, the lower is π-electron delocalization detected by aromaticity indices. In the case of the hydroxy group as a proton-donating one, a decrease of the aromatic character of the ring is caused by an increase in double character of the CO bonds as a result of the H-bond with fluoride. This kind of decrease of aromaticity was also observed in the case of pyrrole rings in porphyrines: the CC bonds in the bridges between the pyrrole rings, C−CH−C, are relatively short, leading in consequence to low HOMA values for pyrrole, in the range of 0.4−0.6 units,[407] whereas for the isolated pyrrole ring (or substituted

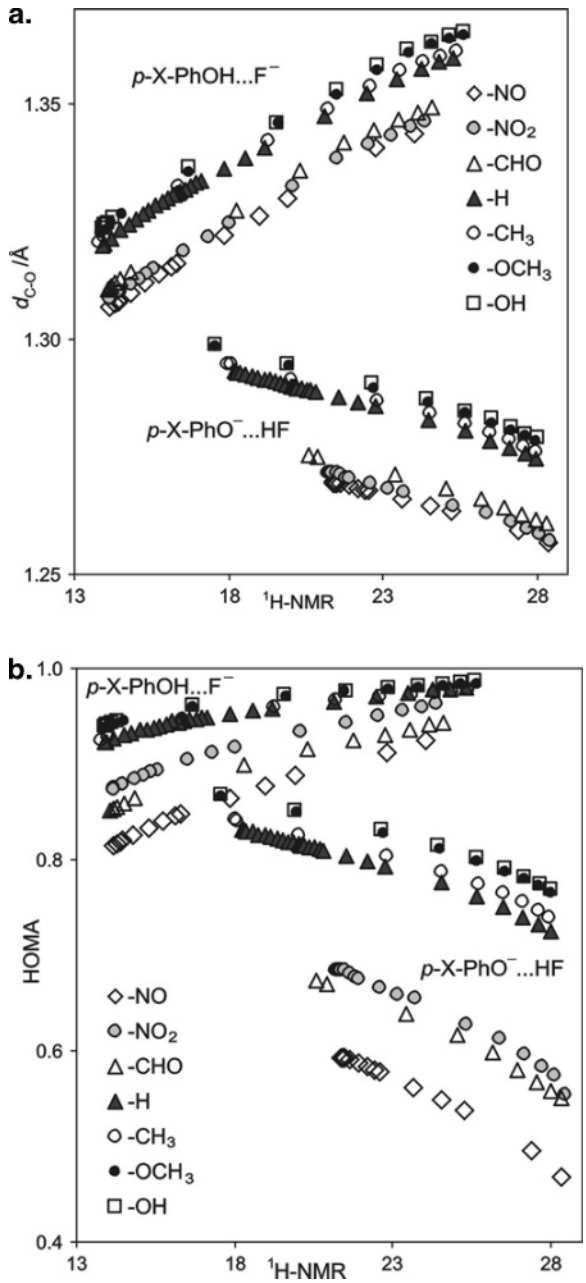

Figure 33. (a) Dependence of two empirical measures of H-bond strengths: the ^{1}H NMR chemical shift of the proton involved and C−O bond length, d_{C-O}, for [*p*-X−PhO···H···F]$^-$ complexes. (b) Dependence of HOMA value on ^{1}H NMR chemical shift of the proton involved in [*p*-X−PhO···H···F]$^-$ complexes. Reprinted with permission from (Krygowski, T. M.; Szatyłowicz H.; Zachara, J. E. *J. Chem. Inf. Model*. **2005**, *45*, 652), copyright 2005, American Chemical Society, Washington, DC.

by a group linked by a single bond) HOMA = ~0.9.[407,408]

A substantial change (an increase) in aromaticity was observed in the heterocyclic bases of DNA and RNA as a consequence of H-bond formation in the Watson−Crick pairs. The effect was found for both, the experimental geometries retrieved from CSD and the *ab initio* optimized systems [at the MP2/6-311+G(d,p) level of approximation].[409] Figure 34 presents the dependence of global HOMA values of the whole molecule in the DNA or RNA bases on the number of C=O or C=N bonds attached to the ring.

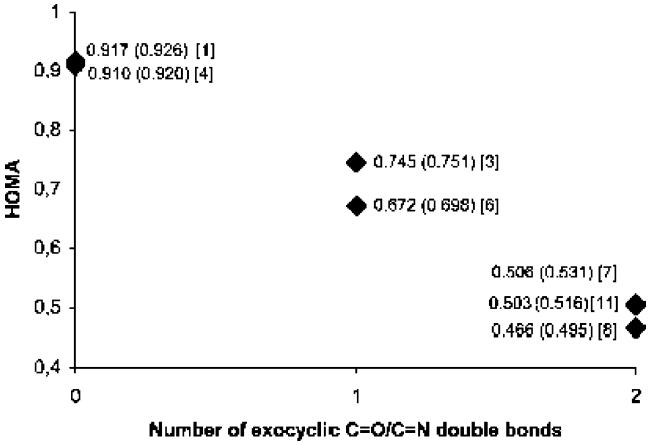

Figure 34. Dependence of the global (i.e., over all molecule) aromaticity index HOMA on the number of C=O and C=N bonds attached to the ring systems. Reprinted with permission from (Cyrański, M. K.; Gilski, M.; Jaskólski, M.; Krygowski T. M. *J. Org. Chem.* **2003**, *68*, 8607), copyright 2004, American Chemical Society, Washington, DC.

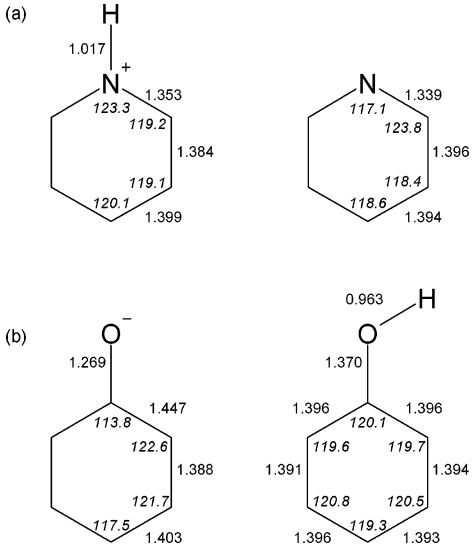

Figure 35. Bond lengths (Å) and bond angles (deg) of pyridine and pyridinium cation (Majerz, I.; Koll, A. *Acta Crystallogr., Sect. B: Struct. Sci.* **2004**, *60*, 406) and of phenol and phenolate (Szatylowicz, H.; Zachara, J. E., private communication).

When the pair of bases is formed via the H-bond, the double-bonded N or O atoms become the proton acceptors and the bonds become longer. In consequence, the aromatic character of the ring to which the bonded N or O atoms are linked increases.

The H-bond complex of pyridine with substituted phenol derivatives has been analyzed recently[410] describing the changes in perturbation of the geometry of the ring because of H-bond formation by use of a function of variance for the CC-bond lengths. Application of the HOMA index to the optimized geometry [B3LYP/6-31G(d,p) level of approximation] of both rings for the limiting situation, i.e., for pyridine and its protonated form,[410] and phenolate and phenol (Figure 35) led to the following HOMA values: pyridine (0.991), pyridinium cation (0.978), phenol (0.971), and phenolate anion (0.577). Additionally, the geometry of phenol and phenolate

anion and HOMA values for these systems are given.[411] The difference in π-electron delocalization is negligible in the case of proton transfer in the pyridine/pyridinium anion pair, whereas in the case of the phenol/phenolate pair, the effect is dramatic. This may be interpreted as follows: the basic atom in pyridine interacts with the proton via the lone electron pair lying in the plane of the molecule; the nitrogen, containing only one π-type electron, affects weakly the ring π-electron structure. A different situation is in the case of the phenol/phenolate pair: the lone pair accepting proton lies also in the plane of the molecule, but the oxygen atom contains a pair of π-type electrons able to conjugate with the ring. Hence, they present some kind of "surplus" and interact stronger with the π-electron structure of the ring, which causes a greater change in π-electron delocalization.

When we look at the changes of the ipso angle in proton-donor and proton-acceptor molecules for both pairs presented in Figure 35, it may be noticed that the same change in both cases, namely, the acceptation of a proton, increases the angle by about 7°. The difference is observed for ipso-ortho bond lengths. In the case of the pyridine−pyridinium cation pair, the difference in this bond after proton transfer is less than 0.02 Å, whereas for the pair phenolate anion−phenol, the difference is slightly greater than 0.05 Å. In the case of both pairs, proton transfer to the base leads to an increase of electronegativity of the proton-accepting site (oxygen and nitrogen atoms) and hence to a substantial change in the ipso angle; the Walsh−Bent rule works.[404] In the case of bond lengths, the effect is associated not only with the changes in electronegativity but also, even to a greater extent, with the mesomeric effect, in other words, with a possibility of π-electron delocalization.[379]

5.5. Intramolecular H-Bond Systems

Molecules or molecular ions containing the intramolecular H-bond consist of two kinds of intramolecular interactions, the H-bond itself and the interactions because of the nature of the spacer. This is a case where in eq 1 (chapter 1) R_1 and R_2 are linked with each other. The part linking A and B is called a spacer.

Chart 26 presents a typical situation, in which B is a basic atom with a lone pair (most often oxygen

Chart 26

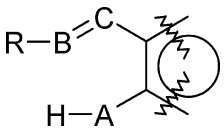

or nitrogen atoms) that may be involved in the acceptation of the proton from the A−H group. The BCCCA fragment is named a spacer. This part may be but not necessarily a π-electron system.

Only a few attempts have been made to estimate π-electron delocalization in the spacer applying standard descriptors, such as for instance aromaticity indices. Application of the HOMA index to experimental geometry of cyclic thioamide β-diketone derivatives,[412] in which the spacer is a π-electron system, gave somewhat unexpected results. The π-electron delocalization in the sulfur-containing (H)OCCCS system is greater than in the oxygen/nitrogen (H)NCCCO···H one (Chart 27); the ranges

Chart 27

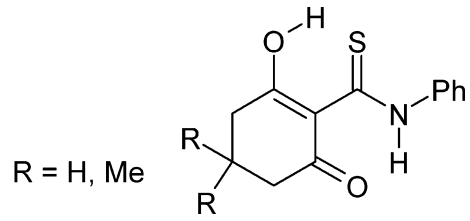

of HOMA values for these two cases are 0.47−0.75 and 0.12−0.40, respectively. It is rather not probable that the NH···O hydrogen bond is weaker than OH···S;[328] thus, a different factor must work here. In the case of the (H)OCCCS system, there is no double-bonded group attached to the spacer, whereas in the case of the (H)NCCCO···H system, the C=S group induces a stronger localization of the π-electron system; hence, there is weaker π-electron delocalization in the (H)NCCCO···H system.

The H-bond in *ortho*-hydroxy derivatives of Schiff bases is a model kind of interaction for the intramolecular H-bond systems.[413] In most bases of this kind studied so far in the crystalline state, the proton is localized at the oxygen atom, but in some cases, the proton position is disordered over two sites, at the nitrogen and oxygen atoms. Hence, the problem of π-electron delocalization in *ortho*-hydroxy Schiff bases is well-represented in the literature. Application of the HOMA index to the experimental geometry of the spacer for seven systems of the shape as in Chart 28[414] gave the range of values 0.20−0.59.

Chart 28

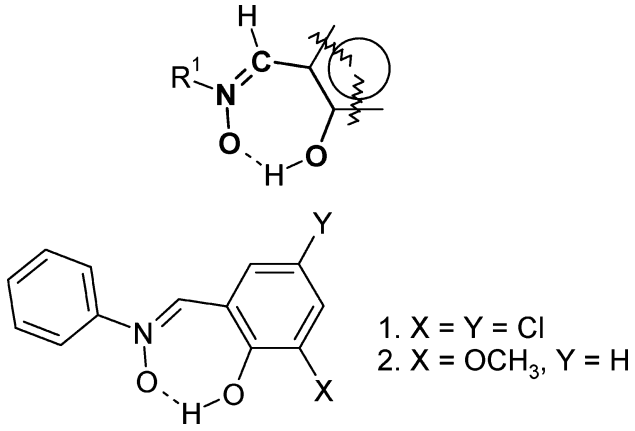

However, these relatively high values of HOMA result rather from the push−pull interaction between C=N and OH groups, which simultaneously are the proton-accepting and proton-donating groups. Optimization of the model system at the B3LYP/6-311+G(d,p) level of approximation and computation of NICS for the quasi-ring built up of the spacer and the OH···N gave values in the range of 1.8−2.5 (depending upon the conformation of OH and NH

groups), indicating a rather anti-aromatic character of this system. Interestingly, when proton in the model system was replaced by lithium cation, Li^+, the NICS values became negative (−1.79) and HOMA for the spacer rose to 0.945. Note that lithium has an empty $2p_z$ orbital that may be used for π-electron conjugation, whereas the energy of this orbital in the hydrogen is much higher.

A much more representative sample ($n = 47$) of experimental geometries of *ortho*-hydroxy Schiff bases was used to study π-electron delocalization of the spacer built up of N=C and two CC and CO bonds between the H-bond-donating OH group and H-bond-accepting nitrogen atom in the C=N bond, leading to a similar conclusion. Moreover, no dependence of HOMA on the N···O interatomic distance was found.[415]

The first experimental detection of the ionic H-bond in *ortho*-hydroxy Schiff bases in the crystal state was done for 5-nitro-*N*-salicydeneathylamine.[416] It revealed a substantial decrease of aromaticity in the ring for the ionic form, HOMA = 0.732. Polysubstitution of benzene usually decreases the ring aromaticity;[417] the mean HOMA value for 154 molecular geometries of 1,2,4-trisubstituted benzene derivatives (topologically equivalent to the studied Schiff base) equals 0.96, which is in line with the value for the neutral form, estimated for an averaged structure of 147 neutral Schiff bases, for which the HOMA = 0.972. Thus, the decrease of π-electron delocalization in the ring is unexpectedly large and is due to an increase of weight of the keto form of canonical structures. These changes are accompanied with the opposite tendency of HOMA values for the spacer, 0.622 for the ionic form and 0.324 for the neutral one. Interestingly, the decrease of aromaticity in the ionic form is dominantly due to the increase of bond-length alternation (GEO term = 0.24), similarly as the decrease of π-electron delocalization in the spacer of the neutral form (GEO = 0.44). Chart 29 presents

Chart 29

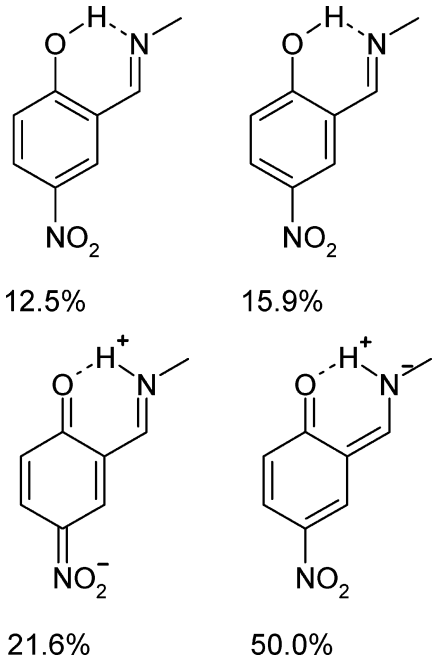

Table 7. HOMA Values for the Ring and for the Spacer for Enol-imine (Abbreviated e-i) and Keto-amine (k-a) Form of Orthohydroxy[a]

level of calculation	HOMA e-i/ring	HOMA k-a/ring	HOMA e-i/spacer	HOMA k-a/spacer
B3LYP/6-31G(d,p)[b]	0.928	0.626	0.284	0.680
B3LYP/6-311+G(d,p)	0.925	0.388	0.382	0.571
B3LYP/aug-ccpVDZ	0.899	0.386	0.341	0.564
MP2/aug-cc-pVDZ	0.845	0.426	0.195	0.585

[a] Schiff bases estimated at different levels of computation. [b] Methyl group attached to the N atom of the base.

canonical structure weights estimated by the use of the HOSE model.[418,419] The ionic form of the H-bond is caused by a strong through-resonance effect between the 4-nitro and 1-hydroxy groups, because of their strong electron-accepting and -donating power, respectively.

A recent comparative structural study on neutral and ionic H-bonds in *ortho*-hydroxy Schiff bases included not only the analysis of geometry patterns but also the experimental charge density studies.[79] The low-temperature, high-resolution X-ray studies employed dianil of 2-hydroxy-5-methylisophthalaldehyde (the case of the neutral H-bond system), 3,5-dinitro-*N*-salicylidenoethylamine, and 3-nitro-*N*-salicylidenocyclo-hexylamine (both ionic H-bond systems).[420] It was concluded that, according to the geometric and bond critical point (BCP) parameters, the neutral OH···N hydrogen bonds seem to be stronger than the ionic ones. Elipticities in BCPs of CC bonds in the ring in a neutral H-bond system (dianil of 2-hydroxy-5-methylisophthalaldehyde) are smaller than in the case of ionic systems. This is in line with the geometry-based conclusion resulting from HOMA values made earlier.[416] The HOMA values for the ring in these three systems (dianil of 2-hydroxy-5-methylisophthalaldehyde, 3,5-dinitro-*N*-salicylidenoethyl-amine, and 3-nitro-*N*-salicylidenocyclo-hexylamine) are 0.92, 0.62, and 0.60, respectively. The changes of HOMA in the spacer are opposite in the sequence: 0.35, 0.49, and 0.55, respectively.

Theoretically based modeling of the consequences of ionic/neutral hydrogen-bonded systems on the π-electron delocalization parameters of the simplest case of *ortho*-hydroxy Schiff base with O···H···N hydrogen bonding[421,422] is presented in Table 7.

A few conclusions result from the data of Table 7. First, the level of theory does not change substantially the qualitative picture of the changes in the π-electron delocalization in the ring and spacer. Second, there is an approximate relation between the π-electron delocalization in the ring and spacer, as it was also found in experimental analyses.[416,423] In the case of neutral systems (or enol−imino systems), high values of the indices in the ring correspond to low values in the spacer. An opposite situation is observed for the keto−amine states (close to ionic states): low values of the indices in the ring correspond to higher values in the spacer.

Recently, an analysis of π-electron delocalization in the aromatic moiety and in the chelate chain was carried out[424] for the H-bond systems as *ortho*-hydroxy ketimines[425] and *ortho*-hydroxy ketones.[426]

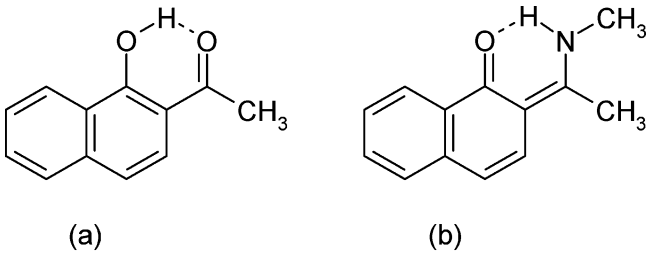

Figure 36. Structures of H-bond in (a) 2-hydroxyacetonaphthone and (b) *ortho*-hydroxyacetonaphthone-imine(2-[1*E*)]-1-methylimono)ethyl]naphthalen-1-olate.

Geometry-based parameters were used, with HOMA for estimation of the aromatic character of the ring and plotted against the aromatic stabilization energy (ASE) of the spacer for the H-bond system, leading to an approximate linear dependence.[418] It results from this dependence that an increase of the aromatic character of the ring in phenol is associated with a decrease of stability of the chelate chain. When HOMA is plotted against d_{OH}, which reflects the strength of the H-bond well, then the increase of the H-bond strength is associated with the decrease of aromaticity monitored by HOMA values.

Application of the same procedure to a system in which the chelate chain belongs partly to naphthalene gives information about how the H-bond interaction affects π-electron delocalization in a more distant ring.[424]

In the crystal structure of 2-hydroxyacetonaphthone (Figure 36a), the prevailing position of the proton is at the hydroxylic oxygen atom, whereas in *ortho*-hydroxy acetonaphthone-imine [2-[(1*E*)]-1-(methylimino)ethyl] naphtha-len-1-olate (Figure 36b), the proton resides at the nitrogen atom. The observed differences bear substantial consequences as far as π-electron delocalization is concerned. In the first case, the aromaticity of the ipso ring is only slightly lower than in naphthalene itself, HOMA = 0.746 (naphthalene = 0.827),[427] whereas for the second ring, the aromaticity is more distant, HOMA = 0.873, even exceeding the value for naphthalene itself. A dramatic difference is observed in the case of the *ortho*-hydroxy acetonaphthone-imine derivative (Figure 36b), with the HOMA value for the first ring = 0.310, whereas for the second one, it is almost the same as for 2-hydroxyacetonaphthone, 0.878. Again, we observe that in the ionic-like H-bond (the case of *ortho*-hydroxy acetonaphthone-imine) system, the π-electron rings become much less aromatic than in the case of typically covalent H-bond systems.

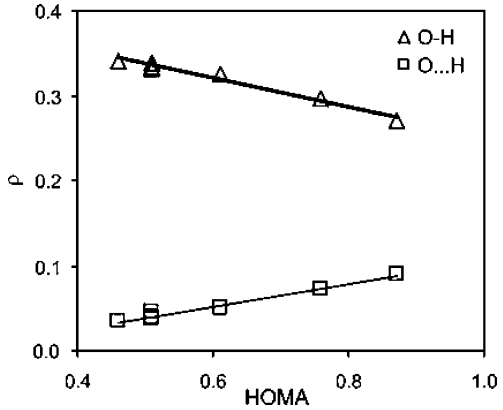

Figure 37. Dependences of electron density in BCP of O−H bond (△) and O···H bond (□) on HOMA values for substituted derivatives of malonaldehyde. Correlation coefficients are −0.989 and 0.990, respectively. Reprinted with permission from (Krygowski, T. M.; Zachara, J. E., *Theor. Chem. Acc.*, in press), copyright Springer, New York.

Another systematic study of the π-electron delocalization is associated with differently substituted (F and Cl in three different positions) derivatives of malonaldehyde.[247,266,268] The schemes in Charts 14 and 15 present labeling and two conformers of malonaldehyde: the bridged and "open" conformers.

Table 8 presents the obtained values of HOMA, EN, and GEO calculated from geometry,[268] the electronic density (in e/a_o^{-3}), and Laplacian in bond critical points (abbreviated BCP) of O−H and O···H and in ring critical point (RCP); all of them were obtained from the optimization made at the MP2/6-311++G(d,p) level of approximation.

Looking at the HOMA values and its components, it is clear that the dominant contribution to the variation in HOMA values results from the changes in bond alternation (GEO term), whereas the EN term is almost negligible. When the electron densities in BCP of OH and H···O, the ρ(O−H) and ρ(O···H), are plotted against HOMA, the scatter plots are as presented in Figure 37.[428]

Surprisingly good are also the dependences of electron density and its Laplacian in ring critical points on HOMA values, as shown in parts a and b of Figure 38. This means that π-electron delocalization, which is undoubtedly monitored by electron density and its Laplacian at the ring critical point is well-correlated with the geometry-based index HOMA (correlation coefficient of 0.98 or better). Similar relationships, although slightly worse, were also

Table 8. Labeling of the Substituted Derivatives of Malonaldehyde, Values of HOMA, EN, and GEO, Electronic Density (in au, e/a_o^3) and Laplacian (in au, e/a_o^5) in Bond Critical Points of O−H and O···H and in Ring Critical Ponts, and Energy of H-Bond, Results Obtained at the MP2/6-311++G(d,p) Level of Approximation

R_1,R_2,R_3	HOMA	EN	GEO	ρ(O−H)	ρ(O···H)	ρ(RCP)	$\nabla^2\rho$(H···O)	$\nabla^2\rho$(RCP)	E_{HB}	E_{HB}[a]
H,H,H	0.61	0.06	0.33	0.326	0.05	0.0205	0.1387	0.1277	−12.15	−10.41
H,F,H	0.51	0.05	0.43	0.335	0.04	0.0185	0.1232	0.1126	−9.73	−8.38
H,Cl,H	0.51	0.07	0.41	0.331	0.046	0.0197	0.1349	0.1215	−10.83	−9.68
H,H,F	0.46	0.02	0.51	0.341	0.035	0.0186	0.1161	0.1096	−9.14	−9.14
H,H,Cl	0.51	0.03	0.46	0.339	0.038	0.0189	0.1222	0.1136	−9.24	−8.63
F,H,H	0.87	0.02	0.11	0.27	0.091	0.0257	0.1386	0.1647	−13.47	−8.67
Cl,H,H	0.76	0.04	0.2	0.296	0.072	0.0237	0.1499	0.1509	−12.49	−8.82

[a] HF/6-311++G(d,p) results.

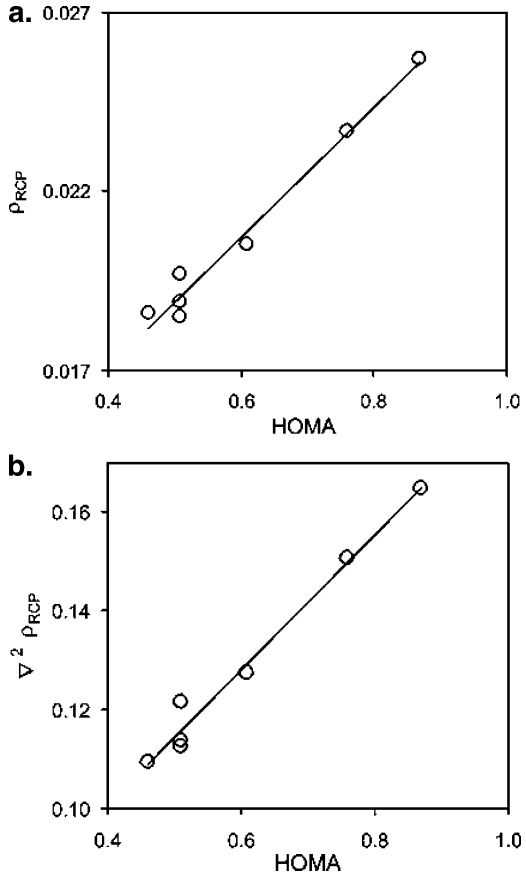

Figure 38. Dependence of (a) electron density and (b) Laplacian of the electron density in RCP on HOMA values; the linear correlation coefficients are equal to 0.988 and 0.990, respectively. Reprinted with permission from (Krygowski, T. M.; Zachara, J. E., *Theor. Chem. Acc.*, in press), copyright Springer, New York.

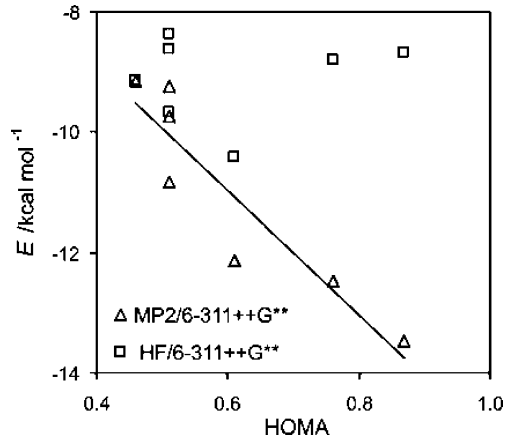

Figure 39. Dependence of H-bond energy on HOMA values for two levels of theory employed: HF/6-311++G(d,p) (□) and including the electron correlation, MP2/6-311++G(d,p) (△). Correlation coefficient for the latest relationship −0.920. Reprinted with permission from (Krygowski, T. M.; Zachara, J. E., *Theor. Chem. Acc.*, in press), copyright Springer, New York.

found for 18 individual rings in 10 benzenoid hydrocarbons.[429]

The HOMA values are also well-correlated with the energy of H-bond computed as the difference of energy between the bridged and open conformers of malonaldehyde (Charts 14 and 15). Figure 39 presents this dependence. Interestingly, if the computations are carried out at the HF/6-311++G(d,p) level of approximation (□ in the figure), thus neglecting almost completely the electron correlation, there is practically no correlation. When the MP2/6-311++G(d,p) level of approximation is employed, which takes into account electron correlation, the correlation is quite acceptable, with a correlation coefficient = −0.92.

Recently, aromaticity of pyromeconic acid and its derivatives has been studied[430] in three states of charging: as cations, a neutral molecule, and anions (see Chart 30).

Chart 30

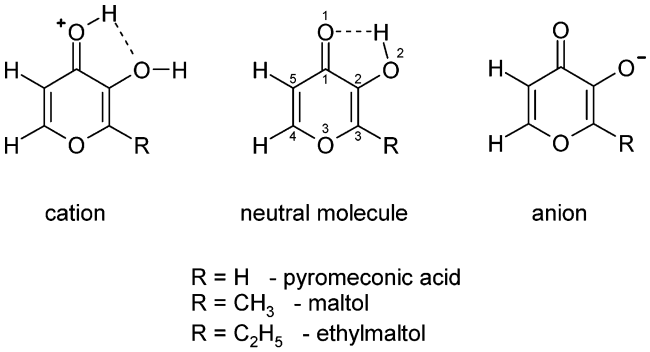

The substituent effect was not significant, but the effect of charge associated with the possibility of H-bond formation was dramatic. Table 9 presents aromaticity indices for pyromeconic acid; the data for both derivatives are very similar.

Independently of the method of optimization geometry, the sequence of aromaticity index HOMA is always the same: the most aromatic is the cation, followed by a neutral molecule, and finally the anion. This finding undoubtedly points nicely to a substantial influence of the H-bond on π-electron delocalization in the pyran ring. Interestingly, if the derivatives of maltol are complexed with oxovanadium(IV) ion,[431] then the π-electron delocalization in the pyran ring resembles a situation between that in the maltol cation and a neutral molecule. The spacer OCCO behaves as in the case of the maltol cation, indicating an important role played by oxovanadium(IV) ion in these complexes.

Table 9. Aromaticity Data for Pyromeconic Acid Determined by Four Different Models of Calculation[a]

aromaticity index	HF	SVWN	B3LYP	B1LYP
neutral molecule				
HOMA	−0.16	0.47	0.16	0.18
GEO	1.15	0.52	0.78	0.75
EN	0.02	0.01	0.06	0.07
cation				
HOMA	0.73	0.85	0.82	0.77
GEO	0.29	0.15	0.18	0.24
EN	−0.02	0.00	0.00	−0.01
anion				
HOMA	−0.66	−0.07	−0.48	−0.47
GEO	1.34	0.71	0.93	0.94
EN	0.33	0.35	0.55	0.52

[a] All computations were carried out by use of 6-311++G(d,p) basis set.

6. Conclusions

The earliest used criterion for the recognition of A−H···B H-bonds was IR spectroscopy and particularly the intensity and location of the ν(AH) band. The changes of these parameters are undoubtedly associated with the changes in charge distribution in the region of the H-bond. The ^{1}H and bridge atoms NMR chemical shifts as a measure of magnetic shielding are also associated with the changes in electron distribution. In both cases, they reveal mainly local electron delocalization.

Sharp changes of IR and NMR parameters are observed when approaching the so-called critical region of the proton-donor−acceptor region associated with the appearance of a double minimum potential for the proton motion. In this region, one observes a jump of the dipole moment connected with complete reorganization of charge distribution. The existence of the double minimum for the proton motion is one of the most characteristic features of H-bonds.

In principle, the H-bond reveals a situation in which a more or less ionized hydrogen atom is immersed in electron clouds of the two closest negatively charged atoms belonging to different or the same molecule (inter- and intramolecular H-bonds). The location of the hydrogen atom and its interactions with both neighboring atoms is undoubtedly associated with electron delocalization. This may be both local and/or observed over a longer distance in the systems involved in the H-bond. The latter may be associated with cooperative interactions discussed in terms of the resonance-assisted H-bond, which lead to π-electron delocalization of distant bonds built of atoms bearing π electrons. Formation of conjugate−chelate rings in which the proton is formally considered as one of the members of the ring leads to some unique features. If the H-bond ring is fused to the aromatic system, it may affect dramatically π-electron delocalization in the aromatic part of the system. These phenomena are revealed in the AIM and aromacity parameters as well as ^{13}C NMR chemical shifts discussed in detail in this review.

7. Acknowledgments

Dedicated to Professor Paul von Rague Schleyer on his 75 birthday. Support has been provided by the State Committee for Scientific Research (KBN number 3T09A 138 26)

8. Note Added in Proof

Since the completion of this manuscript, a paper appeared dealing with the tautomeric equilibria, H-bond, and π-electron delocalization in *o*-nitrosophenol.[432] It has shown that aromaticity of the phenyl ring plays a principal role in stability of the favored tautomer of *o*-nitrozophenol. Localization of the π-electron structure because of a strong push−pull effect of ortho substituents destabilizes the system. H-bond decreasing the push−pull effect interaction between the electron-donating group (OH or O^-) and the electron-accepting group (NO or NOH^+ groups) stabilizes the system and increases π-electron delocalization.

9. References

(1) Lehn, J.-M. *Angew. Chem., Int. Ed. Eng*. **1990**, *29*, 1304.
(2) Lehn, J.-M. *Supramolecular Chemistry*; Verlag-Chemie: Weinheim, Germany, 1995.
(3) Teda, F. *Biorg. Chem*. **1991**, *19*, 157.
(4) Rebek, R., Jr. *Science* **1987**, *235*, 1478.
(5) Jeffrey, G. A.; Saenger, W. *Hydrogen Bonding in Biological Structures*; Springer-Verlag: Berlin, Germany, 1990.
(6) Gerlt, J. A.; Kreevoy, M. M.; Cleland, W. W.; Frey, P. A. *Chem. Biol*. **1997**, *4*, 259.
(7) Perrin, C. L.; Nielson, J. B. *Annu. Rev. Phys. Chem*. **1997**, *48*, 511.
(8) Franks, F., Ed.; *Water. A Comprehensive Treatise*; Plenum Press: New York, 1972.
(9) Benoit, M.; Marx, D.; Parinello, M. *Nature* **1998**, *392*, 258.
(10) Kitaigorodskii, A. I. *Molecular Crystals and Molecules*; Academic Press: New York, 1973.
(11) Braga, D., Grepioni, F., Orpen, A. G., Eds.; *Crystal Engineering: From Molecules and Crystals to Materials*; Kluwer Academic Publishers: Dordrecht, Germany, 1999.
(12) Desiraju, G. R. *Crystal Engineering. The Design of Organic Solids*; Elsevier: Amsterdam, The Netherlands, 1989.
(13) Subramanian, S.; Zaworodko, M. J. *Coord. Chem. Rev*. **1994**, *137*, 357.
(14) Etter, M. C. *Acc.Chem. Res*. **1990**, *23*, 120.
(15) Etter, M. C.; Bernstein, J. B.; McDonald, J. C. *Acta Crystallogr., Sect. B: Struct. Sci.* **1990**, *46*, 256.
(16) Desiraju, G. R. *Angew. Chem., Int. Ed. Eng*. **1995**, *34*, 2311.
(17) Lang, S. B.; Das-Gupta, D. K. *Ferroelectr. Rev*. **2000**, *2*, 217.
(18) Colomban, P., Ed.; *Proton Conductors. Solids, Membranes, and Gels—Materials and Devices*; Cambridge University Press: New York, 1992.
(19) Waluk, J., Ed.; *Conformational Analysis of Molecules in Excited State*; J. Wiley-VCh: New York, 2000.
(20) Borsenberger, P. M.; Weiss, D. S. *Organic Photoreceptors for Imaging Systems*; Marcel Dekker: New York, 1993.
(21) Tour, J. M. *Molecular Electronics. Commercial Insight, Chemistry, Devices, Architecture, and Programming*; World Scientific: Singapore, 2003.
(22) *Pure Appl. Chem*. **1999**, *71*, 1919.
(23) Pauling L. *The Nature of the Chemical Bond*, 3rd ed.; Cornell University Press: Ithaca, NY, 1960.
(24) Kaplan I. G. *Theory of Molecular Interactions; Studies in Physical and Theoretical Chemistry*; Elsevier: Amsterdam, The Netherlands, 1986; Vol. 42.
(25) Grabowski, S. J. *J. Phys. Chem. A* **2001**, *105*, 10739.
(26) Desiraju, G. R. *Acc. Chem. Res*. **2002**, *35*, 565.
(27) Steiner, T. *Angew. Chem. Int. Ed. Eng.* **2002**, *41*, 48.
(28) Gordon, M. S.; Jensen, J. H. *Acc. Chem. Res*. **1996**, *29*, 536.
(29) Gu, Y.; Kar, T.; Scheiner, S. *J. Am. Chem. Soc*. **1999**, *121*, 9411.
(30) Read, W. G.; Flygare, W. H. *J. Chem. Phys*. **1982**, *76*, 2238.
(31) Frisch, M. J.; Pople, J. A.; Del Bene, J. E. *J. Chem. Phys*. **1983**, *78*, 4063.
(32) Leiserowitz, L. *Acta Crystallogr., Sect. B: Struct. Sci.* **1976**, *32*, 775.
(33) Bernstein, J.; Etter, M. C.; Leiserowitz, L. The role of hydrogen bonding in molecular assemblies. In *Structure Correlation*; Bürgi, H.-B., Dunitz, J. D., Eds.; VCH: Weinheim, Germany, 1994.
(34) Gilli, G. Molecules and molecular crystals. In *Fundamentals of Crystallography*; Giacovazzo, C., Ed.; IUCr, Oxford Science Publications: Oxford University Press: New York, 2002.
(35) Jeffrey, G. A. *An Introduction to Hydrogen Bonding*, Oxford University Press: New York, 1997.
(36) Desiraju G. R.; Steiner T. *The Weak Hydrogen Bond in Structural Chemistry and Biology*; Oxford University Press: New York, 1999.
(37) Gilli, G.; Belluci, F.; Ferretti, V.; Bertolesi, V. *J. Am. Chem. Soc*. **1989**, *111*, 1023.
(38) Bergmann, E. D., Pullman, B., Eds.; *Aromaticity, Pseudoaromaticity, Antiaromaticity*; Proceeding of an International Symposium held in Jerusalem 1970, Israel, Academy of Sciences and Humanities, Jerusalem, 1971.
(39) Minkin, V. I.; Glukhovtsev, M. N.; Simkin, B. Ya. *Aromaticity and Antiaromaticity—Electronic and Structural Aspects*; J. Wiley: New York, 1994.
(40) Special issue on aromaticity; Schleyer, P. v. R., Ed.; *Chem. Rev*. **2001**, *101*, 1115.
(41) Krygowski, T. M.; Cyrański, M. K. *Phys. Chem. Chem. Phys*. **2003**, *6*, 249.
(42) Huyskens, P.; Zeegers-Huyskens, T. *J. Chim. Phys*. **1964**, *61*, 84.
(43) Bell, R. P. *The Proton in Chemistry*; Chapman and Hall, London, U.K., 1959.
(44) McWeeney, R. *Coulson's Valence*, Oxford University Press: New York, 1979; chapter 6, table 6.7.

(45) Bartmess, J. E. *Negative Ion Energetics Data in NIST WebBook*, NIST Standard Reference Database Number 69; Linstrom, P. J., Mallard, W. G., Eds.; National Institute of Standards and Technology: Gaithersburg, MD; p 20899.
(46) Scheiner, S.; Grabowski, S. J.; Kar, T. *J. Phys. Chem. A* **2001**, *105*, 10607.
(47) Wessel, J.; Lee, J. C.; Peris, E.; Yap, G. P. A.; Fortin, J. B.; Ricci, J. S.; Sini, G.; Albinati, A.; Koetzle, T. F.; Eisenstein, O.; Rheingold A. L.; Crabtree, R. H. *Angew. Chem., Int. Ed. Engl.* **1995**, *34*, 2507.
(48) Grabowski, S. J. *J. Phys. Chem. A* **2000**, *104*, 5551.
(49) Custelcean, R.; Jackson, J. E. *Chem. Rev*. **2001**, *101*, 1963.
(50) Epstein, L. M.; Shubina, E. S. *Coord. Chem. Rev*. **2002**, *231*, 165.
(51) Aoyama, T.; Matsuoka, O.; Nakagawa, N. *Chem. Phys. Lett*. **1979**, *67*, 508.
(52) Scheiner, S.; Grabowski, S. J. *J. Mol. Struct*. **2002**, 615, 209.
(53) Nishio, M.; Umezawa, Y.; Hirota, M.; Takeuchi, Y. *Tetrahedron* **1995**, *51*, 8701.
(54) Meyer, E. A.; Castellano, R. K.; Diederich, F. *Angew. Chem. Int. Ed.* **2003**, *42*, 1210.
(55) Hadži, D., Thompson, W., Eds.; *The Hydrogen Bonding*; Pergamon Press: London, U.K., 1959.
(56) Pimentel, G.; McClellan, A. *The Hydrogen Bond*; Freeman: San Francisco, CA, 1960.
(57) Vinogradov, S. N.; Linnel, R. H. *The Hydrogen Bond*; van Nostrand-Reinhold: New York, 1971.
(58) Joesten, M. D.; Schaad, L. J. *Hydrogen Bonding*; Marcel Dekker: New York, 1974.
(59) Schuster, P., Zundel, G., Sandorfy, C., Eds.; *The Hydrogen Bond. Recent Development in Theory and Experiments*; North-Holland: Amsterdam, The Netherlands, 1976.
(60) Scheiner, S. *Hydrogen Bonding. A Theoretical Perspective*; Oxford University Press: Oxford, U.K., 1997.
(61) Hadzi, D., Ed.; *Theoretical Treatments of Hydrogen Bonding*; J. Wiley, Chichester, U.K., 1997.
(62) Sobczyk, L., Ed.; *Hydrogen Bonding* (in Polish); PWN: Warszawa, Poland, 1969.
(63) Sokolov, N. D., Ed.; *Hydrogen Bonding* (in Russian); Nauka: Moscow, Russia, 1981.
(64) *J. Mol. Struct.*, special issue, **2004**, *700*.
(65) Szalewicz, K. *Encyclopedia of Physical Science and Technology*, 3rd ed.; Academic Press: New York, 2002; Vol. 7, p 505.
(66) Jeziorski, B.; Moszyński., R.; Szalewicz, K. *Chem. Rev*. **1994**, *94*, 1887.
(67) Lutz, H. D.; Engelen, B. *Trends Appl. Spectrosc*. **2002**, *4*, 355.
(68) Dziembowska, T. *Pol. J. Chem*. **1994**, *69*, 1455.
(69) Müller-Dethlefs, K.; Hobza, P. *Chem. Rev*. **2000**, *100*, 143.
(70) Basilevsky, M. V.; Vener, M. V. *Russ. Chem. Rev*. **2003**, *72*, 1.
(71) Sobczyk, L. *Wiadom. Chem*. (in Polish) **2000**, *55*, 593.
(72) Lutz, H. D. *J. Mol. Struct*. **2003**, *646*, 227.
(73) Grabowski, S. J. *J. Phys. Org. Chem*. **2004**, *17*, 18.
(74) Dziembowska, T. *Pol. J. Chem*. **1998**, *72*, 193.
(75) Buckingham, A. D. The Hydrogen Bond: An Electrostatic Interaction?; van Duijneveldt-van de Rijdt, J. G. C. M., van Duijneveldt, F. B.; In: *Theoretical Treatments of Hydrogen Bonding*; Hadži, D. Ed.; J. Wiley: Chichester, U.K., 1997.
(76) Schuster, P. Energy surfaces for hydrogen bonded systems. In *The Hydrogen Bond*; Schuster, P., Zundel, G., Sandorfy, C., Eds.; North-Holland: Amsterdam, The Netherlands; Vol. 1, pp 25−165.
(77) For best critical approach and collection of van der Waals radii, see Bondi, A. *J. Phys. Chem*. **1964**, *68*, 441.
(78) Bader, R. F. W. *Atoms in Molecules, A Quantum Theory*; Oxford University Press: Oxford, U.K., 1990.
(79) Koritszansky, T. S.; Coppens, P. *Chem. Rev*. **2001**, *101*, 1583.
(80) Koch, U.; Popelier, P. L. *J. Phys. Chem*. **1995**, *99*, 9747.
(81) Morokuma, K. *J. Chem. Phys*. **1971**, *55*, 1236.
(82) Lennard-Jones, J. E. *Proc. R. Soc*. **1924**, *106*, 463.
(83) Watts, R. O.; McGee, I. G. *Liquid-State Chemical Physics*; J. Wiley and Sons: New York, 1976.
(84) Sobczyk, L. *Khim. Phys.* **2005**, *24*, 31.
(85) Hagler, A. T.; Lifson, S.; Dauber, P. *J. Am. Chem. Soc*. **1979**, *101*, 5122.
(86) Katrusiak, A. Pressure-induced H-tansfers in the networks of hydrogen bonds, in: *Frontiers of High-Pressure Research II: Application of High Pressure to Low-Dimensional Novel Electronic Materials*; Hochheimer et al. Eds.; Kluwer Academic Publishers, The Netherlands, 2001, pp 73−85.
(87) Katrusiak, A. *Cryst. Res. Technol*. **1991**, *26*, 52.
(88) Katrusiak, A. *Cryst. Rev*. **2003**, *9*, 91.
(89) Ozeryanskii, V. A.; Pozharskii, A. F.; Głowiak, T.; Majerz, I.; Sobczyk, L.; Grech, E.; Nowicka-Scheibe, J. *J. Mol. Struct*. **2002**, *607*, 1.
(90) Jeziorski, B.; van Hemert, M. *Mol. Phys*. **1976**, *31*, 713.
(91) Chipman, D. M.; Bowman, J. D.; Hirschfelder, J. O. *J. Chem. Phys*. **1973**, *56*, 2427.
(92) Morokuma, K.; Kitaura, K. in *Molecular Interactions*; Ratajczak, H., Orville-Thomas, W. J., Eds.; John Wiley and Sons Ltd.: New York, 1980; Vol. 1, pp 21−66.
(93) Scheiner, S.; Kar, T.; Pattanayak, J. *J. Am. Chem. Soc*. **2002**, *124*, 13257.
(94) Hohenberg, P.; Kohn, W. *Phys. Rev. B* **1964**, *864*, 136.
(95) Kohn, W.; Sham, L. J. *Phys. Rev. A* **1965**, *140*, 1133.
(96) Chałasiński, G.; Szczęśniak, M. M. *Chem. Rev*. **2000**, *100*, 4227.
(97) Novak, A. *Struct. Bonding* **1974**, *18*, 177.
(98) Huyskens, P.; Sobczyk, L.; Majerz, I. *J. Mol. Struct*. **2002**, *615*, 61.
(99) Kollman, P. A.; Allen, L. C. *J. Am. Chem. Soc*. **1970**, *92*, 6101.
(100) Scheiner, S. *J. Phys. Chem*. **1982**, *86*, 376.
(101) Scheiner, S.; Kar, T. *J. Am. Chem. Soc*. **1995**, *117*, 6970.
(102) Bieńko, A. J.; Latajka, Z.; Sawka-Dobrowolska, W.; Sobczyk, L.; Ozeryanskii, V. A.; Pozharskii, A. F.; Grech, E.; Nowicka-Scheibe, J. *J. Chem. Phys*. **2003**, *119*, 4313.
(103) Ozeryanskii, V. A.; Pozharskii, A. F.; Bieńko, A. J.; Sawka-Dobrowolska, W.; Sobczyk, L. *J. Phys. Chem*. **2005**, *109*, 1637.
(104) Perrin, C. L.; Ohta, B. K. *J. Am. Chem. Soc*. **2001**, *123*, 6520.
(105) Smallwood, C. J.; McAllister, M. A. *J. Am. Chem. Soc*. **1997**, *119*, 11277.
(106) Zundel, G. Hydrogen bonds with large proton polarizability and proton-transfer processes in electrochemistry and biology. In *Advanced Chemistry and Physics*; Prigogine, I., Rice, S. A., Eds.; J. Wiley: New York, 2000; Vol. 111.
(107) Benedict, H.; Limbach, H.-H.; Wehlan, M.; Fehlhammer, W.-P.; Golubev, N. S.; Janoschek, R. *J. Am. Chem. Soc*. **1998**, *120*, 2939.
(108) Janoschek, R.; Weideman, E. E.; Pfeifer, H.; Zundel, G. *J. Am. Chem. Soc*. **1972**, *94*, 2387.
(109) Hayd, A.; Zundel, G. *J. Mol. Struct. (THEOCHEM)* **2000**, *500*, 421.
(110) Danninger, W.; Zundel, G. *J. Chem. Phys*. **1981**, *74*, 2769.
(111) Hawranek, J. P.; Muszyński, A. S. *J. Mol. Struct*. **2000**, *552*, 205.
(112) Pearson, R. G. *Coord. Chem. Rev*. **1990**, *100*, 403.
(113) Whiffen, D. H. *Trans. Faraday Soc*. **1958**, *54*, 327.
(114) Zeegers-Huyskens, Th. *J. Mol. Struct*. **1988**, *117*, 125.
(115) Zeegers-Huyskens, Th. *J. Mol. Liq*. **1986**, *32*, 151.
(116) Ault, B. S.; Steinback, E.; Pimentel, G. C. *J. Phys. Chem*. **1975**, *79*, 615.
(117) Sobczyk, L. *Mol. Phys. Rep*. **1996**, *14*, 19.
(118) Smirnov, S. N.; Golubev, N. S.; Denisov, G. S.; Benedict, H.; Schah-Mohammedi, P.; Limbach, H.-H. *J. Am. Chem. Soc*. **1996**, *118*, 4094.
(119) Dega-Szafran, Z.; Szafran, M.; Stefaniak, L.; Brevard, C.; Bourdonneau, M. *Magn. Reson. Chem.* **1996**, *24*, 424.
(120) Majerz, I.; Malarski, Z.; Sobczyk, L. *Chem. Phys. Lett*. **1997**, *274*, 361.
(121) See, e.g., Brycki, B.; Brzeziński, B.; Zundel, G.; Keil, Th. *Magn. Reson. Chem*. **1992**, *30*, 507.
(122) Brycki, B.; Szafran, M. *J. Chem. Soc., Perkin Trans. 2* **1984**, 223.
(123) see, e.g., Kalenik, J.; Majerz, I.; Sobczyk, L.; Grech, E.; Habeeb, M. M. M. *Collect. Czech. Chem. Commun*. **1990**, *55*, 80.
(124) Albrecht, G.; Zundel, G. *J. Chem. Soc., Faraday Trans*. **1984**, *80*, 553.
(125) Huyskens, P.; Cleuren, W.; Franz, M.; van Brabant-Gevaerts, H. M.; Vuylsteke, M. A. *J. Phys. Chem*. **1980**, *84*, 2748.
(126) Huyskens, P. *J. Mol. Struct*. **1986**, *135*, 67.
(127) Lippincott, E.; Schroeder, R. *J. Chem. Phys.* **1955**, *23*, 1099.
(128) Saitoh, T.; Mori, K.; Itoh, R. *Chem. Phys*. **1981**, *60*, 161.
(129) Somorjai, R. L.; Hornig, D. F. *J. Chem. Phys*. **1962**, *36*, 1980.
(130) Krygowski, T. M.; Kalinowski, M. K.; Turowska-Tyrk, I.; Hiberty, P. C.; Milart, P.; Silvestro, A.; Topsom, R. D.; Daehne, S. *Struct. Chem.* **1991**, *2*, 71.
(131) Dziembowska, T.; Szczodrowska, B.; Krygowski, T. M.; Grabowski, S. J. *J. Phys. Org. Chem.* **1994**, *7*, 142.
(132) Krygowski, T. M.; Grabowski, S. J.; Anulewicz-Ostrowska, R.; Izdebski, J.; Fiertek, D. *Pol. J. Chem*. **2002**, *76*, 129.
(133) Biczysko, M.; Latajka, Z. *J. Phys. Chem. A* **2002**, *106*, 3197.
(134) Henrie-Rousseau, O.; Blaise, P. Infrared spectra of hydrogen bond. Basic theories. Indirect and direct relaxation mechanisms in weak hydrogen-bonded systems. In *Theoretical Treatments of Hydrogen Bonding*; Hadži, D., Ed.; J. Wiley: Chichester, U.K., 1997; p 165.
(135) Henrie-Rousseau, O.; Blaise, P.; Chamma, D. *Adv. Chem. Phys*. **2002**, *121*, 241.
(136) Hadži, D.; Bratos, S. Vibrational spectroscopy of the hydrogen bond. In *The Hydrogen Bond. Recent Developments in Theory and Experiments*; Schuster, P., Zundel, G., Sandorfy C., Eds.; North-Holland: Amsterdam, The Netherlands, 1976; Vol. 2, p 565.
(137) Belhayara, K.; Chamma, D.; Henri-Rousseau, O. *J. Mol. Struct*. **2003**, *648*, 93.
(138) Romanowski, H.; Sobczyk, L. *Chem. Phys*. **1977**, *19*, 361.
(139) Romanowski, H.; Sobczyk, L. *Acta Phys. Pol., A* **1981**, *60*, 545.
(140) Bratos, S. J. *Chem. Phys*. **1975**, *63*, 3499.
(141) Borgis, D.; Tarjus, G.; Azzouz, H. *J. Chem. Phys*. **1992**, *97*, 1390.
(142) Witkowski, A. J. *Chem. Phys*. **1983**, *79*, 852.
(143) Witkowski, A. *Phys. Rev. A* **1990**, *41*, 3511.
(144) Marechal, E.; Bratos, S. *J. Chem. Phys*. **1978**, *68*, 1825.
(145) Marechal, E.; Ratajczak, H. *Chem. Phys*. **1986**, *110*, 103.

(146) Brzeziński, B.; Brycki, B.; Zundel, G.; Keil, T. *J. Phys. Chem*. **1991**, *95*, 8598.
(147) Szafran, M. *Wiadom. Chem.* (in Polish) **1988**, *42*, 167.
(148) Golubev, N. S.; Shenderovich, I. G.; Smirnov, S. N.; Denisov, G. S.; Limbach, H.-H. *Chem.—Eur. J*. **1999**, *5*, 492.
(149) *NMR Spectroscopy of Hydrogen-Bonded System*; Limbach, H.-H., Gunther H., Eds.; special issue of *Magn. Reson. Chem*., 2001, Vol. *39*.
(150) Hansen, P. E. *Isotope Effects on Chemical Shift as a Tool in Structural Studies*; Roskilde University Press: Denmark, 1996.
(151) Grech, E.; Klimkiewicz, J.; Nowicka-Scheibe, J.; Pietrzak, M.; Schilf, W.; Pozharskii, A. F.; Ozeryanskii, V. A.; Bolwig, S.; Abildgaard, J.; Hansen, P. E. *J. Mol. Struct*. **2002**, *615*, 121.
(152) Mielke, Z.; Sobczyk, L. In *Isotope Effects in Chemistry and Biology*; Kohen, A., Limbach, H.-H., Eds.; CRC Press: Boca Raton, FL, in press.
(153) Zeegers-Huyskens, Th.; Sobczyk, L. *J. Mol. Liq*. **1990**, *46*, 263.
(154) Ichikawa, M. *J. Mol. Struct*. **2000**, *552*, 63.
(155) Schowen, K. B.; Schowen, R. L. *Methods Enzymol*. **1982**, *87*, 551.
(156) Ichikawa, M.; Gustafsson, T.; Olovsson, I. *J. Mol. Struct*. **1994**, *321*, 21.
(157) Sobczyk, L.; Engelhardt, H.; Bunzl, K. In *The Hydrogen Bonds*; Schuster, P., Zundel, G., Sandorfy, C. Eds.; North-Holland: Amsterdam, The Netherlands, 1976; Vol. 3, p 937.
(158) Hawranek, J. P.; Sobczyk, L. *Acta Phys. Pol. A* **1971**, *33*, 639.
(159) Nouwen, R.; Huyskens, P. P. *J. Mol. Struct*. **1973**, *16*, 459.
(160) Proton solvation and proton mobility, Proceedings of a Research Workshop of the Israel Sience Foundations; Agmon, N., Gutman, M., Eds.; *Isr. J. Chem.* **1999**, *39*, 213.
(161) Mataga, N.; Kubota, T. *Molecular Interactions and Electronic Spectra*; Marcel Dekker: New York, 1970.
(162) Bertolasi, V.; Gilli, P.; Ferretti, V.; Gilli, G. *J. Am. Chem. Soc*. **1991**, *113*, 4917.
(163) Gilli, P.; Bertolasi, V.; Ferretti, V.; Gilli, G. *J. Am. Chem. Soc*. **1994**, *116*, 909.
(164) Bertolasi, V.; Gilli, P.; Ferretti, V.; Gilli, G. *Chem.—Eur. J*. **1996**, *2*, 925.
(165) Madsen, G. K. H.; Iversen, B. B.; Larsen, F. K.; Kapon, M.; Reisner, G. M.; Herbstein, F. H. *J. Am. Chem. Soc*. **1998**, *120*, 10040.
(166) Rozas, I.; Alkorta, I.; Elguero, J. *J. Phys. Chem. A* **2001** *105*, 10462.
(167) Swart, M.; Guerra, F.; Bickelhaupt, F. M. *J. Am. Chem. Soc.* **2004**, *126*, 16718.
(168) Takasuka, M.; Matsui, Y. *J. Chem. Soc., Perkin Trans. 2*, **1979**, 1743.
(169) Schaefer, T. *J. Phys. Chem*. **1975**, *79*, 1888.
(170) Odinokov, S. E.; Nabullin, A. A.; Mashkovsky, A. A.; Glazunov, V. P. *Spectrochim. Acta, Part A* **1983**, *39*, 1055.
(171) Gordy, W. C.; Stanford, S. C. *J. Chem. Phys*. **1940**, *8*, 170.
(172) Josien, M.-L.; Sourisseu, G., p 129; Shigorin, D. M., p 191; Burawoy, A., p 259; Cohen, M. D. et al., p 293; Hunsberger, M. et al., p 461; *Hydrogen Bonding*, papers presented at the symposium on hydrogen bonding held at Ljubljana, July 29—August 3, 1957; Hadži, D., Ed.; Pergamon Press: London, U.K., 1959.
(173) Craig, D. G. in *Nonbenzenoid Aromatic Compounds*; Ginsburg, D., Ed.; Interscience: New York, 1959; p 1.
(174) Lloyd, D.; Marshall, D. R. in *Aromaticity, Pseudoaromaticity and Antiaromaticity*, Proceedings of an International Symposium, Jerusalem, March 31—April 3, 1970; Bergmann, E. D., Pullman, B., Eds.; Israel Academy of Sciences and Humanities: Jerusalem, Israel, 1971; p 85.
(175) Gilli, P.; Bertolasi, V.; Pretto, L.; Antonov, L.; Gilli, G. *J. Am. Chem. Soc*. **2005**, *127*, 4943.
(176) Denisov, G. S.; Sheih-Zade, M. I.; Eskina, M. B. *Zh. Prikl. Spectr*. **1977**, *27*, 1049.
(177) Schreiber, V. M. *J. Mol. Struct.* **1989**, *197*, 73.
(178) Koll, A.; Ratajczak, H.; Sobczyk, L. *Rocz. Chem*. **1970**, *44*, 825.
(179) Burawoy, A.; Chamberlain, J. T. *J. Chem. Soc*. **1952**, 2310 and 3734.
(180) Sucharda-Sobczyk, A.; Sobczyk, L. *J. Chem. Res.* **1985**, *208*.
(181) Lutskii, A. E.; Klepanda, T. I.; Sheina, G. G.; Bartra-kova, L. P. *Zh. Prikl. Spectr*. **1976**, *25*, 735.
(182) Detoni, S.; Hadži, D.; Juranji, M. *Spectrochim. Acta, Part A* **1979**, *30*, 249.
(183) Josien, M.-L.; Fuson, N.; Lebas, J.-M.; Gregory, T. M. *J. Chem. Phys*. **1953**, *21*, 331.
(184) Hadži, D.; Sheppard, N. *Trans. Faraday. Soc*. **1954**, *50*, 911.
(185) Shigorin, D. N. *Hydrogen Bonding* (in Russian); Nauka: Moscow, Russia, 1964; p 195.
(186) Shigorin, D. N.; Shemyakin, M. M.; Kolosov, M. N. *Dokl. Akad. Nauk SSSR* **1956**, *108*, 672.
(187) Kopteva, T. S.; Shigorin, D. N. *Zh. Fiz. Khim*. **1974**, *48*, 532.
(188) Shigorin, D. N.; Gastilovich, Ye. A.; Kopteva, T. S.; Viktorova, N. M. *Opt. Spectrosc.* **1970**, *28*, 241.
(189) Brzezinski, B.; Zundel, G. *J. Phys. Chem*. **1982**, *86*, 5133.
(190) Filarowski, A.; Koll, A.; Głowiak, T. *J. Chem. Soc., Perkin Trans. 2* **2002**, 835.
(191) Filarowski, A.; Koll, A. *Vibr. Spectr*. **1998**, *17*, 123.
(192) Filarowski, A.; Koll, A.; Głowiak, T.; Majewski, E.; Dziembowska, T. *Ber. Bunsen-Ges. Phys. Chem.* **1998**, *102*, 393.
(193) Filarowski, A.; Koll, A.; Głowiak, T. *Monatsh. Chem*. **1999**, *130*, 1097.
(194) Filarowski, A.; Koll, A.; Karpfen, A.; Wolschann, P. *Chem. Phys*. **2004**, *297*, 323.
(195) Mandal, A.; Koll, A.; Filarowski, A.; Mukherjee, S. *Indian J. Chem. A* **2002**, *41*, 1107.
(196) Hansen, P. E. *Prog. NMR Spectrosc*. **1988**, *20*, 207.
(197) Siehl, H.-U. *Adv. Phys. Org. Chem*. **1987**, *23*, 63.
(198) Bolvig, S.; Hansen, P. E. *Curr. Org. Chem*. **2000**, *4*, 19.
(199) Dziembowska, T.; Rozwadowski, Z. *Curr. Org. Chem*. **2001**, *5*, 289.
(200) Bolvig, S.; Duus, F.; Hansen, P. E. *Magn. Reson. Chem*. **1998**, *36*, 315.
(201) Rozwadowski, Z.; Dziembowska, T. *Magn. Reson. Chem*. **1999**, *27*, 274.
(202) Rospenk, M.; Koll, A.; Sobczyk, L. *Chem. Phys. Lett*. **1996**, *261*, 283.
(203) Dziembowska, T.; Rozwadowski, Z.; Filarowski, A.; Hansen, P. E. *Magn. Reson. Chem*. **2001**, *39*, S67.
(204) Abildgaard, J.; Bolwig, S.; Hansen, P. E. *J. Am. Chem. Soc*. **1998**, *126*, 9063.
(205) Khatipov, S. A.; Shapetko, N. N.; Bogatchev, Yu. S.; Andreytchikov, Yu. S. *Zh. Fiz. Khim*. **1985**, *59*, 2095.
(206) Reuben, J. *J. Am. Chem. Soc*. **1986**, *108*, 1735; **1987**, *109*, 316.
(207) Andresen, B.; Duus, F.; Bolvig, S.; Hansen, P. E. *J. Mol. Struct*. **2000**, *552*, 45.
(208) Hansen, P. E.; Sitkowski, J.; Stefaniak, L.; Rozwadowski, Z.; Dziembowska, T. *Ber. Bunsen-Ges. Phys. Chem*. **1998**, *102*, 410.
(209) Hansen, A.; Kolonicny, P. E.; Lycka, A. *Magn. Reson. Chem*. **1992**, *30*, 786.
(210) Rozwadowski, Z.; Majewski, E.; Dziembowska, T.; Hansen, P. E. *J. Chem. Soc., Perkin Trans 2* **1999**, 2809.
(211) Hansen, P. E.; Skibsted, U.; Duus, F. *J. Phys. Org. Chem*. **1991**, *4*, 225.
(212) Filarowski, A.; Koll, A.; Rospenk, M.; Król-Starzomska, I.; Hansen, P. E. *Chem. Phys. Phys. Chem.*, manuscript submitted.
(213) Jameson, C. J. In *Isotopes in the Physical and Biomedical Sciences*; Buncel, E., Jones, J. R., Eds.; Elsevier: Amsterdam, The Netherlands, 1991; Vol. 2.
(214) Jameson, C. J.; Osten, H. J. *Annu. Rep. NMR Spectrosc*. **1986**, *17*.
(215) Forsyth, D. A.; Yang, J.-R. *J. Am. Chem. Soc*. **1986**, *108*, 2157.
(216) Rospenk, M.; Koll, A.; Sobczyk, L. *J. Mol. Liq*. **1995**, *67*, 63.
(217) Karplus, M.; Pople, J. A. *J. Chem. Phys*. **1963**, *38*, 2803.
(218) Dunitz, J. D. X-ray *Analysis and the Structure of Organic Molecules*; Cornell University Press: Ithaca, NY, 1979.
(219) Grabowski, S. J. Simulations of hydrogen bonds in crystals and their comparison with neutron diffraction results. In *Neutrons and Numerical Methods—N_2M*, Grenoble, France, December 1998, AIP Conference Proceedings 479; Johnson, M. R., Kearley, G. J., and Büttner, H. G., Eds.; American Institute of Physics, 1999.
(220) Glusker, J. P.; Lewis, M.; Rossi, M. *Crystal Structure Analysis for Chemists and Biologists*; VCH: New York, 1994.
(221) *Cambridge Structural Database System*; Cambridge Crystallographic Data Centre: Cambridge, U.K., 2001.
(222) Grabowski, S. J.; Krygowski, T. M. *Tetrahedron* **1998**, *54*, 5683.
(223) Steiner, T. *J. Phys. Chem*. **1998**, *102*, 7041.
(224) Taylor, R.; Kennard, O. *J. Am. Chem. Soc*. **1982**, *104*, 5063.
(225) Grabowski, S. J. *Tetrahedron* **1998**, *54*, 10153.
(226) Bader, R. F. W. *Acc. Chem. Res*. **1985**, *18*, 9.
(227) Bader, R. F. W.; MacDougall, P. J.; Lau, C. D. H. *J. Am. Chem. Soc*. **1984**, *106*, 1594.
(228) Bader, R. F. W. *Chem. Rev*. **1991**, *91*, 893.
(229) Popelier, P. *Atoms in Molecules. An Introduction*; Prentice Hall, Pearson Education Limited: New York, 2000.
(230) Grabowski, S. J.; Pfitzner, A.; Zabel, M.; Dubis, A. T.; Palusiak, M. *J. Phys. Chem. B* **2004**, *108*, 1831.
(231) Gilli, G.; Gilli, P. *J. Mol. Struct*. **2000**, *552*, 1.
(232) Flensburg, C.; Larsen, S.; Stewart, R. F. *J. Phys. Chem*. **1995**, *99*, 10130.
(233) Madsen, D.; Flensburg, C.; Larsen, S. *J. Phys. Chem. A* **1998**, *102*, 2177.
(234) Popelier, P. L. A. *J. Phys. Chem. A* **1998**, *102*, 1873.
(235) Mó, O.; Yánez, M.; Elguero, *J. Chem. Phys*. **1992**, *97*, 6628.
(236) Mó, O.; Yánez, M.; Elguero, J. *J. Mol. Struct. (THEOCHEM)* **1994**, *314*, 73.
(237) Espinosa, E.; Molins, E.; Lecomte, C. *Chem. Phys Lett.* **1998**, *285*, 170.
(238) Rozas, I.; Alkorta, I.; Elguero, J. *J. Am. Chem. Soc*. **2000**, *122*, 11154.
(239) Galvez, O.; Gomez, P. C.; Pacios, L. F. *Chem. Phys. Lett.* **2001**, *337*, 263.
(240) Galvez, O.; Gomez, P. C.; Pacios, L. F. *J. Chem. Phys*. **2001**, *115*, 11166.

(241) Galvez, O.; Gomez, P. C.; Pacios, L. F. *J. Chem. Phys*. **2003**, *118*, 4878.
(242) Pacios, L. F. *J. Phys. Chem. A* **2004**, *108*, 1177.
(243) Grabowski, S. J. *J. Mol. Struct*. **2002**, *615*, 239.
(244) Arnold, W. D.; Oldfield, E. *J. Am. Chem. Soc*. **2000**, *122*, 12835.
(245) Jenkins, S.; Morrison, I. *Chem. Phys. Lett*. **2000**, *317*, 97.
(246) Grabowski, S. J.; Sokalski, W. A. S.; Leszczyński, J. *J. Phys. Chem. A* **2005**, *109*, 4331.
(247) Grabowski, S. J. *Monatsh. Chem.* **2002**, *133*, 1373.
(248) Rybarczyk-Pirek, A. J.; Grabowski, S. J.; Małecka, M.; Nawrot-Modranka, J. *J. Phys. Chem. A* **2002**, *106*, 11956.
(249) Mallison, P. R.; Woźniak, K.; Wilson, C. C.; McCormack, K. L.; Yufit, D. S. *J. Am. Chem. Soc*. **1999**, *121*, 4640.
(250) Mallison, P. R.; Woźniak, K.; Smith, G. T.; McCormack, K. L.; Yufit, D. S. *J. Am. Chem. Soc.* **1997**, *119*, 11502.
(251) Mallison, P. R.; Smith, G. T.; Wilson, C. C.; Grech, E.; Woźniak, K. *J. Am. Chem. Soc*. **2003**, *125*, 4259.
(252) Woźniak, K.; Mallison, P. R.; Smith, G. T.; Wilson, C. C.; Grech, E. *J. Phys. Org. Chem*. **2003**, *16*, 764.
(253) Abramov, Y. A. *Acta Crystallogr., Sect. A: Found. Crystallogr.* **1997**, *53*, 264.
(254) Espinosa, E.; Alkorta, I.; Elguero, J.; Molins, E. *J. Chem. Phys*. **2002**, *117,* 5529.
(255) Jeffrey, G. A.; Gress, M. E.; Takagi, S. *Carbohydr. Res*. **1978**, *60*, 179.
(256) Rincón, L.; Almeida, R.; Garcia-Aldea, D.; Diez y Riega, H. *J. Chem. Phys*. **2001**, *114*, 5552.
(257) Viswamitra, M. A.; Radhakrishnan, R.; Bandekar, J.; Desiraju, G. R. *J. Am. Chem. Soc.* **1993**, *115*, 4868.
(258) Hunt, S. W.; Higgins, K. J.; Craddock, M. B.; Brauer, C. S.; Leopold, K. R. *J. Am. Chem. Soc*. **2003**, *125*, 13850.
(259) Huggins, M. L. *J. Org. Chem*. **1936**, *1*, 405.
(260) Coulson, C. A. *Valence*; Oxford University Press: Oxford, U.K., 1952.
(261) Bailinger, W. F.; Schleyer, P. v R.; Murty, T. S. S. R.; Robinson, L. *Tetrahedron* **1964**, *20*, 1635.
(262) Staab, H. A. *Einführung in die Theoretische Organische Chemie*; Verlag Chemie, Weinheim/Bergstrasse, Germany, 1959.
(263) Emsley, J. *Struct. Bonding* **1984**, *57*, 147.
(264) Gilli, P.; Bertloasi, V.; Pretto, L.; Ferretti, V.; Gilli, G. *J. Am. Chem. Soc*. **2004**, *126*, 3845.
(265) Buemi, G. J. *Mol. Struct. (THEOCHEM)* **2000**, *499*, 21.
(266) Grabowski, S. J. *J. Phys. Org. Chem*. **2003**, *16*, 797.
(267) Cuma, M.; Scheiner, S.; Kar, T. *J. Mol. Struct. (THEOCHEM)* **1999**, *467*, 37.
(268) Grabowski, S. J. *J. Mol. Struct*. **2001**, *562*, 137.
(269) Buemi, G.; Zuccarello, F. *Chem. Phys*. **2004**, *306*, 115.
(270) Grabowski, S. J.; Krygowski, T. M. *Chem. Phys. Lett.* **1999**, *305*, 247.
(271) Bürgi, H.-B. *Angew. Chem., Int. Ed. Eng.* **1975**, *14*, 460.
(272) Bürgi, H.-B., Dunitz, J. D., Eds.; *Structure Correlation*; VCH: Weinheim, Germany, 1994; Vols. 1−2.
(273) Coppens, P. *X-ray Charge Densities and Chemical Bonding*; IUCr; Oxford University Press: New York, 1997.
(274) Johnston, H. S. *Adv. Chem. Phys*. **1960**, *3*, 131.
(275) Johnston, H. S.; Parr, Ch. *J. Am. Chem. Soc*. **1963**, *85*, 2544.
(276) Pauling, L. *J. Am. Chem. Soc*. **1947**, *69*, 542.
(277) Auf der Heyde, T. P. E.; Bürgi, H.-B. *Inorg. Chem*. **1989**, *28*, 3960.
(278) Cieplak, A. S. Organic addition and elimination reactions; transformation paths of carbonyl derivatives. In *Structure Correlation*; Bürgi, H.-B., Dunitz, J. D., Eds; Weinheim, Germany, 1994.
(279) Auf der Heyde, T. Ligand rearrangement and substitution reactions of transition metal complexes. In *Structure Correlation*; Bürgi, H.-B., Dunitz, J. D., Eds; Weinheim, Germany, 1994.
(280) Bürgi, H.-B.; Shklover, V. Reaction paths for nucleophilic substitution (S_N2) reactions. In *Structure Correlation*; Bürgi, H.-B., Dunitz, J. D., Eds; Weinheim, Germany, 1994.
(281) Grabowski, S. J.; Krygowski, T. M. Molecular geometry as a source of chemical information—Application of the bond valence−bond number models. In *Advances in Quantitative Structure Property Relationships*; Charton, B., Charton, M., Eds.; Elsevier Science B.V.: New York, 2002; Vol. 3, pp 27−66.
(282) Brown, I. D. *Chem. Soc. Rev*. **1978**, *7*, 359.
(283) Brown, I. D. Altermat, D. *Acta Crystallogr., Sect. B: Struct. Sci.* **1985**, *41*, 244.
(284) Brown, I. D. *Acta Crystallogr., Sect. B: Struct. Sci.* **1992**, *48*, 553.
(285) Steiner, T. *J. Chem. Soc*., *Perkin Trans. 2* **1996**, 1315.
(286) Kim, Y. *J. Am. Chem. Soc*. **1996**, *118*, 1522.
(287) Neumann, M. A.; Craciun, S.; Corval, A.; Johnson, M. R.; Horsewill, A. J.; Benderskii, V. A.; Trommsdorff, H. P. *Ber. Bunsen-Ges. Phys. Chem*. **1998**, *102*, 325.
(288) Guallar, V.; Moreno, M.; Lluch, J. M.; Arnat-Guerri, F.; Douhal, A. *J. Phys. Chem*. **1996**, *100*, 19789.
(289) Garcia-Viloca, M.; González-Lafont, A.; Lluch, J. M. *J. Phys. Chem. A* **1997**, *101*, 3880.
(290) Garcia-Viloca, M.; Gelabert, R.; González-Lafont, A.; Moreno, M.; Lluch, J. M. *J. Phys. Chem. A* **1997**, *101*, 8727.
(291) Garcia-Viloca, M.; González-Lafont, A.; Lluch, J. M. *J. Am. Chem. Soc*. **1997**, *119*, 1081.
(292) Allen, F. H.; Davies, J. E.; Galloy, J. E.; Johnson, J. J.; Kennard, O.; Macrave, C. F.; Mitchel, E. M.; Smith, J. M.; Watson, D. G. *J. Chem. Inf. Comput. Sci*. **1991**, *31*, 187.
(293) Grabowski, S. J. *J. Mol. Struct*. **2000**, *552*, 153.
(294) Robertson, J. M.; Ubbelohde, A. R. *Proc. R. Soc. London* **1939**, *170*, 222.
(295) Ubbelohde, A. R.; Gallagher, K. J. *Acta Crystallogr.* **1955**, *8*, 71.
(296) Cleland, W. W.; Kreevoy, M. M. *Science* **1994**, *264*, 1887.
(297) Cleland, W. W.; Frey, P. A.; Gerlt, J. A. *J. Biol. Chem*. **1998**, *273,* 25529.
(298) Gerlt, J. A.; Gassman, P. G. *Biochemistry* **1993**, *32*, 11934.
(299) Gerlt, J. A.; Gassman, P. G. *J. Am. Chem. Soc.* **1993**, *115*, 11552.
(300) Frey, P. A.; Whitt, S. A.; Tobin, J. B. *Science* **1994**, *264*, 1927.
(301) Warshel, A.; Papazyan, A.; Kollman, P. A. *Science* **1995**, *269*, 102.
(302) Abu-Dari, K.; Raymond, K. N.; Freyberg, D. P. *J. Am. Chem. Soc.* **1979**, *101*, 3688.
(303) Abu-Dari, K.; Freyberg, D. P.; Raymond, K. N. *Inorg. Chem.* **1979**, *18*, 2427.
(304) James, M. N. G.; Matsushima, M. *Acta Crystallogr.* **1976**, *B32*, 1708.
(305) Currie, M.; Speakman, J. C. *J. Chem. Soc. A* **1970**, 1923.
(306) Ellison, R. D.; Levy, H. A. *Acta Crystallogr.* **1965**, *19*, 260.
(307) Küppers, H.; Kvick, Å.; Olovsson, J. *Acta Crystallogr.* **1981**, *B37*, 1203.
(308) Lundgren, J. O.; Telgren, R. *Acta Crystallogr., Sect. B: Struct. Sci.* **1974**, *30*, 1937.
(309) Brunton, G. D.; Johnson, C. G. *J. Chem. Phys*. **1975**, *62*, 3797.
(310) Coulson, C. A.; Danielsson, U. *Ark. Fysik* **1954**, *8*, 239.
(311) Coulson, C. A.; Danielsson, U. *Ark. Fysik* **1954**, *8*, 245.
(312) Pimental, G. C. *J. Chem. Phys.* **1951**, *19,* 446.
(313) Reid, C. *J. Chem. Phys*. **1959**, *30*, 182.
(314) Stevens, E. D.; Lehmann, M. S.; Coppens, P. *J. Am. Chem. Soc*. **1977**, *99*, 2829.
(315) Ferguson, G.; Marsh, W. C.; Restivo, R. J.; Lloyd, D. *J. Chem. Soc., Perkin Trans. 2* **1975**, 998.
(316) Grabowski, S. J.; Sokalski, W. A.; Leszczynski, J. *J. Phys. Chem. A* **2004**, *108*, 1806.
(317) Cioslowski, J.; Surján, P. *J. Mol. Struct. (THEOCHEM)* **1992**, *255*, 9.
(318) Wojtulewski, S.; Grabowski, S. J. *J. Mol. Struct.* **2003**, *645*, 287.
(319) Cuma, M.; Scheiner, S.; Kar, T. *J. Mol. Struct. (THEOCHEM)* **1999**, *467*, 37.
(320) Rozas, I.; Alkorta, I.; Elguero, J. *J. Phys. Chem. A* **2001**, *105*, 10462.
(321) Bertolasi, V.; Gilli, P.; Ferretti, V.; Gilli, G.; Vaughan, K. *New J. Chem*. **1999**, *23*, 1261.
(322) Gilli, P.; Bertolasi, V.; Ferretti, V.; Gilli, G. *J. Am. Chem. Soc.* **2000**, *122*, 10405.
(323) Allen, F. H.; Kennard, O.; Watsan, D. G.; Brammer, L.; Orpen, A. G.; Taylor, R. *J. Chem. Soc., Perkin Trans. 2* **1987**, S1.
(324) Malecka, M.; Grabowski, S. J.; Budzisz, E. *Chem. Phys*. **2004**, *297*, 235.
(325) Rybarczyk-Pirek, A. J.; Grabowski, S. J.; Nawrot-Modranka, J. *J. Phys. Chem. A* **2003**, *107*, 9232.
(326) Steiner, T. *Chem. Commun*. **1998**, 411.
(327) González, L.; Mó, O.; Yáñez, M. *J. Org. Chem*. **1999**, *64*, 2314.
(328) Wojtulewski, S.; Grabowski, S. J. *Chem. Phys. Lett*. **2003**, *378*, 388.
(329) Sanz, P.; Yánez, M.; Mó, O. *J. Phys. Chem. A* **2002**, *106*, 4661.
(330) Malarski, Z.; Rospenk, M.; Sobczyk, L.; Grech, E. *J. Phys. Chem*. **1982**, *86*, 401.
(331) Zeegers-Huyskens, T. In *Intermolecular Forces*; Huyskens, P. L., Luck, W. A., Zeegers-Huyskens, T., Eds.; Springer-Verlag: Berlin, Germany, 1991; chapter 6.
(332) Sobczyk, L. *Ber. Bunsen-Ges. Phys. Chem*. **1998**, *102*, 377.
(333) Reinhard, L. A.; Sacksteder, K. A.; Cleland, W. A. *J. Am. Chem. Soc*. **1998**, *120*, 13366.
(334) Gilli, P.; Bertolasi, V.; Pretto, L.; Lyčka, A.; Gilli, G. *J. Am. Chem. Soc*. **2002**, *124*, 13554.
(335) Hammond, G. S. *J. Am. Chem. Soc*. **1955**, *77*, 334.
(336) Bertolasi, V.; Gilli, P.; Ferretti, V.; Gilli, G. *Acta Crystallogr., Sect. B: Struct. Sci.* **1995**, *51*, 1004.
(337) Guerra, C. F.; Bickelhaupt, F. M.; Snijders, J. G.; Baerends, E. J. *Chem.—Eur. J*. **1999**, *5*, 12.
(338) Jensen, F. *Introduction to Computational Chemistry*; John Wiley and Sons: Chichester, U.K., 1999.
(339) Bickelhaupt, F. M.; Hommes, N. J. R. van Eikema; Guerra, C. F.; Baerends, E. J. *Organometallics* **1996**, *15*, 2923.
(340) Dubis, A.; Grabowski, S. J.; Romanowska, D. B.; Misiaszek, T.; Leszczynski, J. *J. Phys. Chem. A* **2002**, *106*, 10613.
(341) Grabowski, S. J.; Dubis, A. T.; Martynowski, D.; Glowka, M.; Palusiak, M.; Leszczynski, J. *J. Phys. Chem. A* **2004**, *108*, 5815.
(342) Krygowski, T. M.; Cyrański, M. K.; Czarnocki, Z.; Hafelinger, G.; Katritzky A. R. *Tetrahedron* **2000**, *56*, 1783.

(343) Elvidge, J. A.; Jackman, L. M. *J. Chem. Soc.* **1961**, 859.
(344) Sondheimer, F. *Pure Appl. Chem*. **1963**, *7*, 363.
(345) Dewar, M. J. S. *Tetrahedron Suppl.* **1966**, *8*, 75.
(346) Pauling L.; Sherman J. *Chem. Phys.* **1933**, *1*, 362.
(347) Kistiakowski, G. B.; Ruhoff, J. R.; Smith, H. A.; Vaughan, W. E. *J. Am. Chem. Soc.* **1936**, *58*, 146.
(348) Wheland, G. W. *The Theory of Resonance and Its Application to Organic Chemistry*; J. Wiley: New York, 1944.
(349) Julg, A.; Francoise, P. *Theor. Chim. Acta* **1967**, *7*, 249.
(350) Kruszewski, J.; Krygowski, T. M. *Tetrahedron Lett.* **1972**, 3839.
(351) Bird, C. W. *Tetrahedron* **1985**, *41*, 1409.
(352) Krygowski, T. M. *J. Chem. Inf. Comput. Sci.* **1993**, *33*, 70.
(353) Krygowski, T. M.; Cyrański, M. K. *Tetrahedron* **1996**, *52*, 1713.
(354) Krygowski, T. M.; Cyrański, M. K. *Chem. Rev.* **2001**, *101*, 1385.
(355) Flygare, W. H. *Chem. Rev*. **1974**, *74*, 653.
(356) Dauben, H. J.; Wilson, J. D.; Laity, J. L. *J. Am. Chem. Soc*. **1968**, *90*, 811.
(357) Dauben, H. J.; Wilson, J. D.; Laity, J. L. *J. Am. Chem. Soc.* **1969**, *91*, 1991.
(358) Dauben, H. J.; Wilson, J. D.; Laity, J. L. in *Non-Benzoid Aromatics*; Snyder, J. P., Ed.; Academic Press: New York, 1971; Vol. 2.
(359) For a recent review, see Lazzeretti, P. *Prog. NMR Spectrosc*. **2000**, *36*, 1.
(360) Mitchell, R. G. *Chem. Rev*. **2001**, *101*, 1301.
(361) For the idea, see also Esler, V.; Haddon, R. C. *Nature* **1987**, *325*, 792.
(362) Schleyer, P. v. R.; Maerker, C.; Dransfeld, H.; Jiao, H.; van Eikemma Hommes, N. J. R. *J. Am. Chem. Soc.* **1996**, *118*, 6317.
(363) Katritzky, A. R.; Barczyñski, P.; Mussumura G.; Pisano, D.; Szafran, M. *J. Am. Chem. Soc*. **1989**, *111*, 7.
(364) Jug, K.; Koester, A. *J. Phys. Org. Chem.* **1991**, *4*, 163.
(365) Krygowski, T. M.; Ciesielski, A.; Bird, C. W.; Kotschy A. *J. Chem. Inf. Comput. Sci*. **1995**, *35*, 203.
(366) Subramanian, G.; Schleyer P. v. R.; Jiao, H. *Angew. Chem., Int. Ed. Eng.* **1995**, *35*, 2638.
(367) Katritzky, A. R.; Karelson, M.; Sild, S.; Krygowski, T. M.; Jug, K. *J. Org. Chem.* **1998**, *63*, 5228.
(368) Katritzky, A. R.; Jug, K.; Onciu, D. C. *Chem. Rev.* **2001**, *101*, 1421.
(369) Cyrański, M. K.; Krygowski, T. M.; Katritzky, A. R.; Schleyer, P. v. R. *J. Org. Chem*. **2002**, *67*, 1333.
(370) Stępień, B. T.; Krygowski, T. M.; Cyrański, M. K. *J. Org. Chem*. **2002**, *67*, 5987.
(371) Stępień, B. T.; Krygowski, M. K.; Cyrański M. K. *J. Phys. Org. Chem*, **2003**, *16*, 426.
(372) Hellmann, H. *Einfürung in die Quantenchemie*, Franz Deuticke, Leipzig, Germany, 1937. (b) Feynman, R. P. *Phys. Rev*. **1939**, *56*, 340.
(373) Jeffrey, G. A.; Ruble, J. R.; McMullan, R. K.; Pople, J. A. *Proc. R. Soc. London, Ser. A* **1987**, *414*, 47.
(374) Cyrański, M. K.; Krygowski, T. M. *Tetrahedron* **1996**, *52*, 1713.
(375) Schleyer, P. v. R.; Monoharan, M.; Wang, Z.; Kiran, X. B.; Jiao, H.; Puchta, R.; van Eikemma Hommes, N. J. R. *Org. Lett.* **2001**, *3*, 2465.
(376) Lazzeretti, P. *Phys. Chem. Chem. Phys*. **2004**, *6*, 217.
(377) Wiberg, K. B. *Chem. Rev*. **2001**, *101*, 1317.
(378) Corminboeuf, C.; Heine, T.; Seifert, G.; Schleyer, P. v. R.; Weber, J. *Phys. Chem. Chem. Phys*. **2004**, *6*, 273.
(379) Woźniak, K.; Krygowski, T. M.; Kariuki, B.; Jones, W. *J. Mol. Struct.* **1991**, *248*, 331.
(380) Woźniak, K.; Heyong, He.; Klinowski, J.; Jones, W.; Dziembowska, T.; Grech, E. *J. Chem. Soc., Faraday Trans.* **1995**, *91*, 77.
(381) Iczkowski, R. P.; Margrave J. L. *J. Am. Chem. Soc*. **1961**, *83*, 3547.
(382) Walsh, A. D. *Discuss. Faraday Soc*. **1947**, *2*, 18.
(383) Bent, H. A. *Chem. Rev*. **1961**, *61*, 275.
(384) Vilkov, L. V.; Mastryukov, V. S.; Sadova, N. I. *Determination of the Geometrical Structure of Free Molecules*, Mir, Moscow, Russia, 1983.
(385) Georgiou, K.; Kroto, W. H. *J. Mol. Spectrosc.* **1980**, *83*, 94.
(386) Larsen, N. W. *J. Mol. Struct.* **1979**, *51*, 175.
(387) Szatyłowicz, H.; Krygowski, T. M. *Pol. J. Chem*. **2004**, *78*, 1719.
(388) Campanelli, A. R.; Domenicano, A.; Ramondo, F. *J. Phys. Chem. A* **2003**, *107*, 6429.
(389) Bõhm, S.; Exner, O. *Acta Crystallogr., Sect. B: Struct. Sci.* **2004**, *60*, 103.
(390) These problems are discussed more in details in the paper by T. M. Krygowski and B. T. Stępień, this issue: "σ and π-electron delocalization: Focus on substituent effects".
(391) Krygowski, T. M.; Szatyłowicz, H.; Zachara, J. E. *J. Chem. Inf. Comput. Sci*. **2004**, *44*, 2077.
(392) Krygowski, T. M.; Zachara, J. E.; Szatyłowicz, H. *J. Phys. Org. Chem*. **2005**, *18*, 110.
(393) The Cambridge Structure Database, the 5.25 version, November 2003, updated January 2004.
(394) Krygowski, T. M.; Szatyłowicz, H.; Zachara, J. E. *J. Chem. Inf. Model.* **2005**, *45*, 652.
(395) Bernstein, J. In *Accurate Molecular Structures—Their Determination and Importance*; Domenicano, A., Hargittai, I., Eds.; IUCr; Oxford University Press: New York, 1992; chapter 19, p 469 ff.
(396) Malinowski, E. R.; Howery, D. G. *Factor Analysis in Chemistry*; Wiley: New York, 1980.
(397) Zalewski, R. I. In S*imilarity Models in Organic Chemistry, Biochemistry, and Related Fields*; Zalewski, R. I., Krygowski, T. M., Shorter, J., Eds.; Elsevier: Amsterdam, The Netherlands, 1991; chapter 9, p 456 ff.
(398) Lee, C.; Yang, W.; Parr, R. G. *Phys. Rev. B* **1988**, *37*, 785.
(399) Becke, A. D. *J. Phys. Chem.* **1993**, *98*, 1372.
(400) Becke, A. D. *J. Chem. Phys.* **1993**, *98*, 5648.
(401) Stephens, P. J.; Devlin, F. J.; Chabalowski, C. F.; Frisch, M. J. *J. Phys. Chem.* **1994**, *98*, 11623.
(402) Kwiatkowska, E.; Majerz, I.; Koll, A. *Chem. Phys. Lett*. **2004**, *398*, 130.
(403) Boys, S. F.; Bernardi, F. *Mol. Phys*. **1970**, *19*, 553.
(404) Krygowski, T. M.; Zachara, J. E.; Szatyłowicz, H. *J. Org. Chem*. **2004**, *69*, 7038.
(405) Pross, A.; Radom, L.; Taft, W. R. *J. Org. Chem.* **1980**, *45*, 818.
(406) Hansch, C.; Leo, A.; Taft, W. R. *Chem. Rev*. **1991**, *91*, 165.
(407) Cyrański, M. K.; Krygowski, M. K.; Wisiorowski, M.; van Eikemma Hommes, N. J.; Schleyer, P. v. R. *Angew. Chem. Int. Ed.* **1998**, *37*, 177.
(408) Krygowski, T. M.; Cyranski, M. K. *Tetrahedron* **1996**, *52*, 10255.
(409) Cyrański, M. K.; Gilski, M.; Jaskólski, M.; Krygowski, T. M. *J. Org. Chem.* **2003**, *68*, 8607.
(410) Majerz, I.; Koll, A. *Acta Crystallogr., Sect. B: Struct. Sci.* **2004**, *60*, 406.
(411) Szatylowicz, H.; Zachara, J. E., private communication.
(412) Anulewicz, R.; Krygowski, T. M.; Jagodziñski, T. *Pol. J. Chem.* **1998**, *72*, 439.
(413) Dziembowska, T. *Pol. J. Chem.* **1998**, *72*, 193.
(414) Krygowski, T. M.; Stepien, B. T.; Anulewicz-Ostrowska, R.; Cyranski, M. K.; Grabowski, S. J.; Rozwadowski, Z.; Dziembowska, T. *Collect. Czech. Chem. Commun.* **1999**, *64*, 1797.
(415) Krygowski, T. M.; Stępień, B. T.; Anulewicz-Ostrowska, R.; Dziembowska, T. *Tetrahedron* **1999**, *55*, 5457.
(416) Krygowski, T. M.; Woźniak, K.; Anulewicz, R.; Pawlak, D.; Kołodziejski, W.; Grech, E.; Szady, A. *J. Phys. Chem.* **1997**, *101*, 9399.
(417) Cyrański, M.; Krygowski, T. M. *J. Chem. Inf. Comput. Sci.* **1996**, *36*, 1142.
(418) Krygowski, T. M.; Anulewicz R.; Kruszewski, J. *Acta Crystallogr., Sect. B: Struct. Sci.* **1983**, *39*, 732.
(419) For review, see Krygowski, T. M.; Cyrański, M. K. In *Theoretical Organic Chemistry*; Parkanyi, C., Ed.; Elsevier: Amsterdam, The Netherlands, 1998; chapter 6, Vol. 5.
(420) Dominiak, P.; Grech, E.; Barr, G.; Teat, S.; Mallison, P.; Woźniak, K. *Chem.—Eur. J*. **2003**, *9*, 963.
(421) Koll, A. *Int. J. Mol. Sci.* **2003**, *4*, 434.
(422) Krygowski, T. M.; Zachara, J. E. *J. Chem. Inf. Model* **2005**, in press.
(423) Filarowski A. *J. Phys. Org. Chem*. **2005**, *18*, 686.
(424) Filarowski, A.; Kochel, A.; Cieślik, K.; Koll, A. *J. Phys. Org. Chem*. **2005**, *18*, 986.
(425) Data from (a) Filarowski, A.; Koll, A.; Głowiak, T.; Majewski, E.; Dziembowska, T. *Ber. Bunsen-Ges. Phys. Chem.* **1998**, *102*, 393. (b) Filarowski, A.; Koll, A.; Głowiak, T. *J. Chem. Soc., Perkin Trans. 2* **2002**, 835. (c) Mandal, A.; Koll, A.; Filarowski, A.; Mukherjee, S. *Indian J. Chem. A* **2002**, *41*, 1107. (d) Filarowski, A.; Koll, A.; Głowiak, T. *J. Mol. Struct.* **1999**, *484*, 75. (e) Filarowski, A.; Koll, A.; Głowiak, T. *Monatsh. Chem.* **1999**, *130*, 1097. (f) Filarowski, A.; Koll, A.; Głowiak, T. *J. Mol. Struct.* **2002**, *615*, 97. (g) Król-Starzomska, I.; Rospenk, M.; Filarowski, A.; Koll, A. *J. Phys. Chem.* **2004**, *108*, 2131. (h) Filarowski, A.; Koll, A.; Karpfen, G.; Wolschann, P. *Chem. Phys.* **2004**, *297*, 323.
(426) Data from Cambridge Structural Database (CSD; Allen, F. H.; Kennard, O. *Chem. Des. Autom. News* **1993**, *8*, 1), update 5.20 (October 2003).
(427) Cyrański, M. K.; Stępień, B. T.; Krygowski, T. M. *Tetrahedron* **2000**, *56*, 9663.
(428) Krygowski, T. M.; Zachara, J. E. *Theor. Chem. Acc*. **2005**, 13 ASAP on-line June 15, 2005.
(429) Howard, S. T.; Krygowski, T. M. *Can. J. Chem.* **1997**, *75*, 1174.
(430) Zborowski, K.; Grybos, R.; Proniewicz, L. M. *J. Phys. Org. Chem.* **2005**, *18*, 250.
(431) Zborowski, K.; Proniewicz, L. M. *Pol. J. Chem.* **2004**, *78*, 2219.
(432) Raczynska, E. D.; Krygowski, T. M.; Zachara, J. E.; Osmialowski, B.; Gawinecki, R. *J. Phys. Org. Chem.* **2005**, *18*, 892.

CR030083C